Electrochemical Dehumidification and Adsorption Thermal Energy Storage

August 2023

Yunho Hwang

Center for Environmental Energy Engineering
Department of Mechanical Engineering
University of Maryland
College Park, MD 20742-3035

Energy Efficiency and Heat Pumps Consortium

CENTER FOR ENVIRONMENTAL ENERGY ENGINEERING

Introduction

- Using air conditioners and electric fans accounts for about 20% of all global electricity consumption (IEA).
- According to the U.S. Energy Information Administration (EIA), the electricity used for cooling was about 389 billion kilowatt-hours (kWh), or about 10% of total U.S. electricity consumption in 2021.
- Since the typical latent load is about 25% of the total building's cooling loads, dehumidification is responsible for 2.5% of total U.S. electricity consumption.
- When we can use innovative energy-efficient dehumidification technologies while using waste from the conventional cooling system, this cooling electricity consumption share can be decreased to 7% with a 30% energy savings in air conditioning.

Dehumidification

PRINCIPLE

- Refrigerant Dehumidifier
- Desiccant Dehumidifier
- Petlier Dehumidifier

APPLICATIONS

- Home Dehumidifier
- Pool Dehumidifier
- Industrial Dehumidifier

Part 1: Electrochemical Dehumidification

- **Y. Hwang*, L. Cao, J. Baker, C. Wang, R. Radermacher, Electrochemical Mass Transfer for Dehumidification and Gas Compression, 08/2023, DOI: 10.18462/iir.icr.2023.1150.**

- L. Cao, J. Baker, Y. Hwang*, C. Wang, R. Radermacher, Development of An Electrochemical Membrane Dehumidifier, 08/2023, DOI: 10.18462/iir.icr.2023.0849.

Introduction

- **Comparison of Alkaline fuel cell (AEMFC) and electrochemical dehumidifier**

Alkaline Fuel Cell (AEMFC)

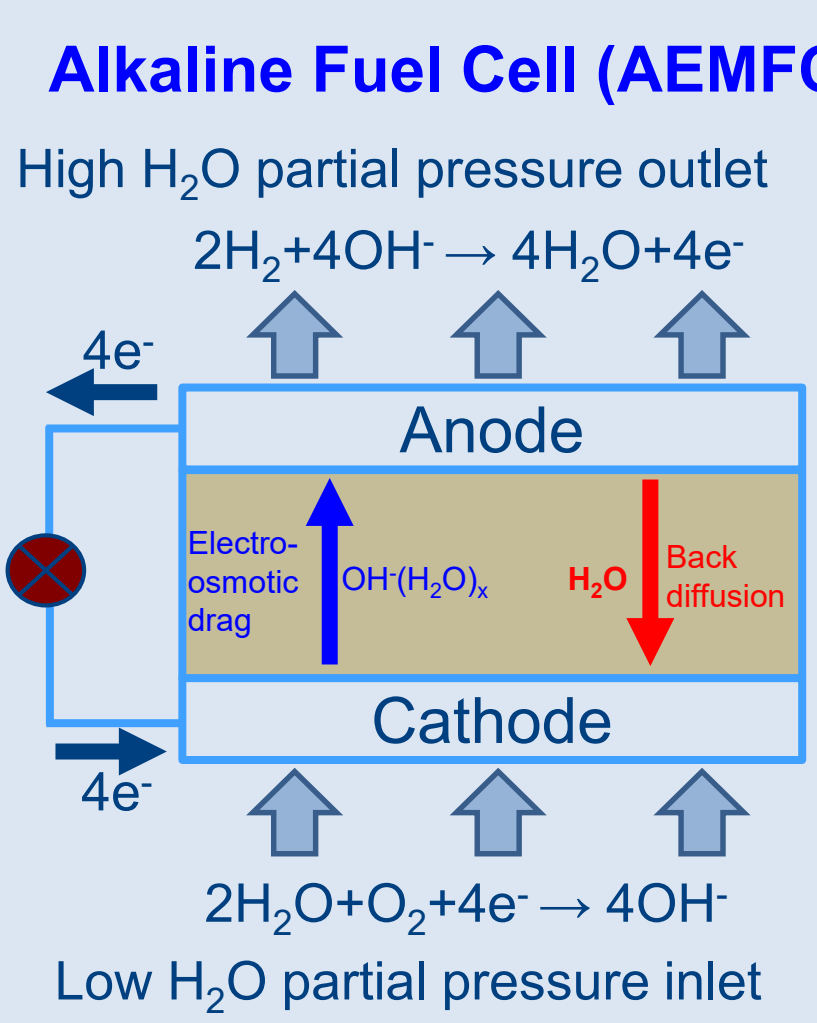

Electrochemical Dehumidifier (ECD)

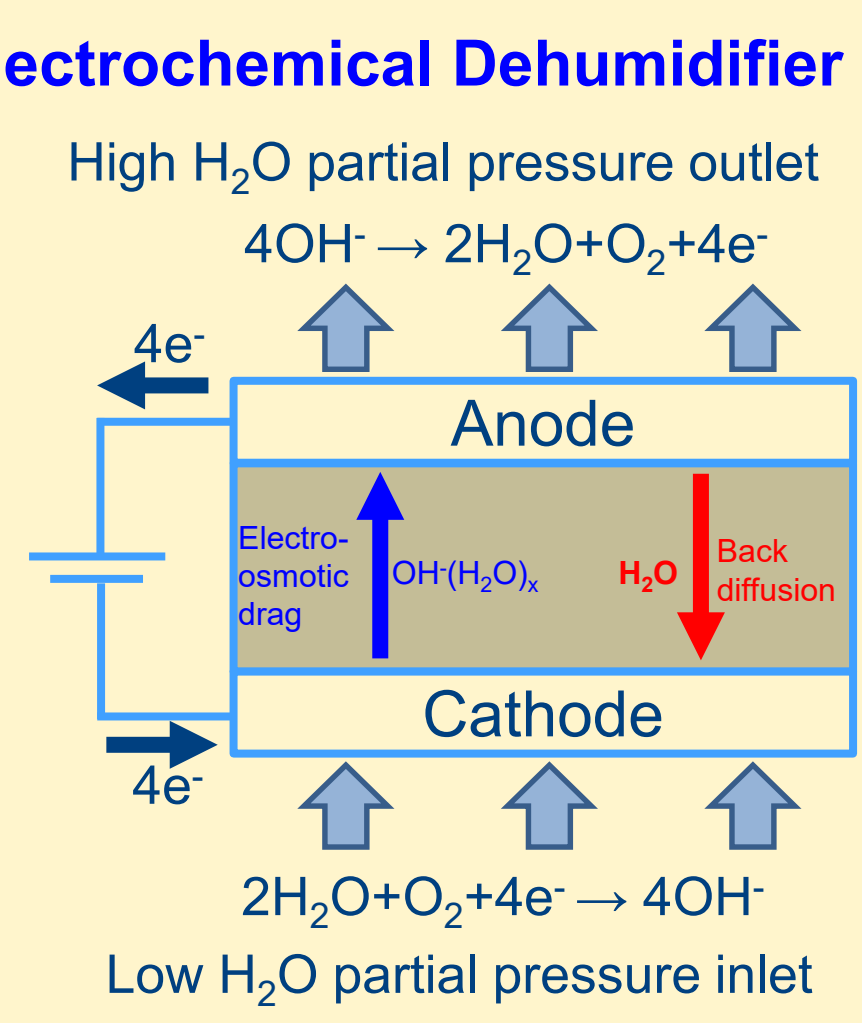

MEA Fabrication

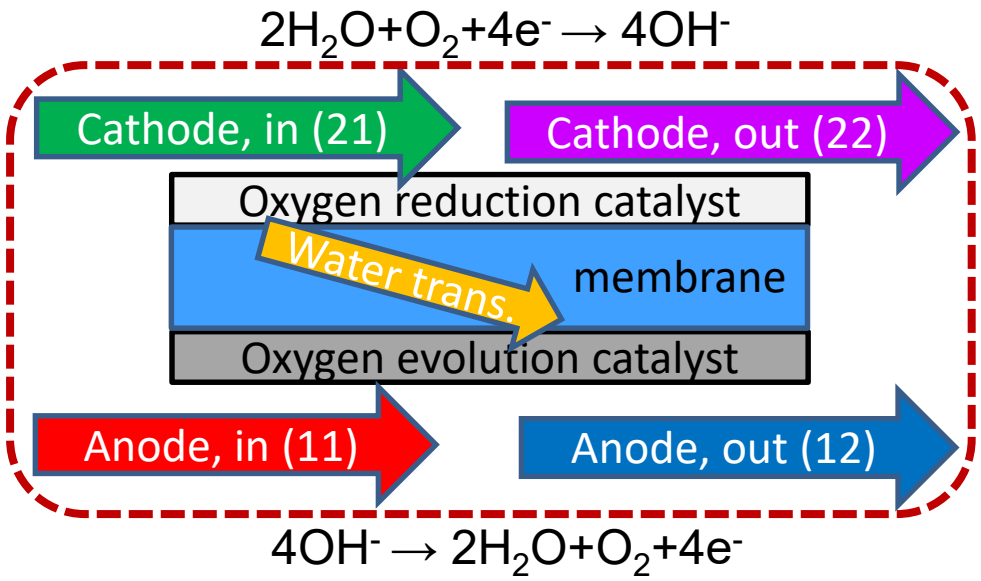

MEA (Membrane electrode assembly) Fabrication Procedure:

- **The anode/cathode catalysts and ionomer binder were mixed to form ink solutions: catalyst/binder ratio, ultrasound.**
- **The ink solutions were painted on the membrane at a pre-determined amount: spray speed.**
- **Two gas diffusion layers were hot-pressed against each other with the catalyst-coated membrane to form the MEA: temperature and pressure.**

Hydrophilic carbon cloth

Catalyst coated membrane

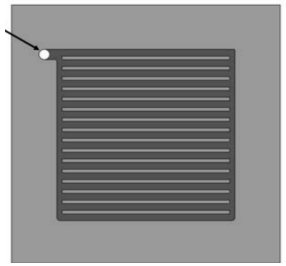

Designed parallel gas distribution channel

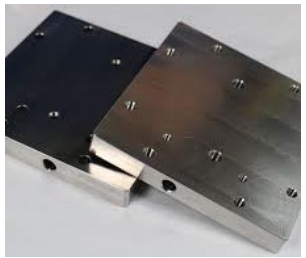

Titanium endplate

In-house MEA developed had:

- **active membrane area of 5 cm^2,**
- **cathode catalyst loading of 1 $mgPt \cdot cm^{-2}$,**
- **anode catalyst loading of 1 $mgIrO_2 \cdot cm^{-2}$,**
- **cathode catalyst was 60 wt.%Pt/40 wt.%C, and the anode catalyst was IrO_2.**

ECD – Test Facility and Matrix

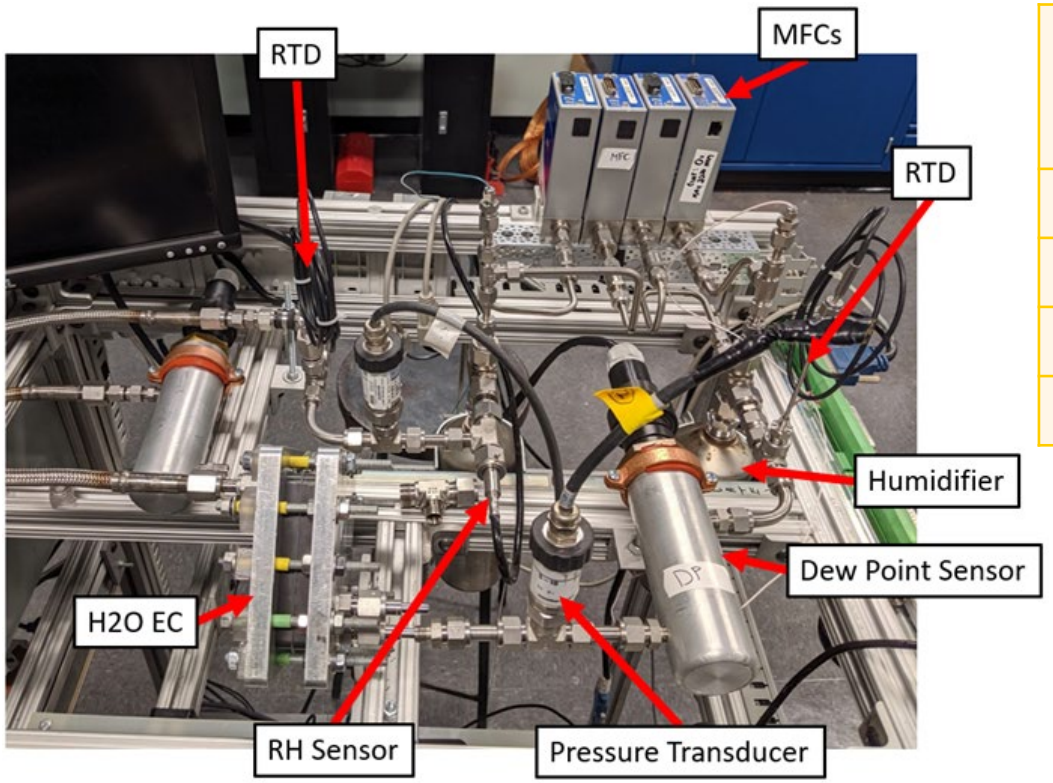

Picture of the MEA Test Facility

Test No.	Cathode RH - Set (Actual) (%)	Anode RH -Set (Actual) (%)	Dry Oxygen Flow Rate (mL/min)	Voltage (V)
1	50 (59)	50 (49)	600	0
2	50 (59)	50 (49)	600	2
3	50 (59)	50 (49)	600	3
4	50 (59)	50 (49)	800	2

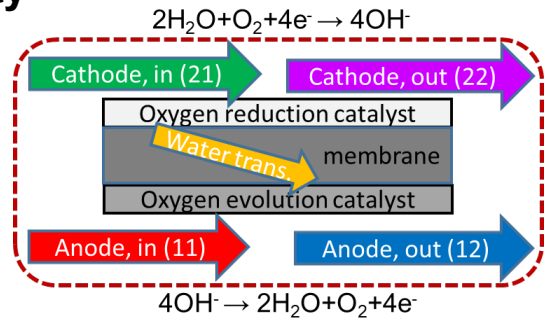

Schematic of the MEA Test Facility

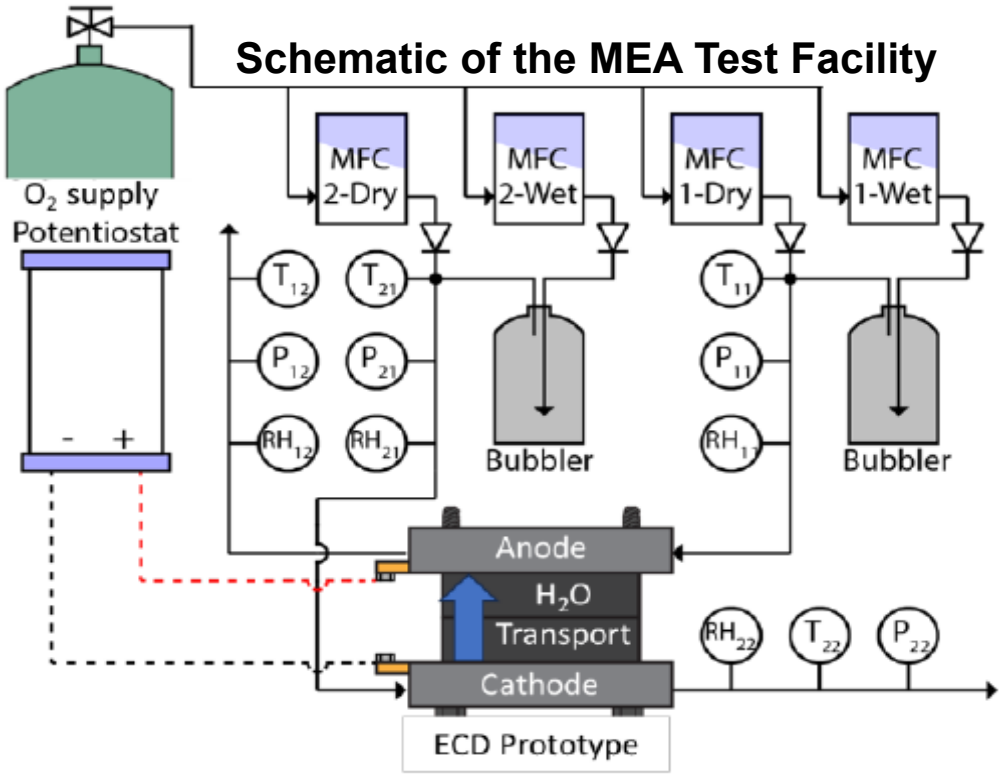

Energy Efficiency and Heat P

ECD Test Results (I)

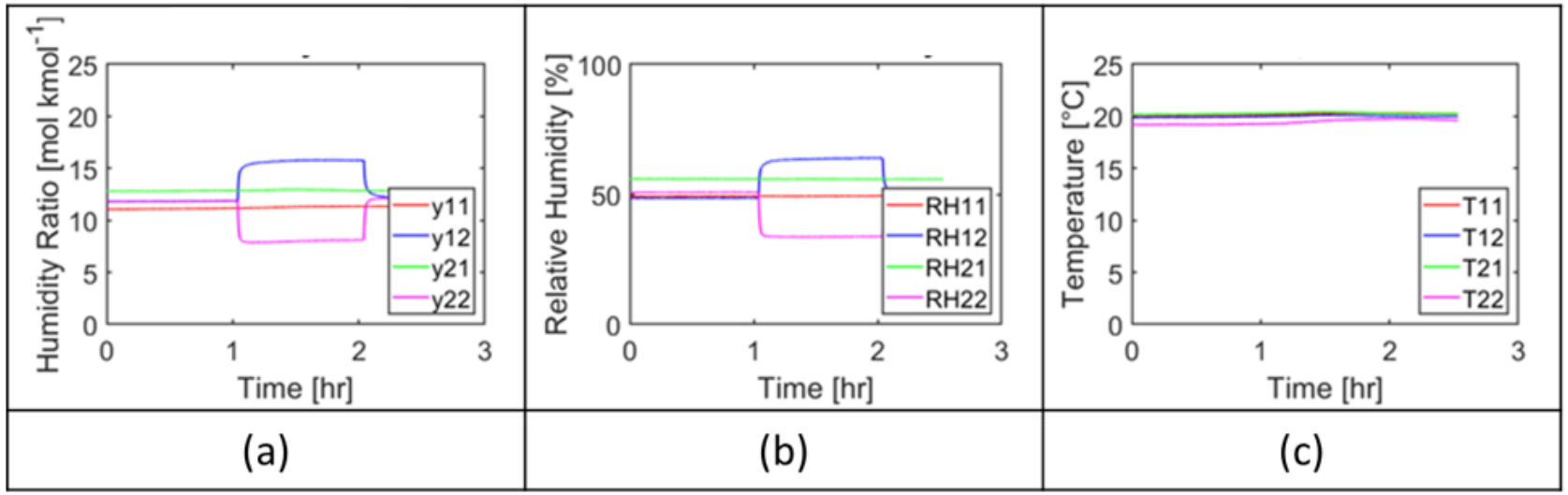

Fig. 4: ECD process with a dry oxygen flow rate of 600 mL·min^{-1}, 0/2 V, RH 50/50%. (Test 1 and 2)

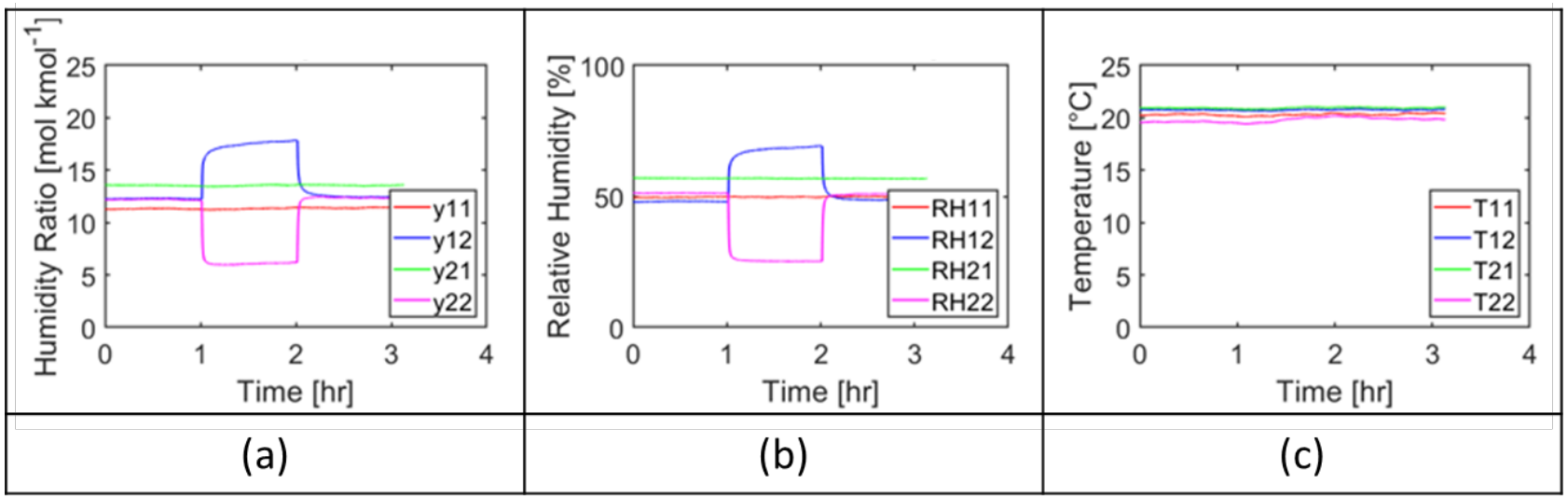

Fig. 5: ECD process with a dry oxygen flow rate of 600 mL·min^{-1}, 0/3 V, RH 50/50%. (Test 1 and 3)

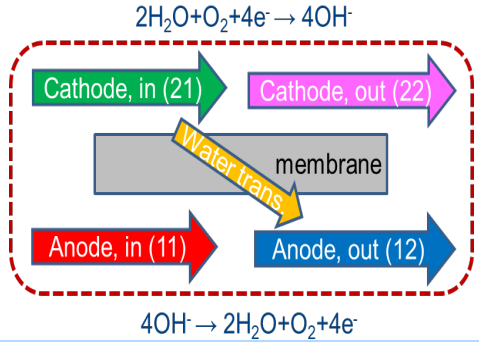

Actual water removal rate 0.69 g/day/cm^2 is 48% smaller than Faradic water removal rate 1.33 g/day/cm^2 when water is moved from high RH 59% to low RH 49% at 2 V (neutral diffusion).

Actual water removal rate 0.97 g/day/cm^2 is 33% smaller than Faradic water removal rate 1.45 g/day/cm^2 when water is moved from high RH 59% to low RH 49% at 3 V (neutral diffusion).

ECD Test Results (II)

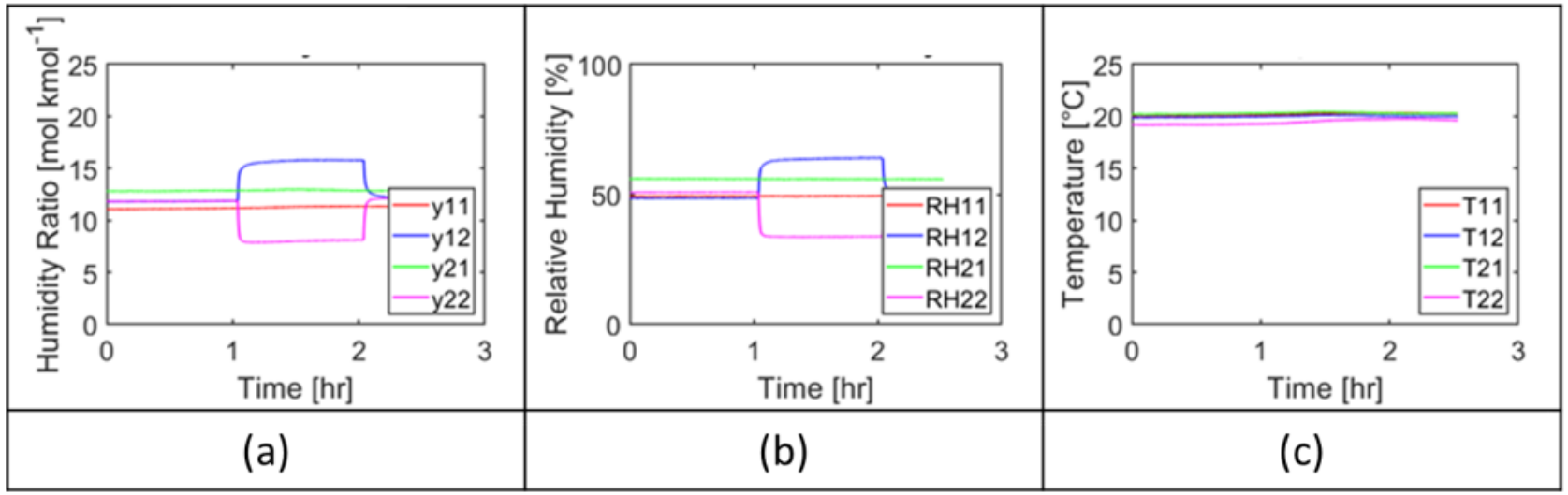

Fig. 4: ECD process with a dry oxygen flow rate of 600 mL·min^{-1}, 0/2 V, RH 50/50%. (Test 1 and 2)

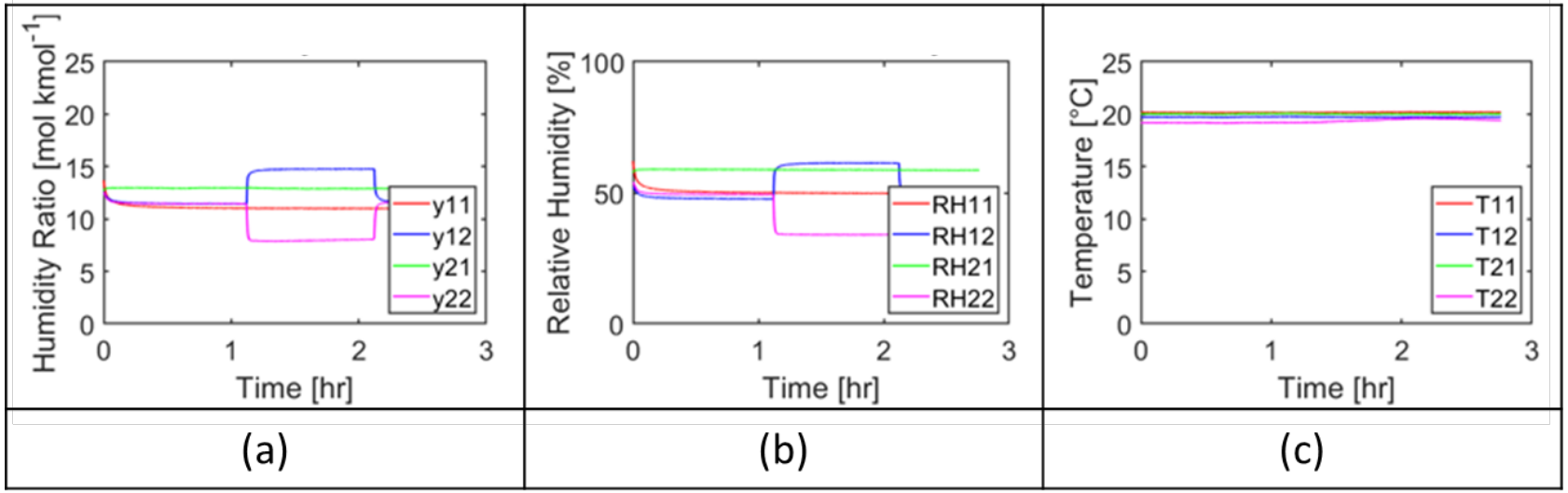

Fig. 6: ECD process with a dry oxygen flow rate of 800 mL·min^{-1}, 0/2 V, RH 50/50%. (Test 1 and 4)

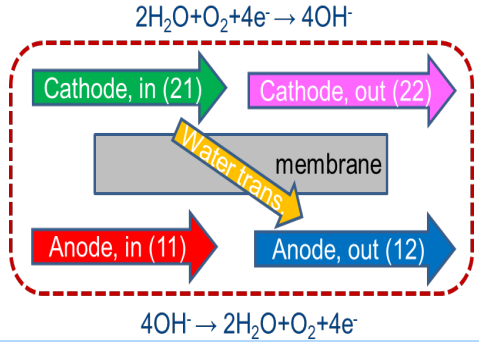

Actual water removal rate 0.69 g/day/cm^2 is 48% smaller than Faradic water removal rate 1.33 g/day/cm^2 when water is moved from high RH 59% to low RH 49% at 2 V (neutral diffusion).

Actual water removal rate 0.93 g/day/cm^2 is 34% smaller than Faradic water removal rate 1.40 g/day/cm^2 when oxygen flow rate is increased from 600 to 800 ml/min at 2 V (neutral diffusion).

ECD Test Results (III)

We analyzed the steady-state mass flux and power consumption and calculated the water removal rate and dehumidification efficiency.

$$\dot{M}_{removal} = \dot{m}_{air}(\omega_{cathode-in} - \omega_{cathode-out}) \quad \text{Eq. (3)}$$

$$\eta_{dehumidification} = \dot{m}_{removal}/(P \times A) \quad \text{Eq. (4)}$$

where ω is humidity ratio, P is power input, and A is membrane area.

No.	Electric Field (V)	Air inlet of Anode side				Air inlet of Cathode side				Water removal (g/day/m^2)	Dehumidification efficiency (g/(J·m^2))
		m_a (g/s)	V_a (mL/min)	T(°C)	HR (g/kg)	m_a (g/s)	V_a (mL/min)	T(°C)	HR (g/kg)		
1	3	0.0324	1502	21.5	14.7	0.0324	1502	21.5	10.7	4,020	0.0225
2	3	0.0111	516	21.5	14.7	0.0111	516	21.5	10.7	2,539	0.0195
3	3	0.0270	1251	22.6	13.2	0.0270	1251	22.9	12.6	2,610	0.0150
4	3	0.0111	516	22.6	13.2	0.0111	516	22.9	12.6	1,975	0.0155
5	3	0.0323	1497	21.9	11.3	0.0323	1497	22.3	11.6	2,116	0.0140
6	3	0.0111	516	21.9	11.3	0.0111	516	22.3	11.6	1,622	0.0150
7	3	0.0163	755	19.5	13.4	0.0163	755	19.3	8.6	2,821	0.0190
8	3	0.0113	524	17.7	12.1	0.0113	524	17.4	8.0	2,328	0.0190
9	3	0.0054	250	16.6	11.3	0.0054	250	16.5	8.0	1,693	0.0155
10	3	0.0143	600	20	7.2	0.0143	600	20	8.7	9,700	0.0417
11	2	0.0143	600	20	7.2	0.0143	600	20	8.7	6,900	0.0307
12	2	0.0190	800	20	7.2	0.0190	800	20	8.5	9,300	0.0619

Work by Qi et al. (2017a)

Work by Qi et al. (2017b)

Current work

2.8 times higher dehum. efficiency

System Modeling Approach

- **Use experimental data and other modeling approaches to simulate:**
  - **EC dehumidifier**
  - **Sensible evaporator**
- **Combine system components using a numerical model**

Conveniently solve different system configurations

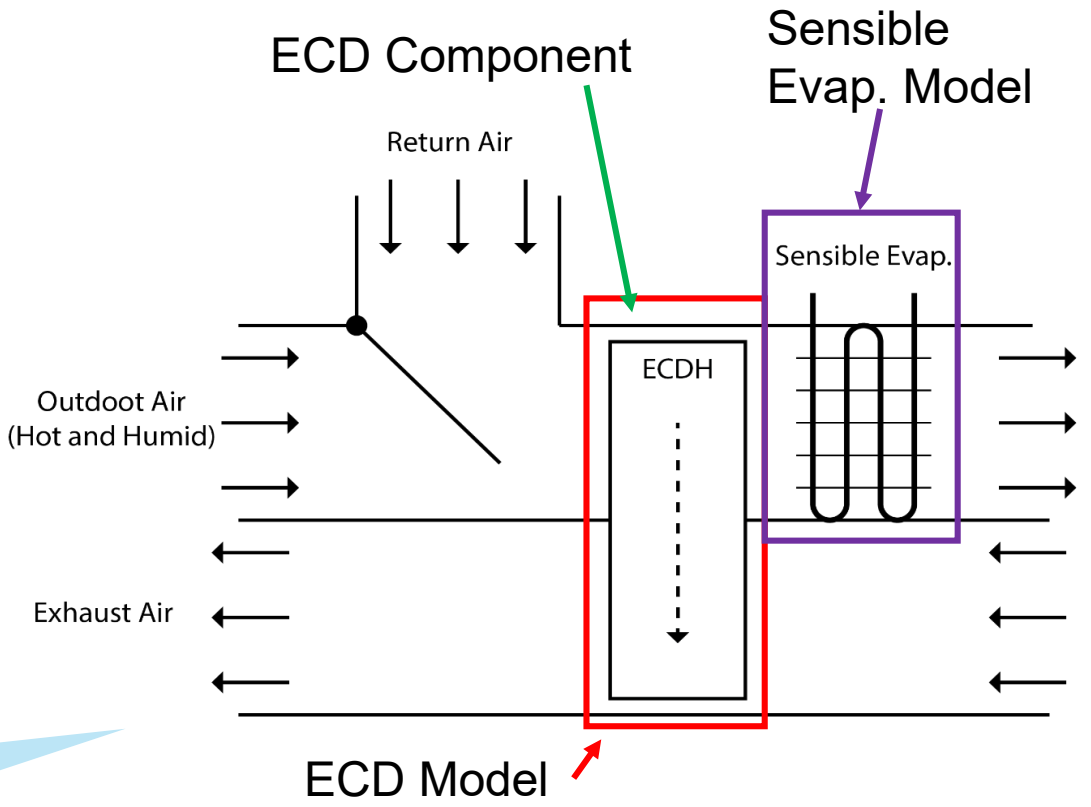

Proposed modeling approach: combine system components using independent sub-models validated by experimental data.

SSLC System Configurations

Conf. 1: 20%V, ECDin OA

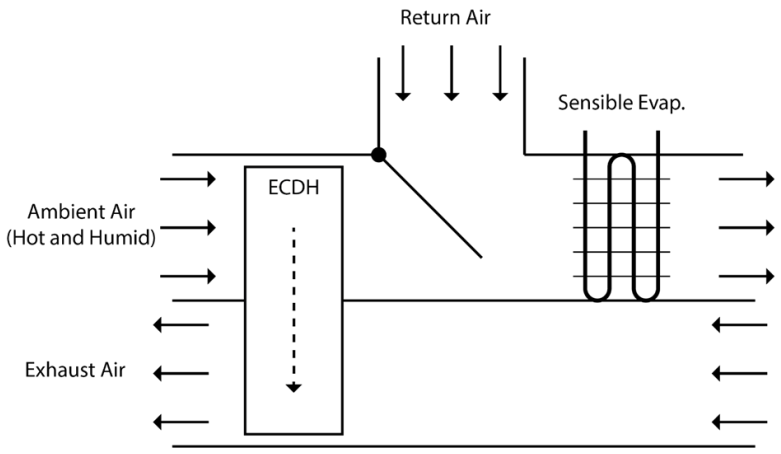

Conf. 2: 100%V, ECDin OA

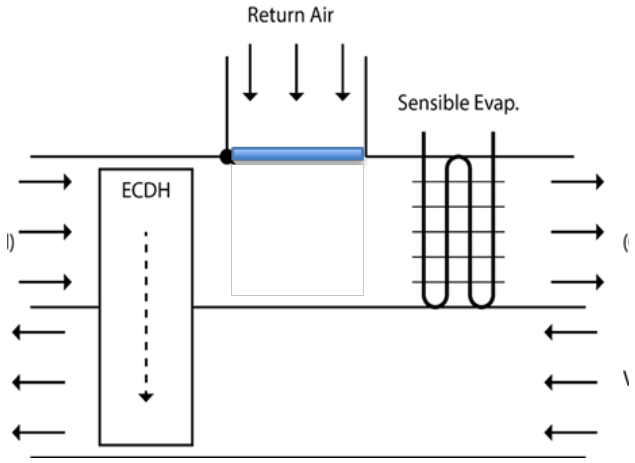

Conf. 3: 0%V, ECDin RA

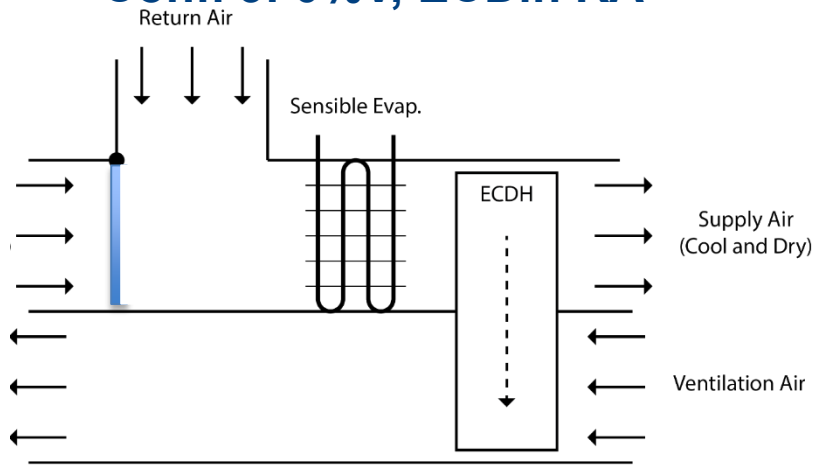

Conf. 4: 0%V, ECDin RA

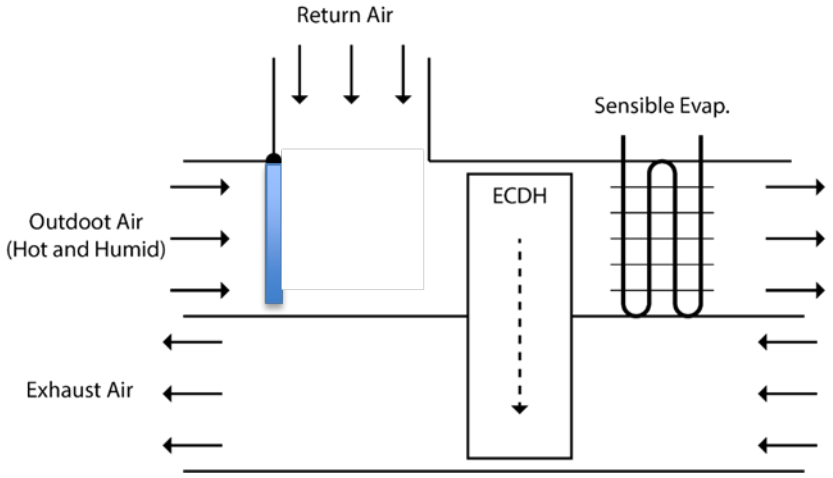

Conf. 5: 20%V, ECDin MixA

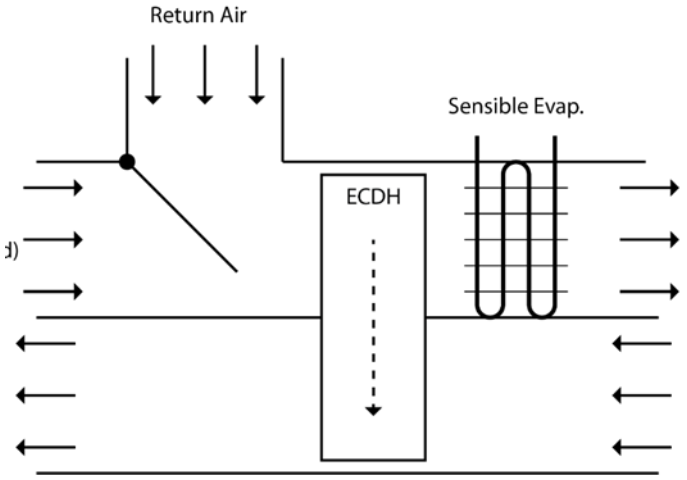

Conf. 6: 20%V, ECDin MixA

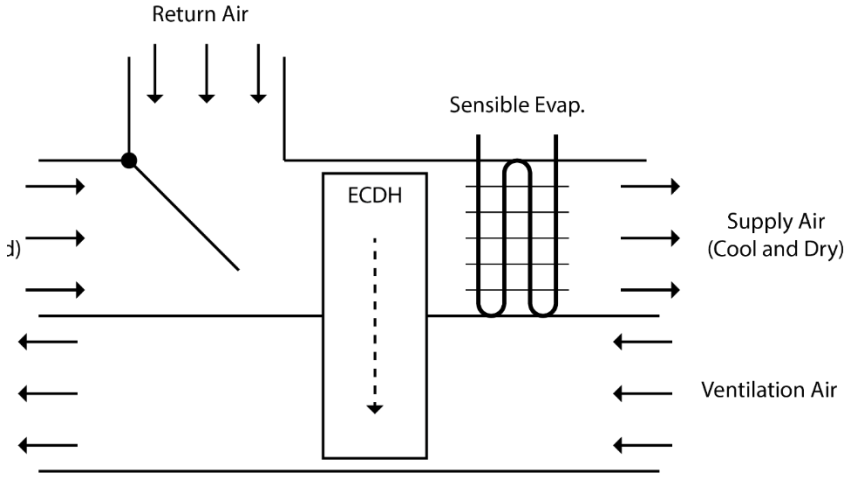

ECD Conclusions

- Dehumidification represents a significant portion of air conditioning energy requirements. Separate sensible and latent cooling using EC dehumidification may provide an energy-efficient thermal comfort solution for the hot and humid parts of the world.
- We developed several EC dehumidifiers, considering both proton exchange and anion exchange processes, and conducted experiments.
- The diffusion of the water vapor was significant in this application.
- Test results show that the dehumidification performance was increased from 0.69 $g \cdot day^{-1} \cdot cm^{-2}$ to 0.93 $g \cdot day^{-1} \cdot cm^{-2}$ when the dry oxygen flow rate is increased by the enhanced water mass transfer kinetics. The highest dehumidification efficiency achieved was 0.0619 $g \cdot J^{-1} \cdot m^{-2}$, which is 175% higher than the previous work.

Part 2: Adsorption Heat Pump

- Qian, S., K. Gluesenkamp, Y. Hwang*, R. Radermacher, H. Chun, Cyclic steady-state performance of adsorption chiller with low regeneration temperature zeolite, Energy, V. 60, pp. 517-516, 10/2013.

Adsorption Heat Pump Schematic

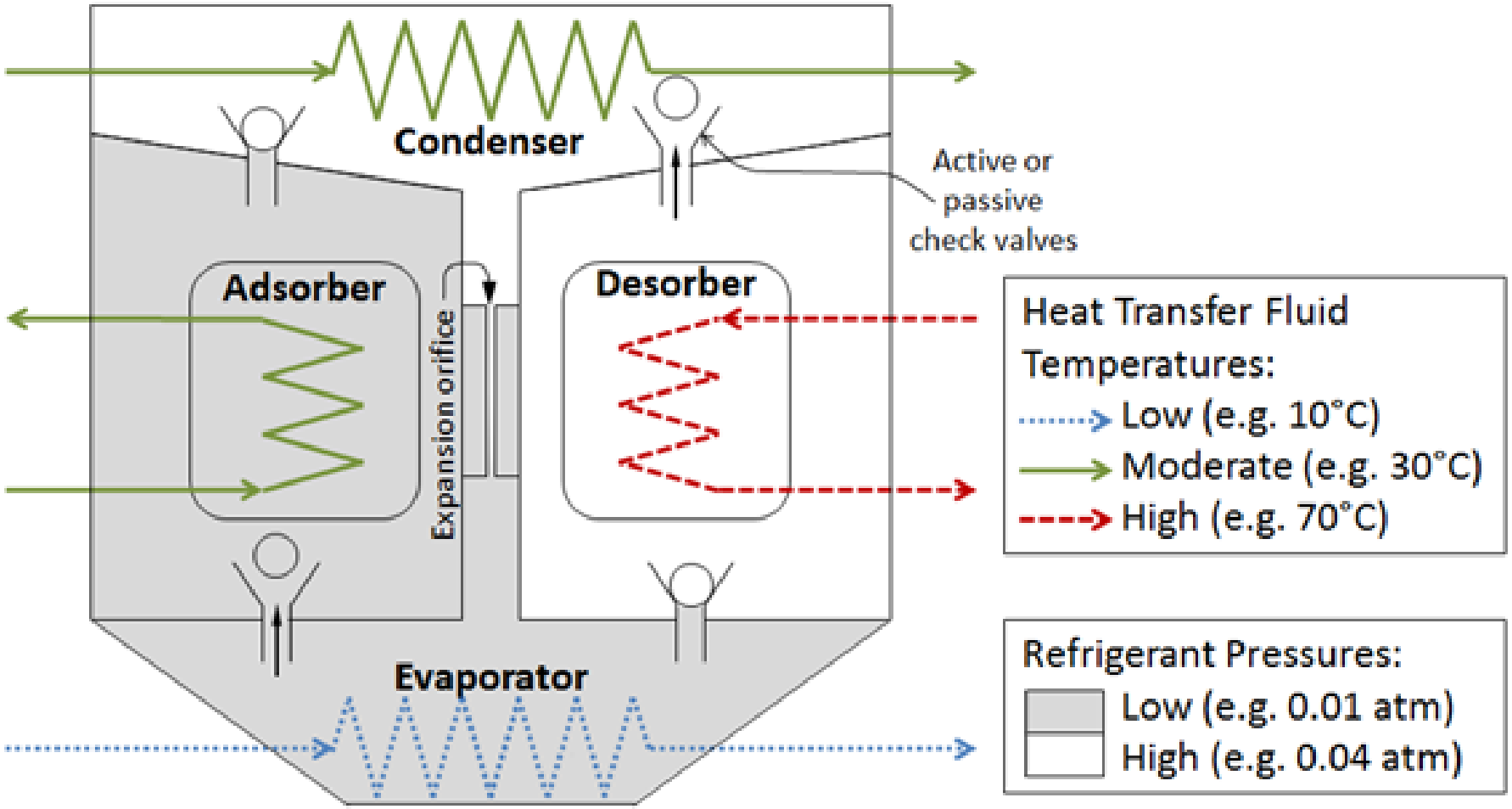

Experimental Facility

Nominal cooling capacity	3 kW
Number of adsorber HXs	2
Working pair (refrigerant/adsorbent)	water/zeolite
Adsorber HX finned-volume dimensions (excludes headers and u-tubes)	600 x 264 x 102 mm
Calculated adsorbent mass (per HX)	2.82 kg
Adsorbent substrate area (per HX)	16.7 m^2
Charge of HTF (per HX, excl. headers)	2.47 liter

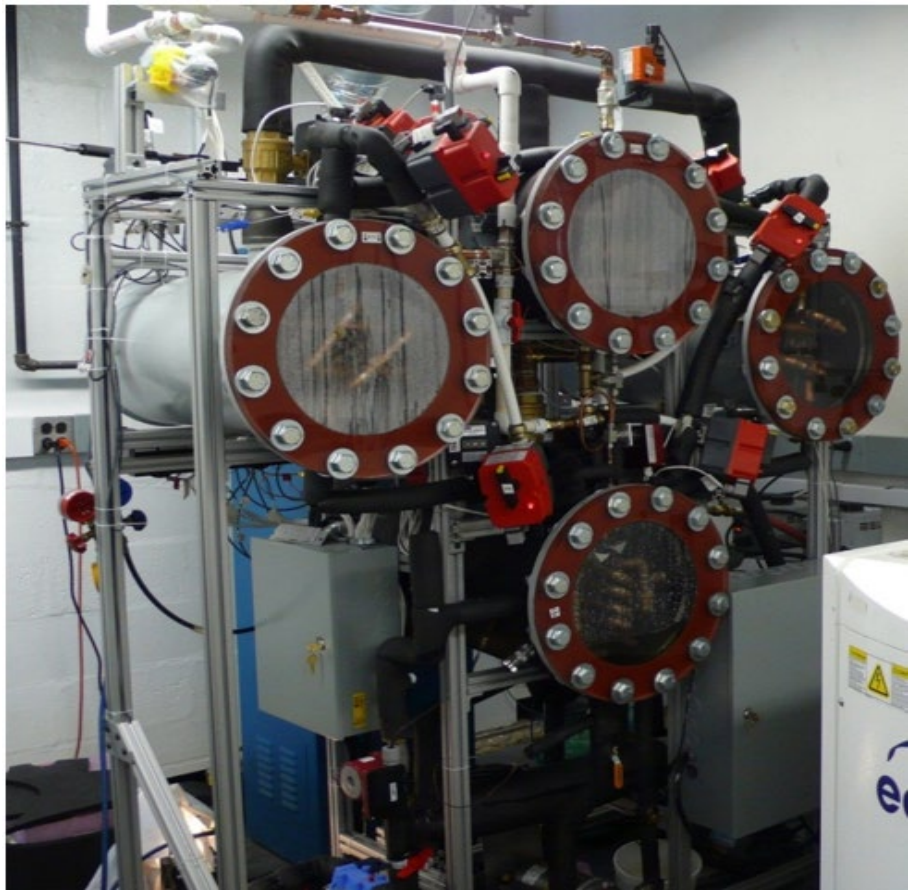

Adsorbent Heat Exchanger

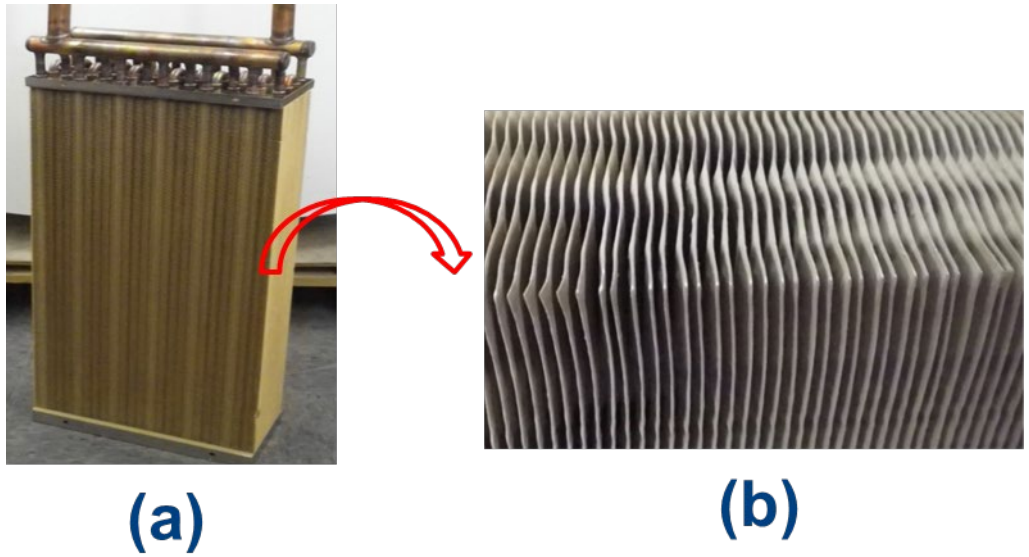

(a) Prototype of adsorber HX
(b) Close-up of adsorber HX-coated fins (1.8 mm fin spacing, 0.115 mm fin thickness, 0.25 mm zeolite coating thickness)

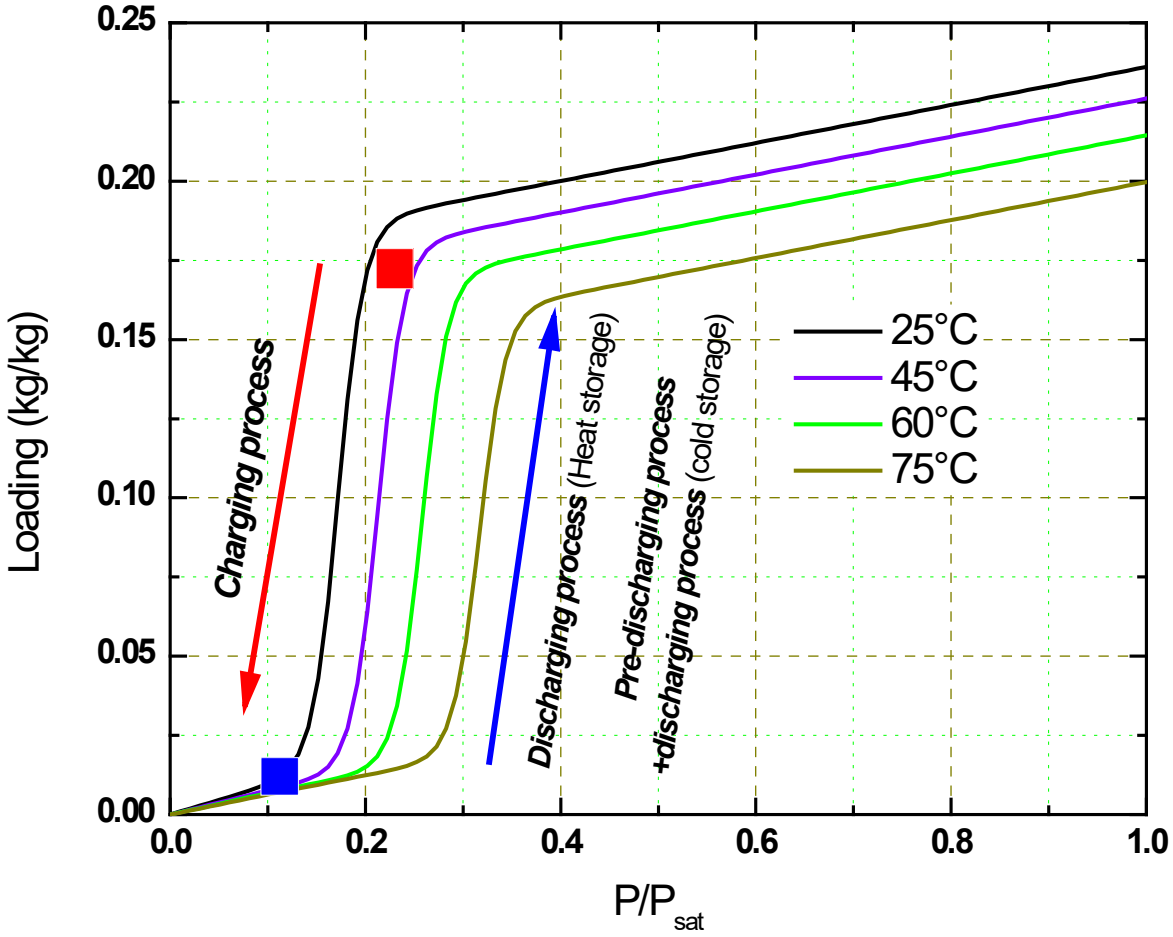

Isotherm Data of *Zeolite-H2O* (Mitsubishi Plastic Inc., Z01)

Adsorption System w/ Heat Recovery

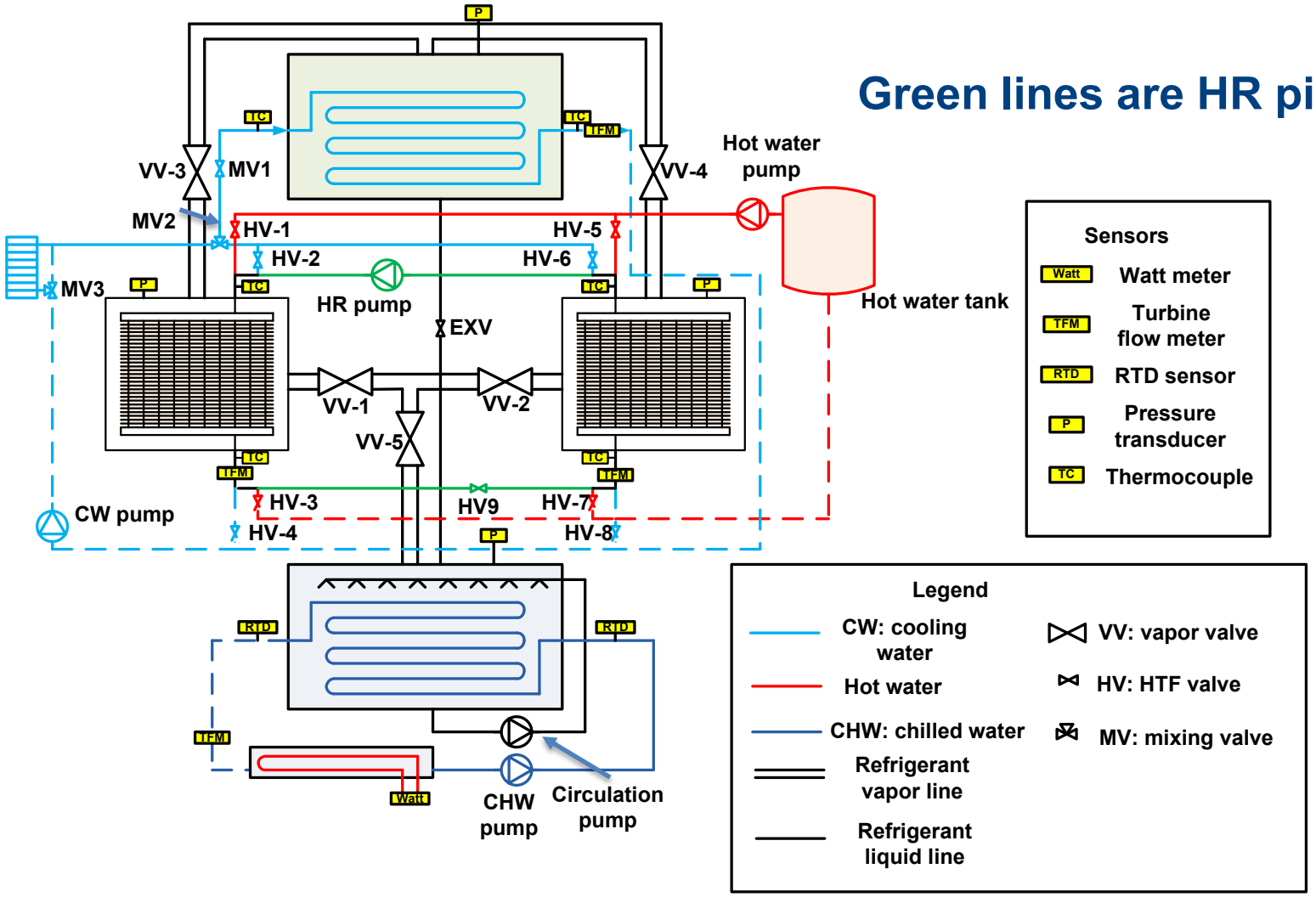

Adsorption Time Impact

- Generally, the longer the adsorption time, more refrigerant can be adsorbed
- Too long adsorption time reduces the system capacity

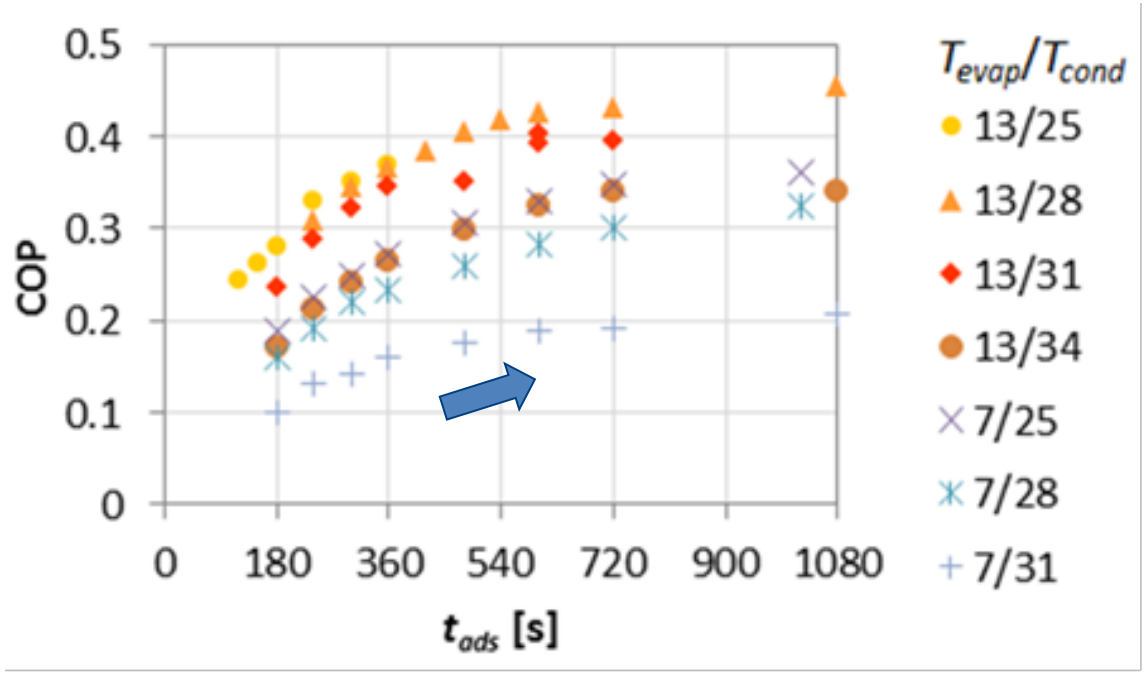

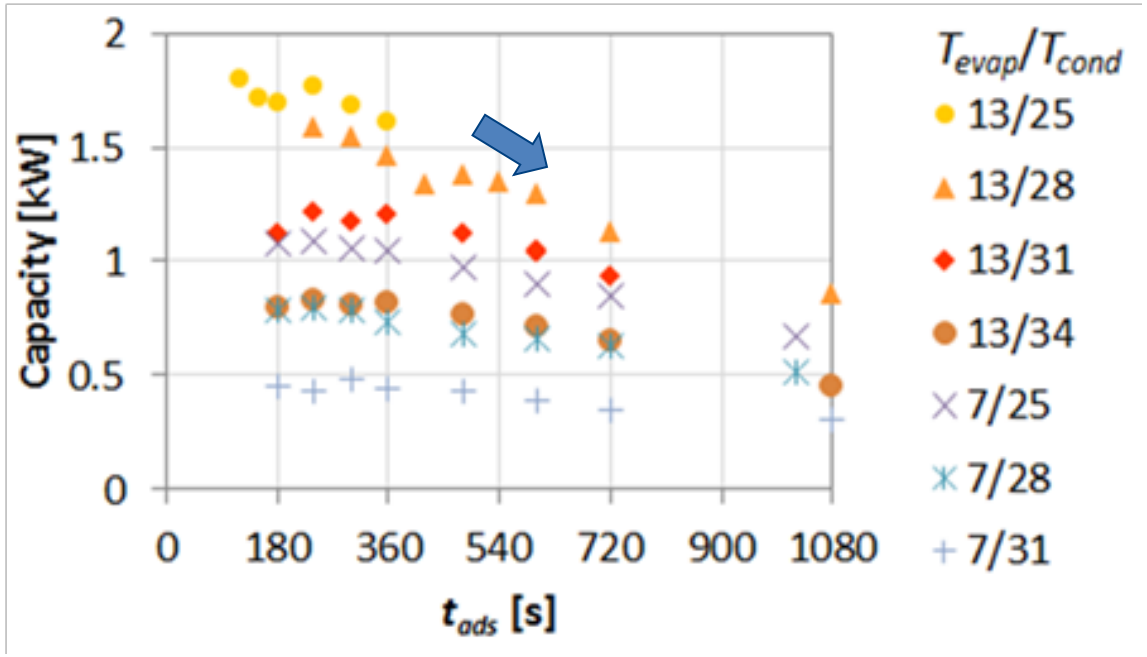

Heat Recovery Impact

- Heat transfer fluid (HTF) flows between the desorber and adsorber
- HTF in the desorber preheats the adsorber; HTF in the adsorber precools the desorber
- Heat recovery time is essential to the system COP and capacity

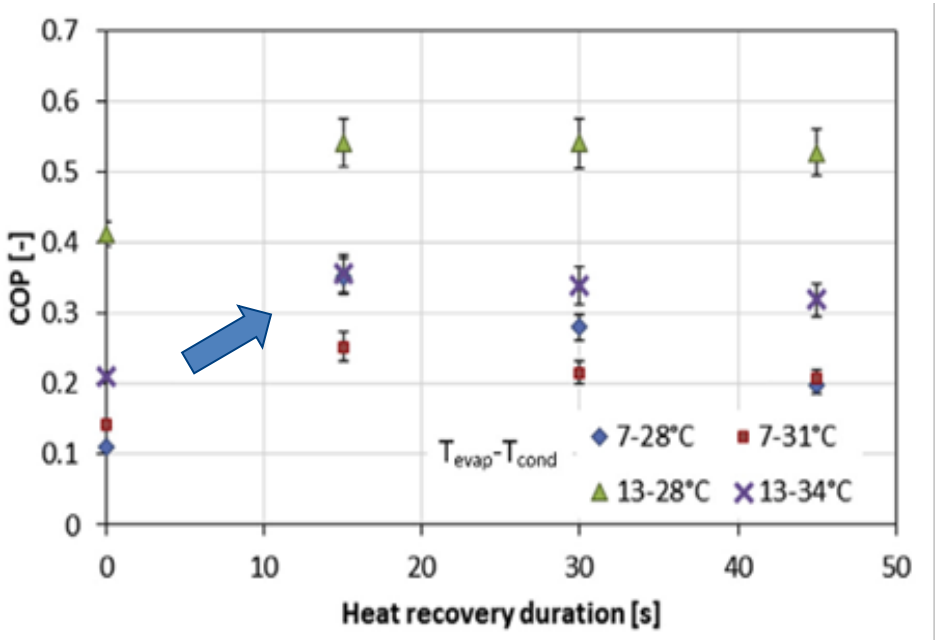

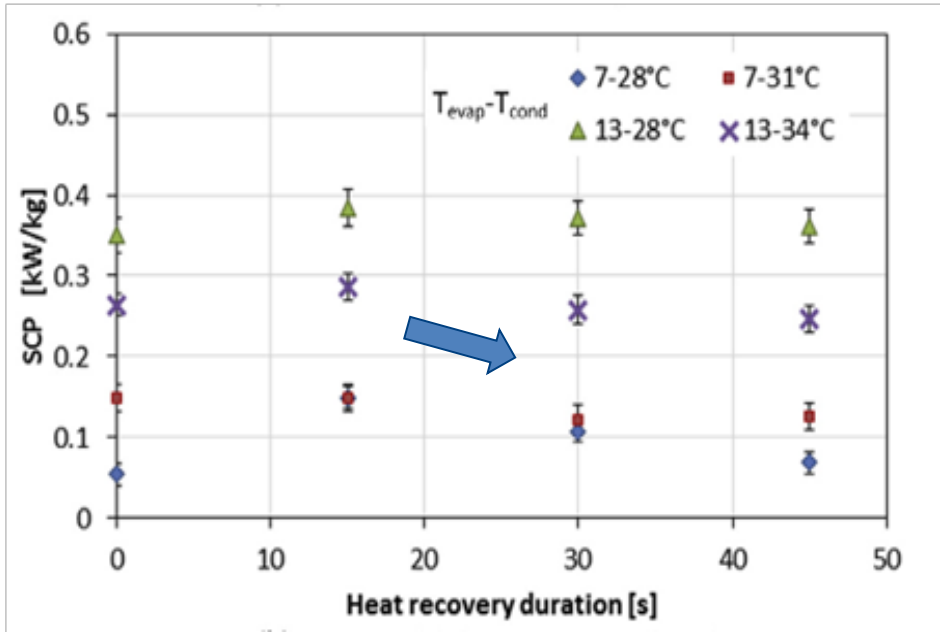

Experimental Data

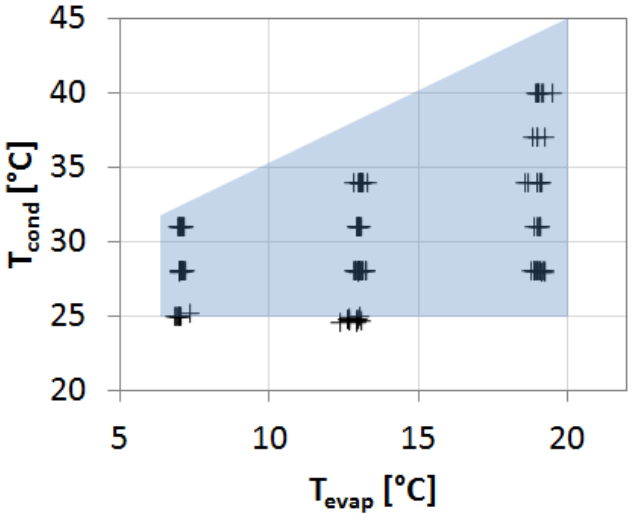

Range of temperature tested

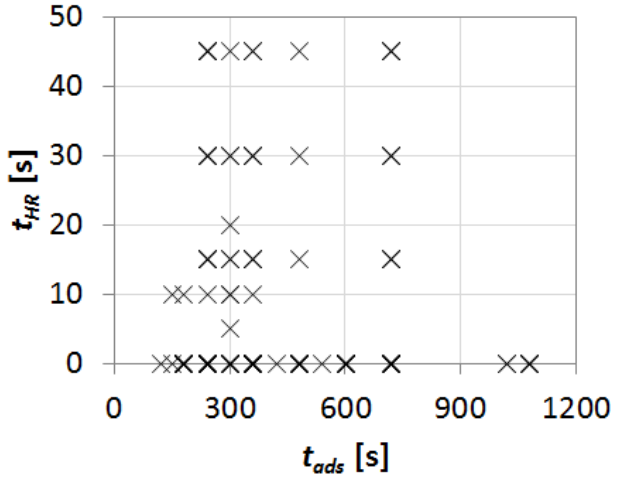

Range of time constants tested

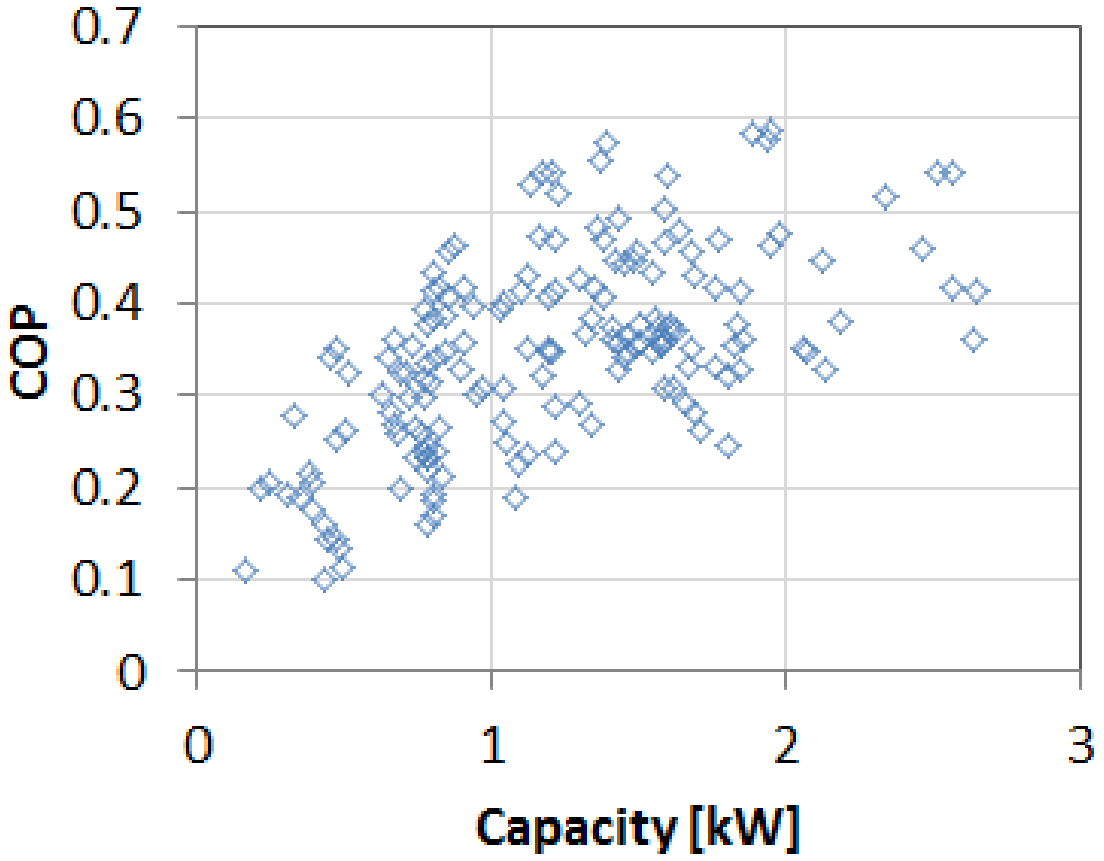

145 Measured COP and capacity

In this study, a curve-fit performance model-based feedforward control strategy is proposed from the unique chiller performance characteristics.

Part 2 Conclusions

- Synthetic zeolite/water was implemented into a 3 kW adsorption chiller test facility driven by hot water at 70°C.
- The zeolite was coated onto two fin-and-tube heat exchangers, with heat recovery employed between the two.
- Cyclic steady-state parametric studies were conducted to evaluate the chiller's performance, resulting in a cooling COP ranging from 0.1 to 0.6.

Part 3: Short-Term Adsorption Heat Storage

- **Li, G., S. Qian, H. Lee*, Y. Hwang, R. Radermacher, Experimental investigation of energy and exergy performance of short-term adsorption heat storage for residential application, Energy, V. 65, 1, pp. 675-691, 02/2014.**

- Li, G., Y. Hwang*, R. Radermacher, Experimental investigation of energy and exergy performance of adsorption cold storage for space cooling application, investigation, Int. J. of Refrigeration, V. 44, pp. 23-35, 03/2014.

TES Classification

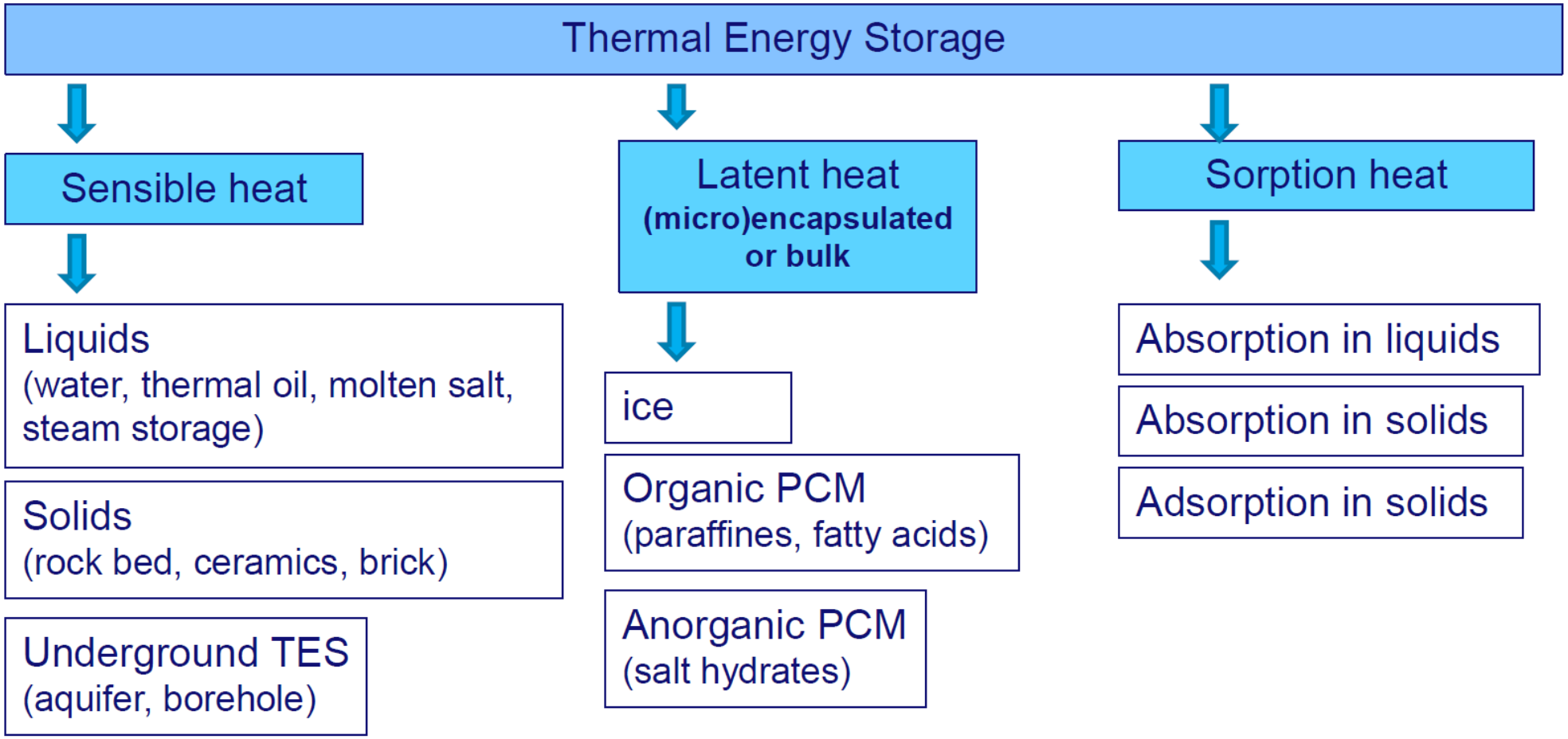

H.A. Zondg, Seasonal and daily heat storage for heating and cooling of building, TU/e Mechanical Engineering, 2012.

Sorption TES

- Relies on the physical or chemical attraction of the refrigeration gas on a liquid (absorption) or solid (adsorption) sorbent.
- Sorption TES has been suggested as a technique for a long-term storage period with limited heat loss.
- Higher energy density
- Stores energy as chemical potential, and potential does not degrade with time.

Adsorbent Heat Exchanger

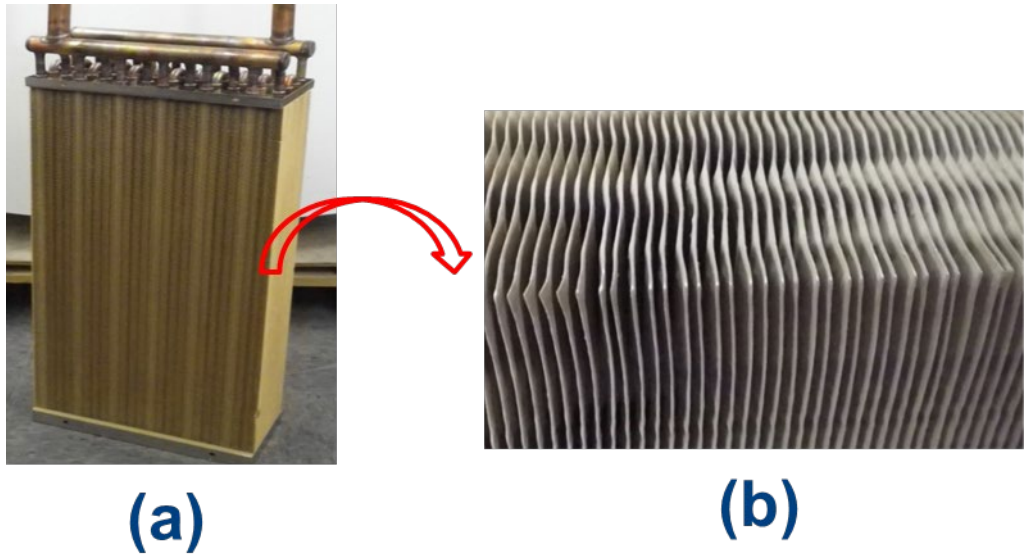

(a) Prototype of adsorber HX
(b) Close-up of adsorber HX-coated fins (1.8 mm fin spacing, 0.115 mm fin thickness, 0.25 mm zeolite coating thickness)

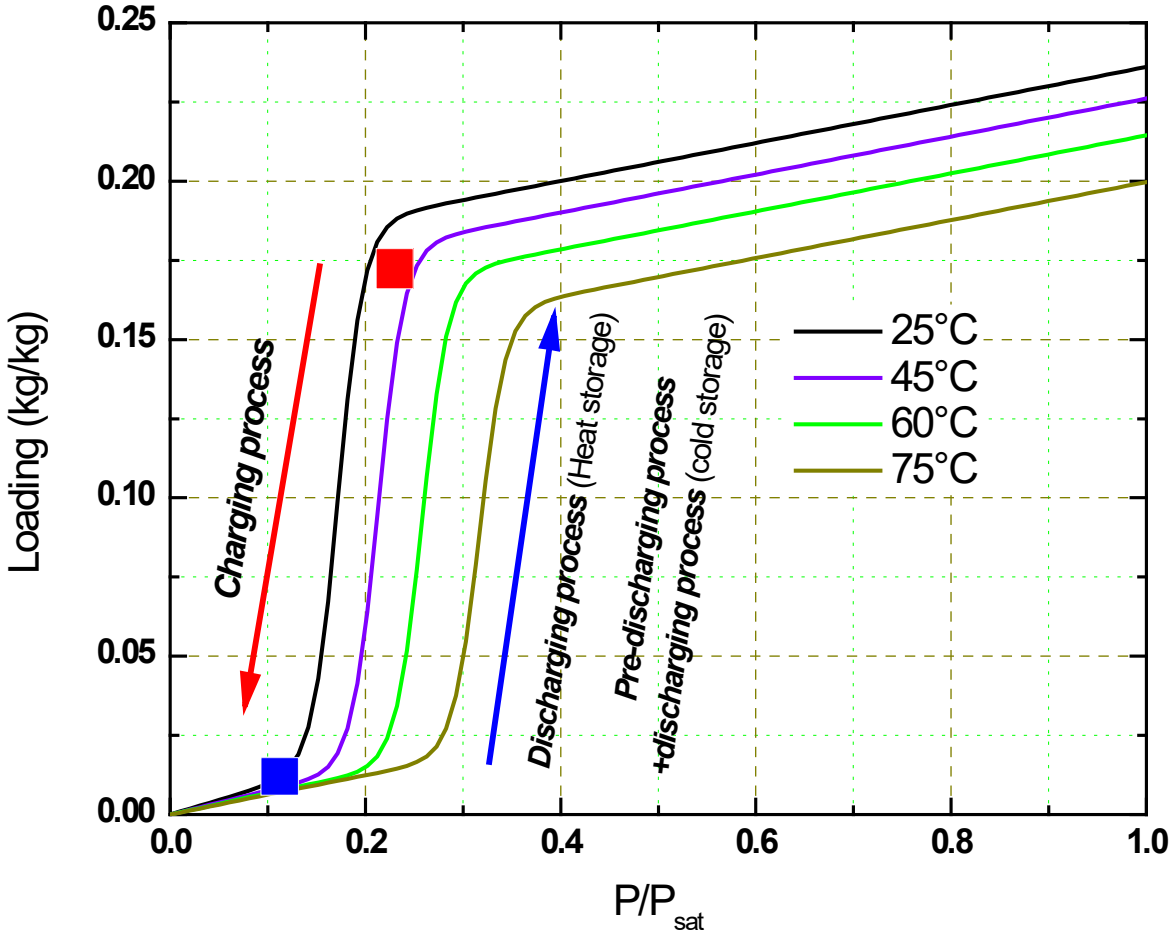

Isotherm Data of *Zeolite-H2O* (Mitsubishi Plastic Inc., Z01)

Heat Storage Test Facility

(a)

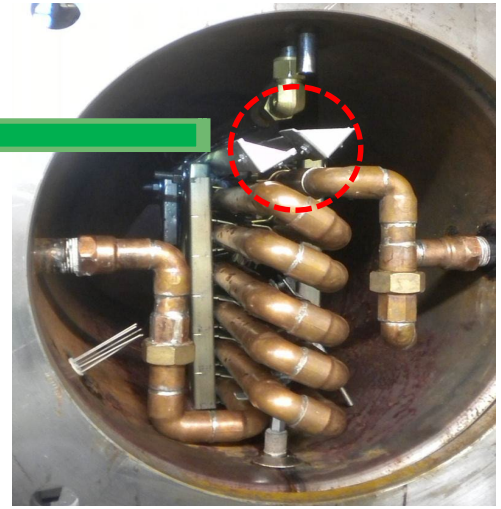

(b)

(a) Close-up of falling film distributor
(b) Condenser/evaporator

Adsorption TES Powered by Engine Waste Heat

Heat Storage Test Facility

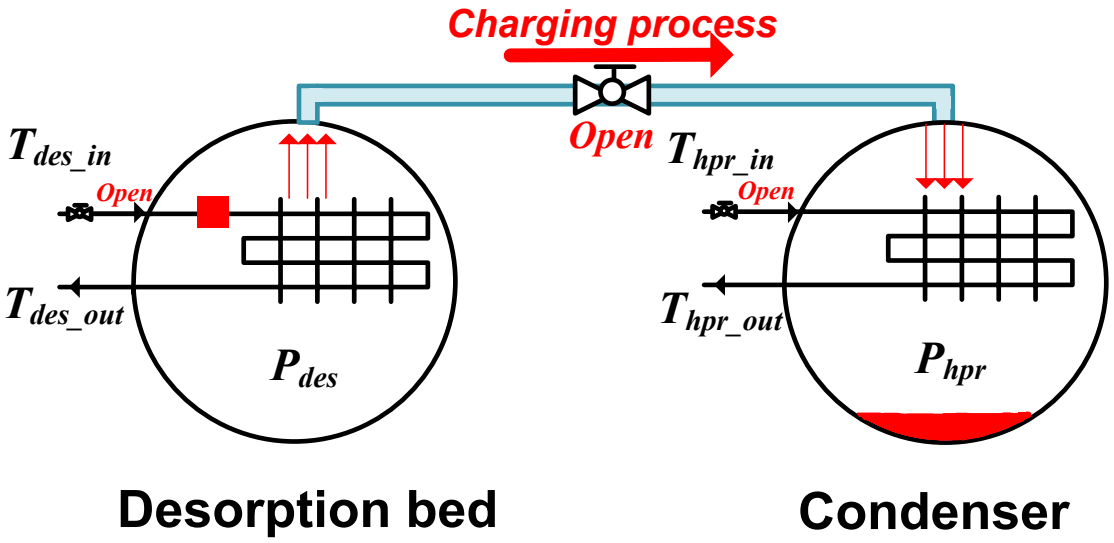

Desorption bed

Condenser

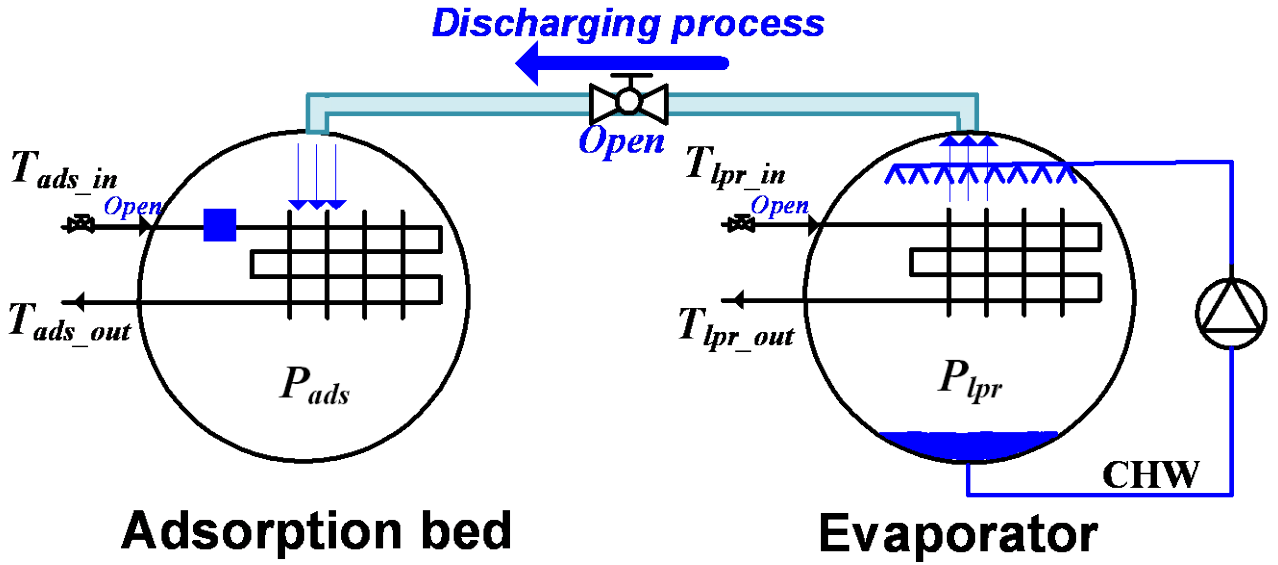

Adsorption bed

Evaporator

Cold Storage Test Facility

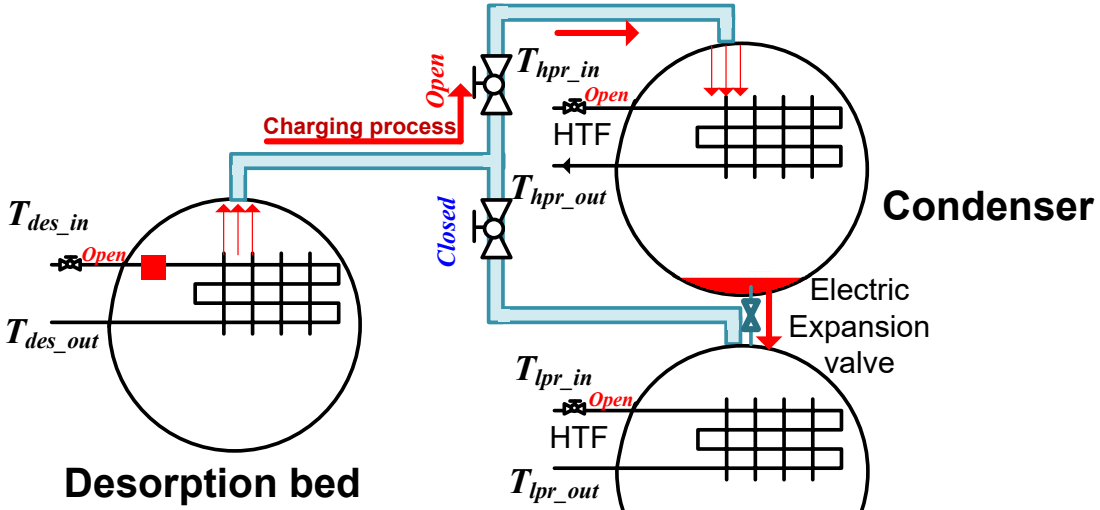

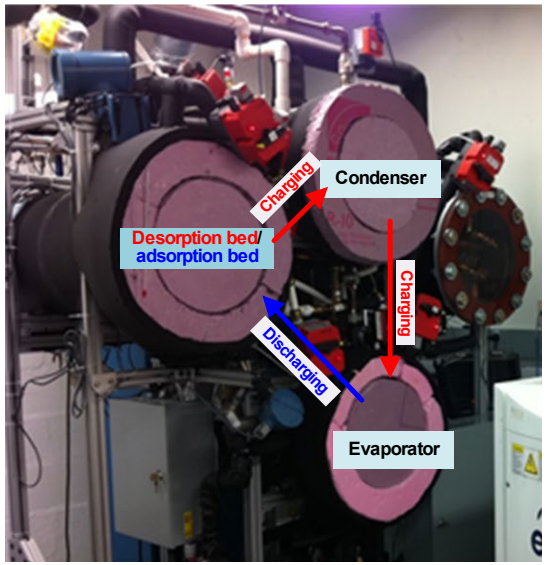

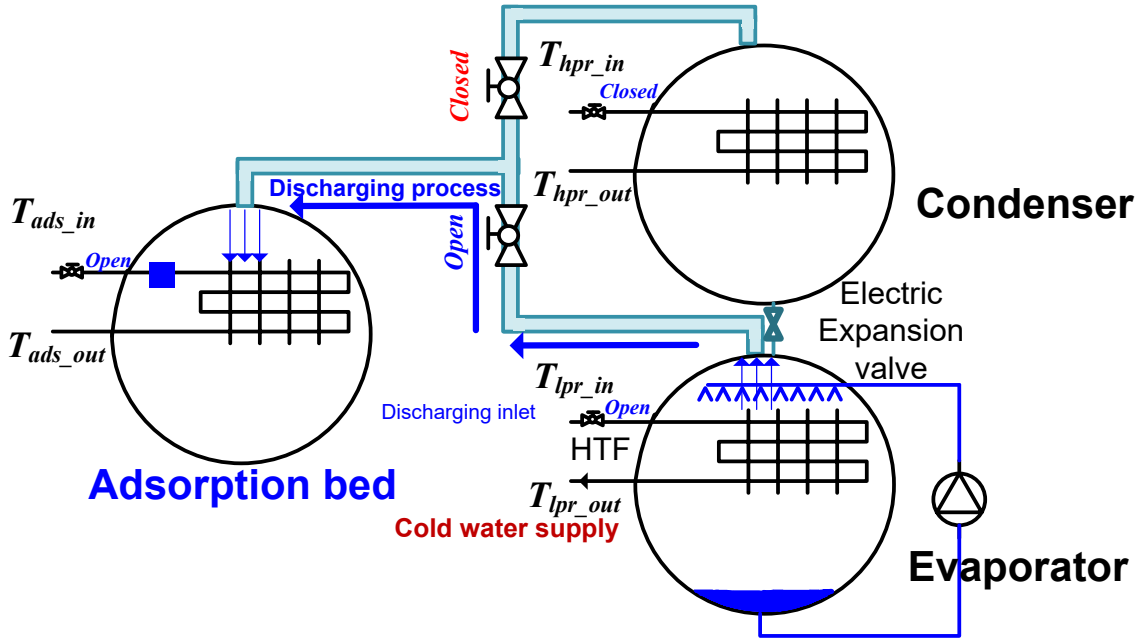

Charging and Discharging

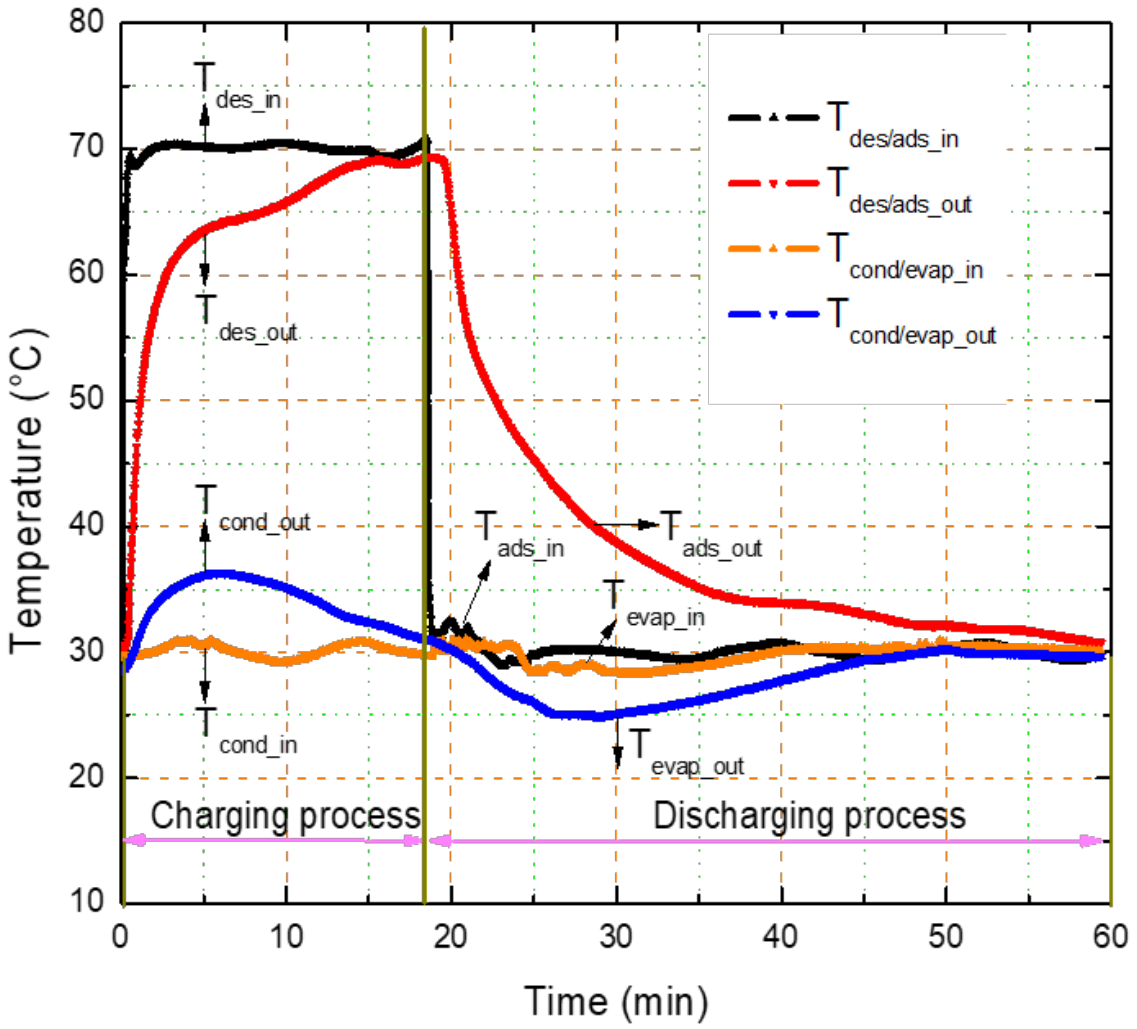

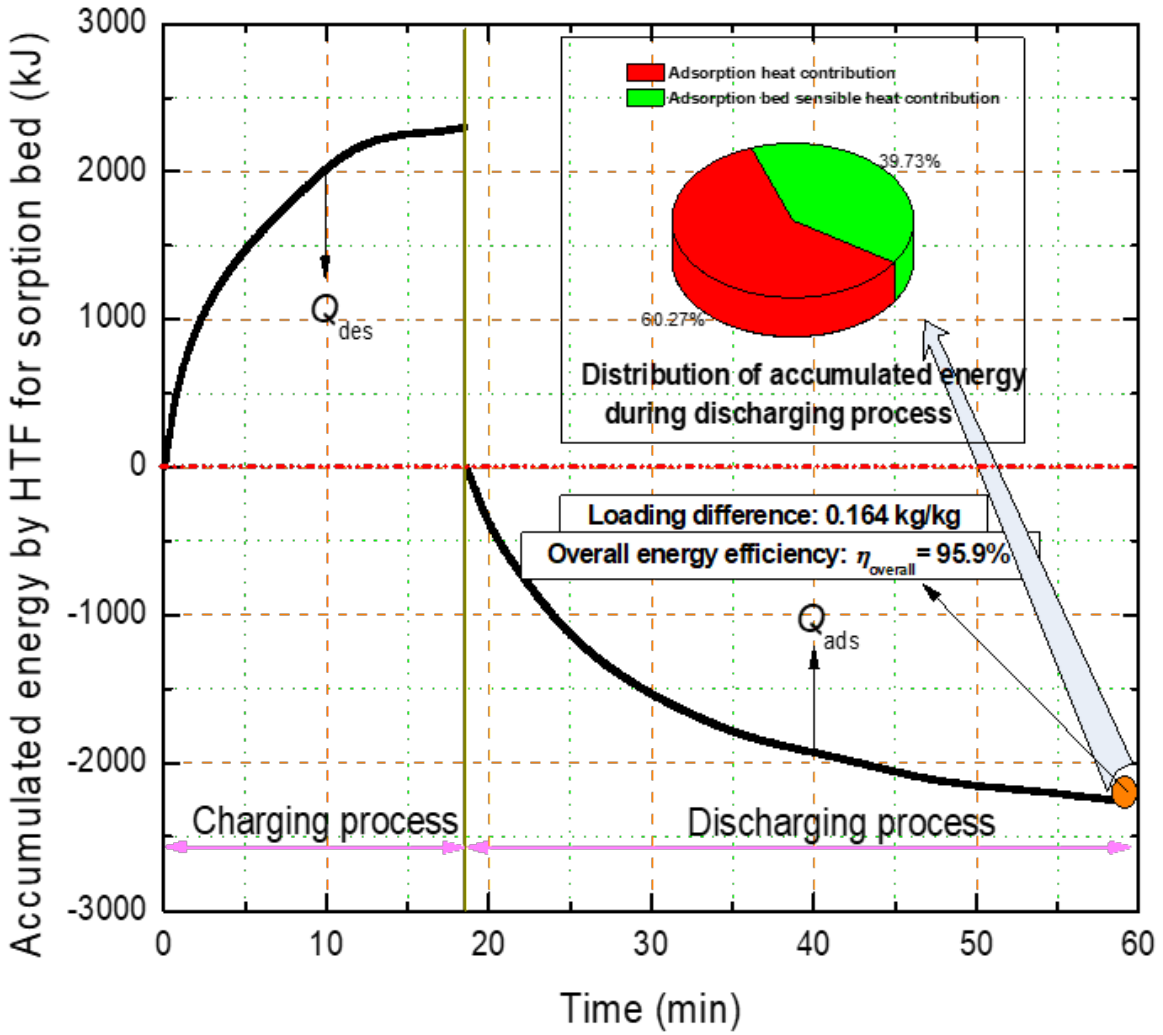

Overall Storage Performance

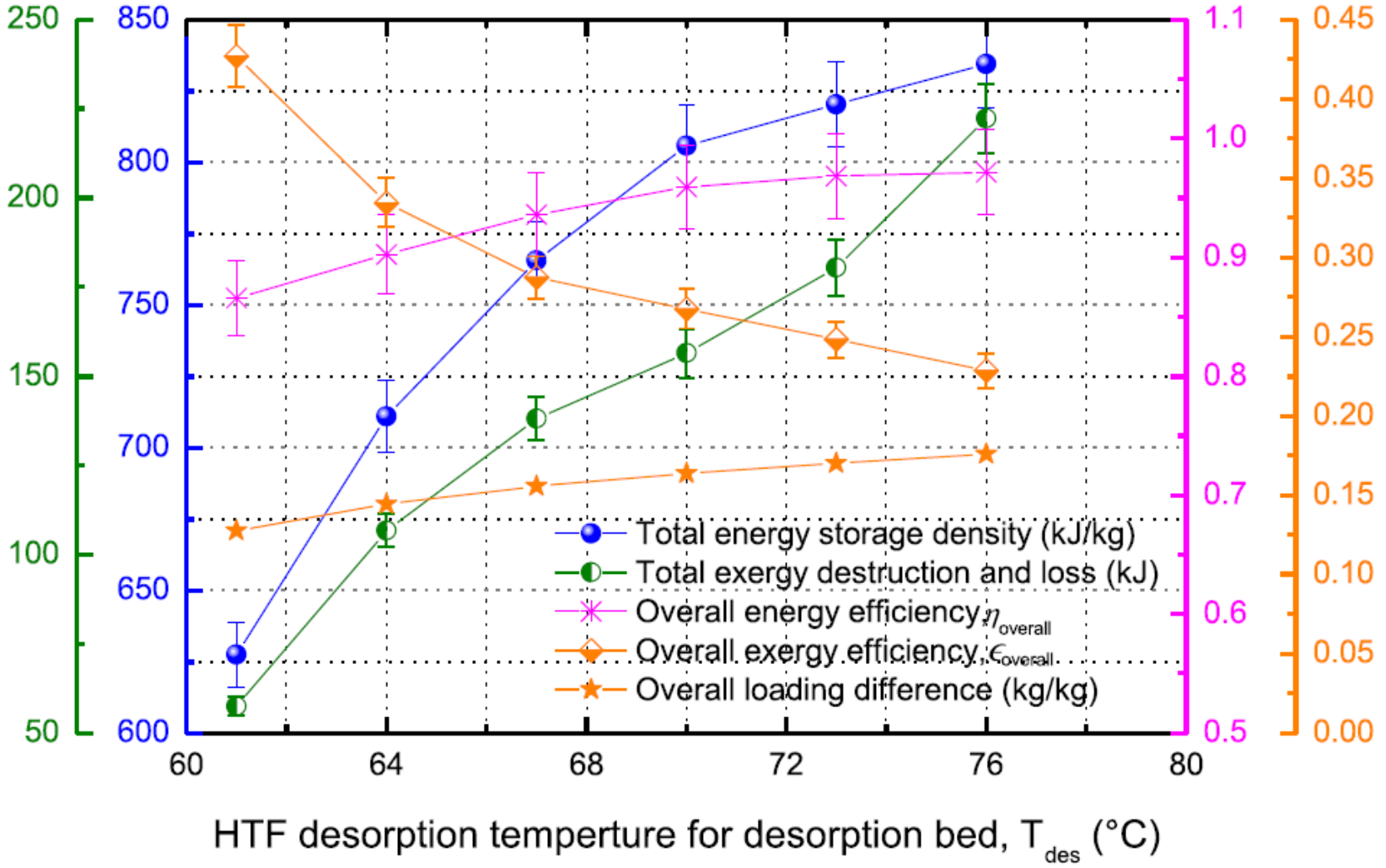

Common PCM TES Technologies

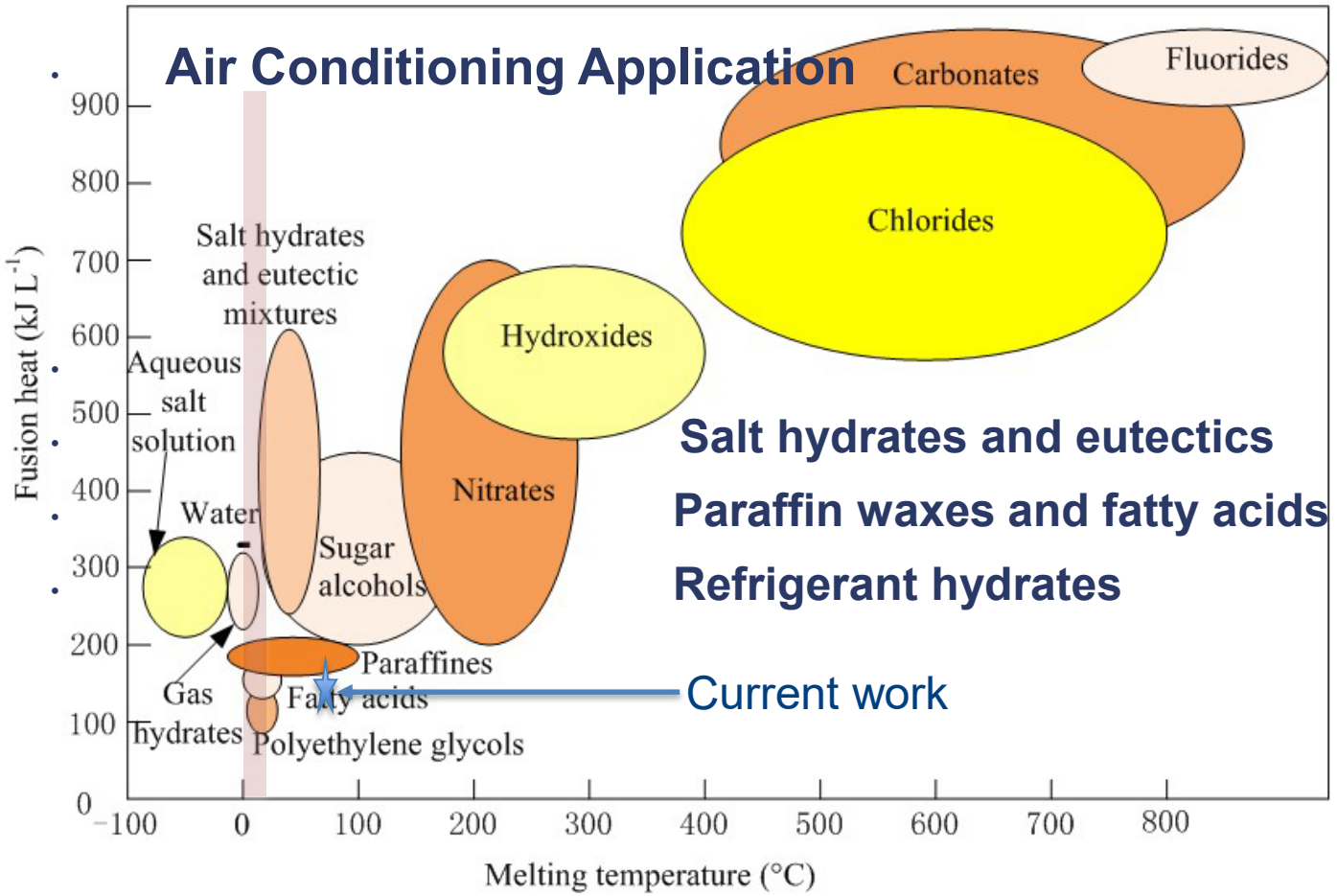

Fig. 10: Melting temperature and phase change enthalpy of existing PCMs [43]

Part 3 Conclusions

- A fin-coated heat exchanger was adopted for a sorption bed to quicken the charging process.
- When the regeneration temperature was 70°C, ambient temperature was 30°C, HTF (heat transfer fluid) inlet temperature for the adsorption bed was 30°C, results show that the heat ESD (energy storage density) was approximately 805 kJ/kg with the energy efficiency approximately 96%.

Contact: yhhwang@umd.edu

Back Up

Part 1: Desiccant Dehumidification

1. Tu, R., Y. Hwang*, Efficient configurations for desiccant wheel cooling systems using different heat sources for regeneration, Int. J. of Refrigeration, 86, 14-27, February 2018.
2. Tu, R., Y. Hwang*, T. Cao, M. Hou, H. Xiao, Investigation of adsorption isotherms and rotational speeds for low-temperature regeneration of desiccant wheel systems, Int. J. of Refrigeration, 86, 495-509, February 2018.
3. Al-Alili, A., Y. Hwang*, R. Radermacher, Performance of a desiccant wheel cycle utilizing new zeolite material: Experimental investigation, Energy, V. 81, pp. 137-145, March 2015.
4. **Cao, T., H. Lee, Y. Hwang*, R. Radermacher, Experimental Investigation on Thin Polymer Desiccant Wheel Performance, Int. J. of Refrigeration, V. 44, pp. 1-11, 08/2014.**

Introduction

- Desiccant wheel (DW) is widely used in the advanced cooling system and dehumidification process.
- The current standard available for DW testing is *ANSI/ASHRAE Standard 139-2007 "Method of Testing for Rating Desiccant Dehumidifiers Utilizing Heat for the Regeneration Process*".
- Most experimental studies were conducted with silica gel at high regeneration temperatures.
- Studies on polymer desiccant material are limited.
- Studies on DWs with thicknesses below 100 mm are rare.

Introduction of Components

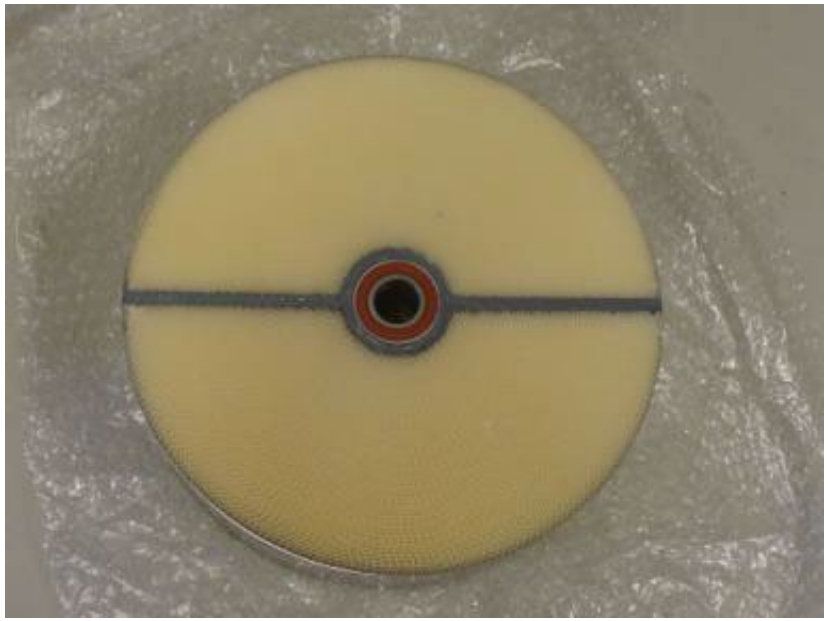

Desiccant wheel (DW)

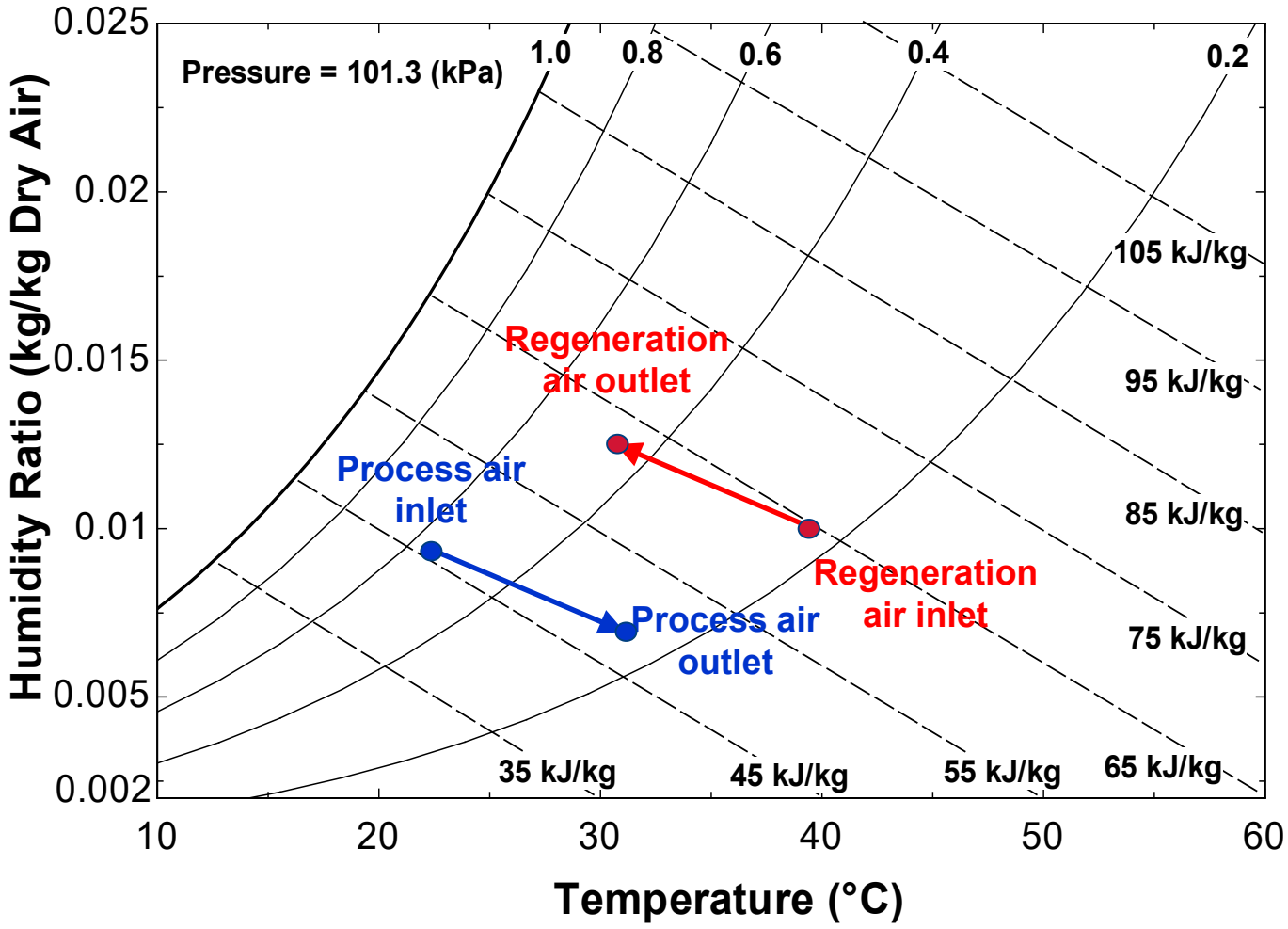

Polymer Desiccant

Lee, D.Y. (2012) introduced a novel poler desiccant by ion modification of polyacrylic acid sodium salt.

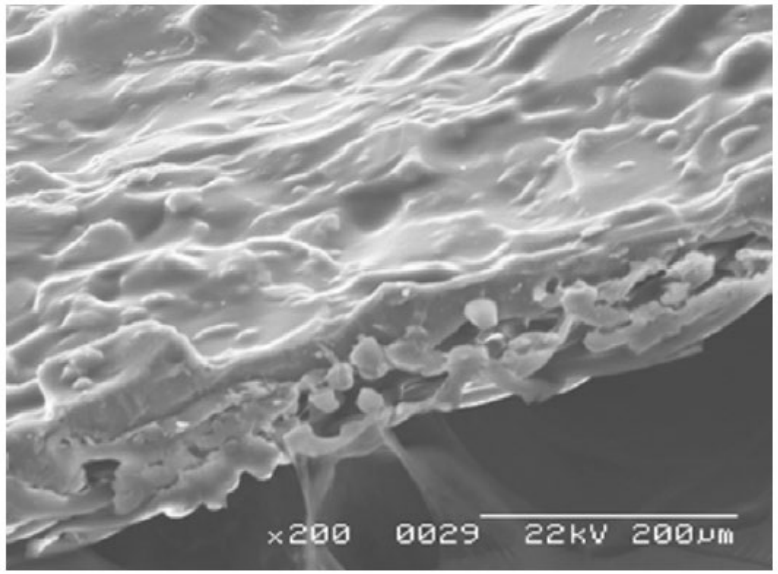

Fig. 1 – SEM picture of the super desiccant polymer coating.

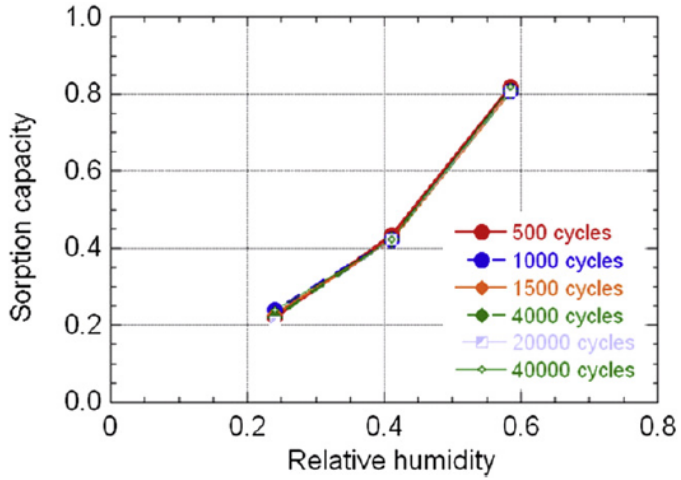

ig. 13 – Sorption capacity variation of SDP rotor sample luring 40,000 cycles of dehumidification and regeneration.

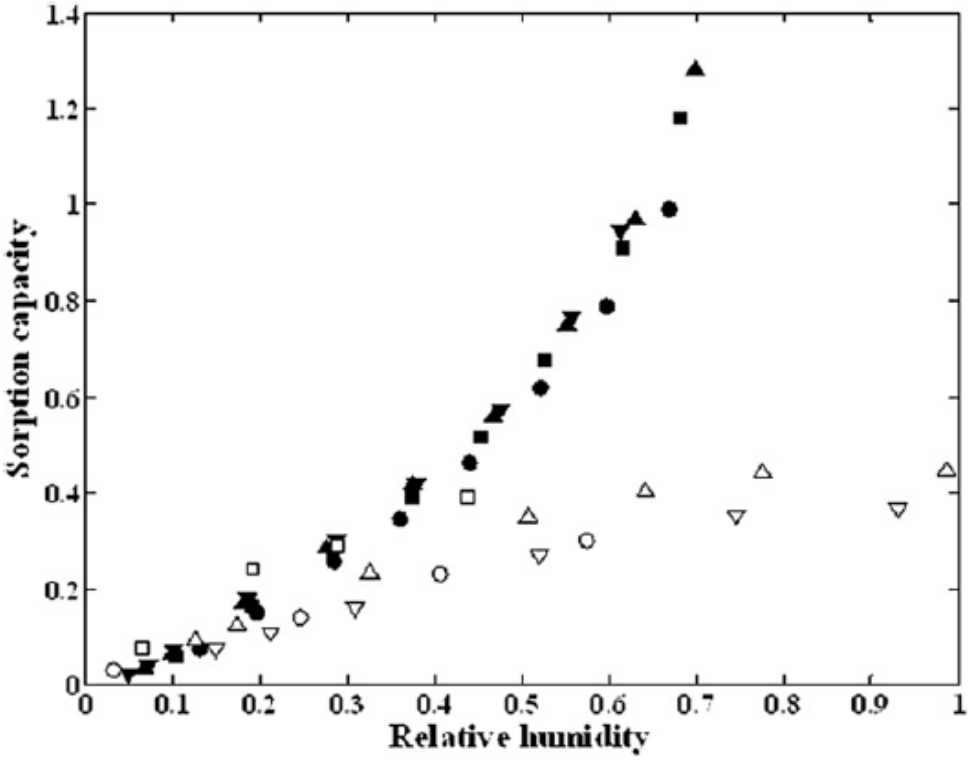

Fig. 5 – Isotherms of water vapor on silica gel (○, 50 °C, (Xia et al., 2008)), lithium chloride-silica gel composite adsorbent (□, 50 °C, (Gong et al., 2010)), type A silica gel (▽, 30 °C, (Chua et al., 2002)), type RD silica gel (△, 30 °C, (Chua et al., 2002), SDP (●, 30 °C), SDP (■, 40 °C), SDP (▲, 50 °C), SDP (▼, 60 °C).

https://doi.org/10.1016/j.ijrefrig.2012.07.009

Experimental Setup

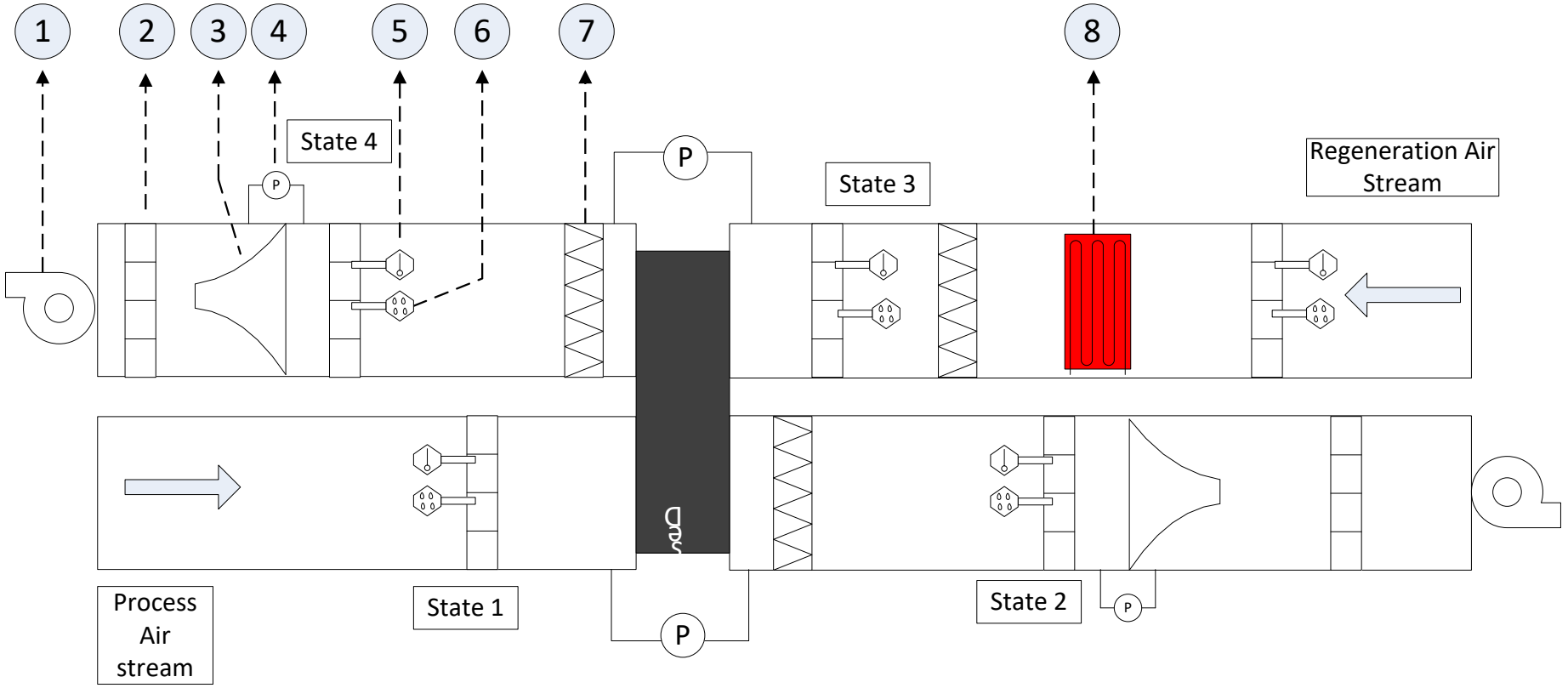

Schematics for polymer desiccant wheel testing system

(1) Fans; (2) Straightener; (3) Nozzles; (4) Differential pressure transducers; (5) Thermocouple grids; (6) Humidity sensors; (7) Air mixers; (8) Electric heaters.

System Designed with **ANSI/ASHRAE 41.2-1987 (RA 92),** Standard Methods for Laboratory Airflow Measurement

Experimental Setup (continued)

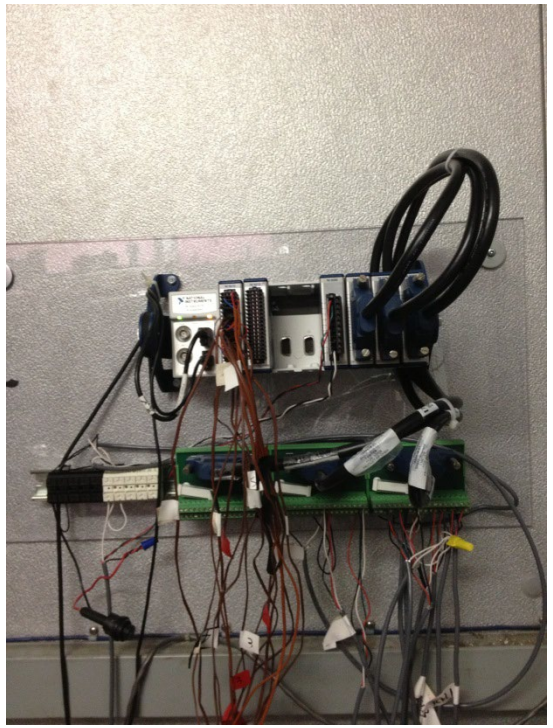

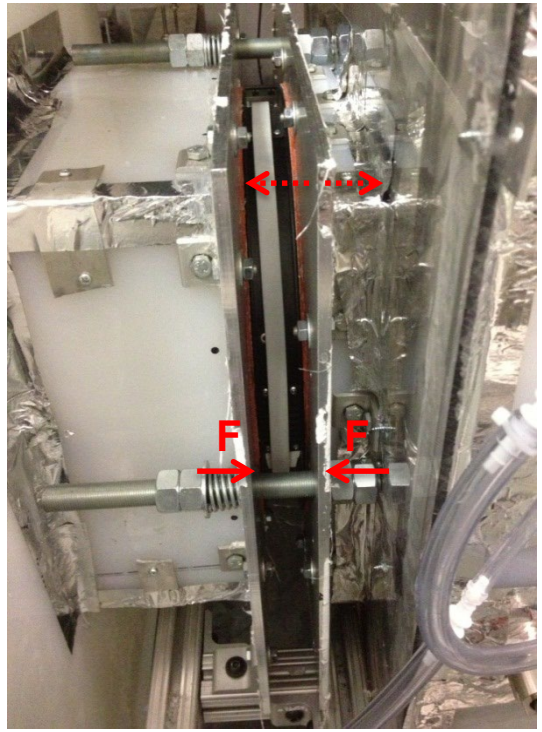

Overview of testing system (left); Data acquisition system (middle); Desiccant wheel assembly (right)

Heat Pump Desiccant Unit

- **Heating season:**
  - **Using only outdoor and return air moisture to humidify the indoors during the ventilation**
  - **Does not require additional water sources**

Air-side:
Two fans (supply & exhaust) at the SA & EA outlets

Refrigerant-side:
One hermetic compressor, two heat exchangers covered with adsorption material (AHX), expansion valve, and a 4-way valve

Dimensions: 1300x1000x450 mm, Weight: 155 kg, Design air flow rate = 500 m^3/h

HPD Operations

HPD operates in cycle during the dehumidification mode

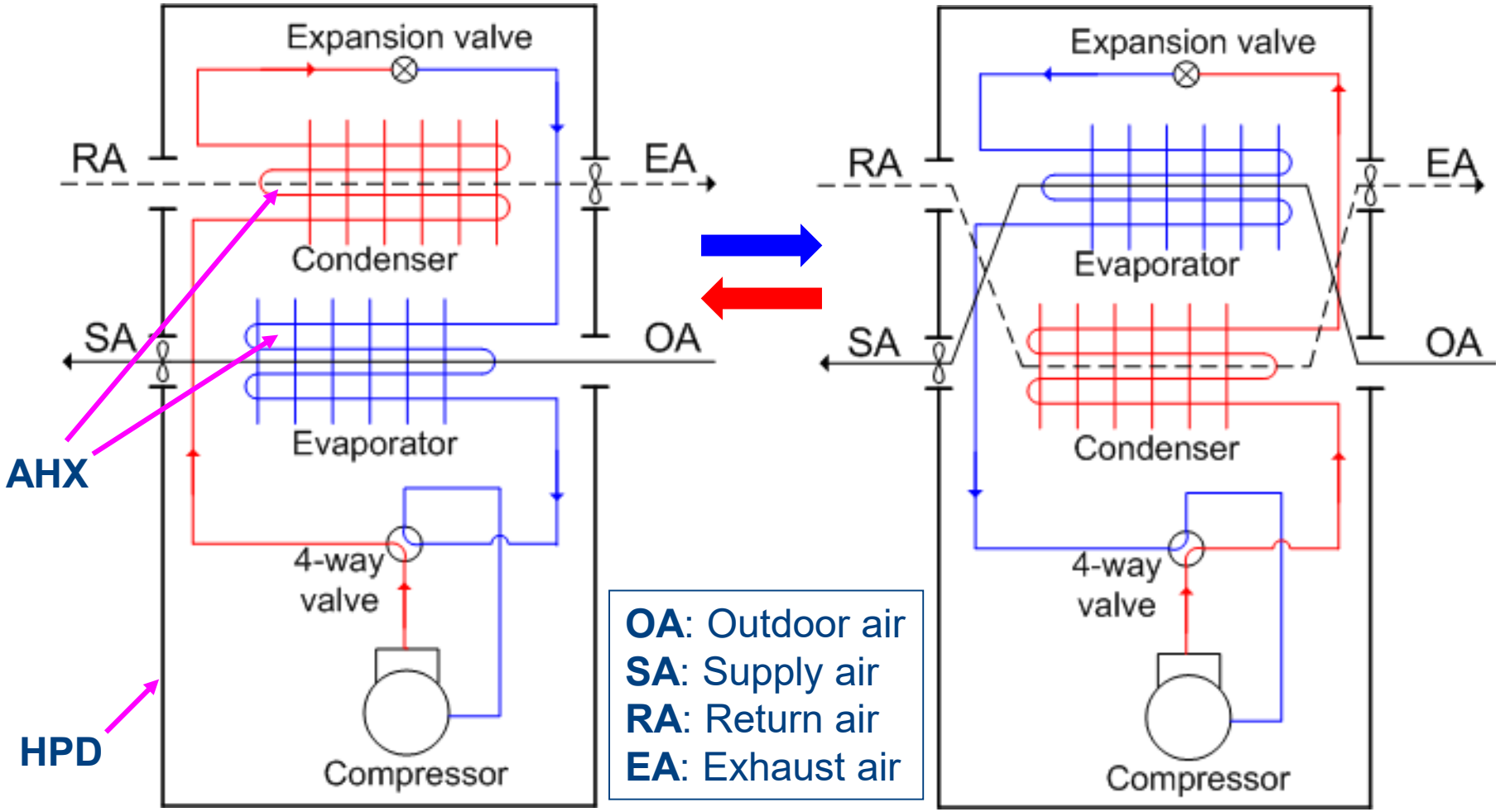

HPD Operations

HPD operates in cycle during the humidification mode

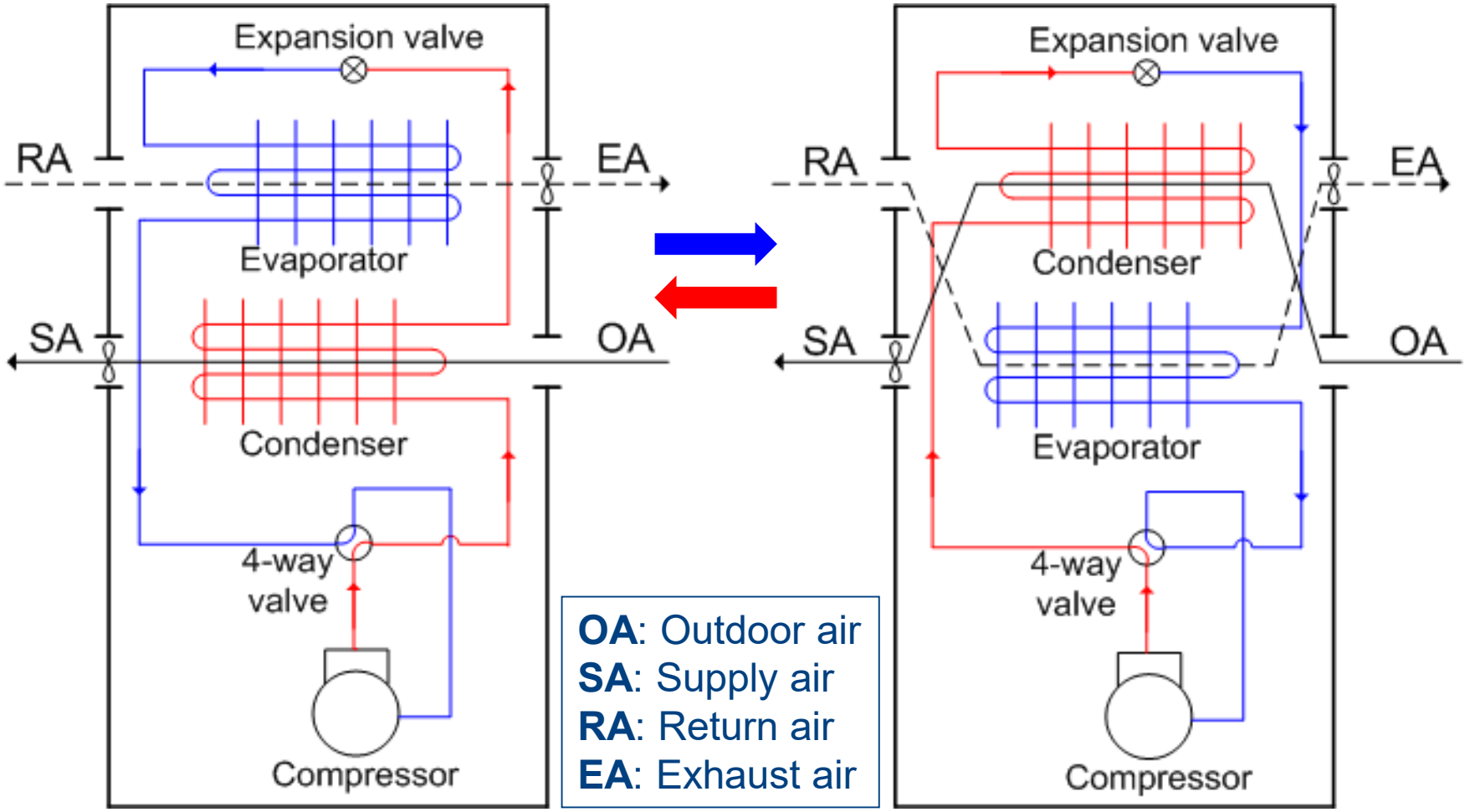

HPD Performance

Cooling & Dehumidification Mode

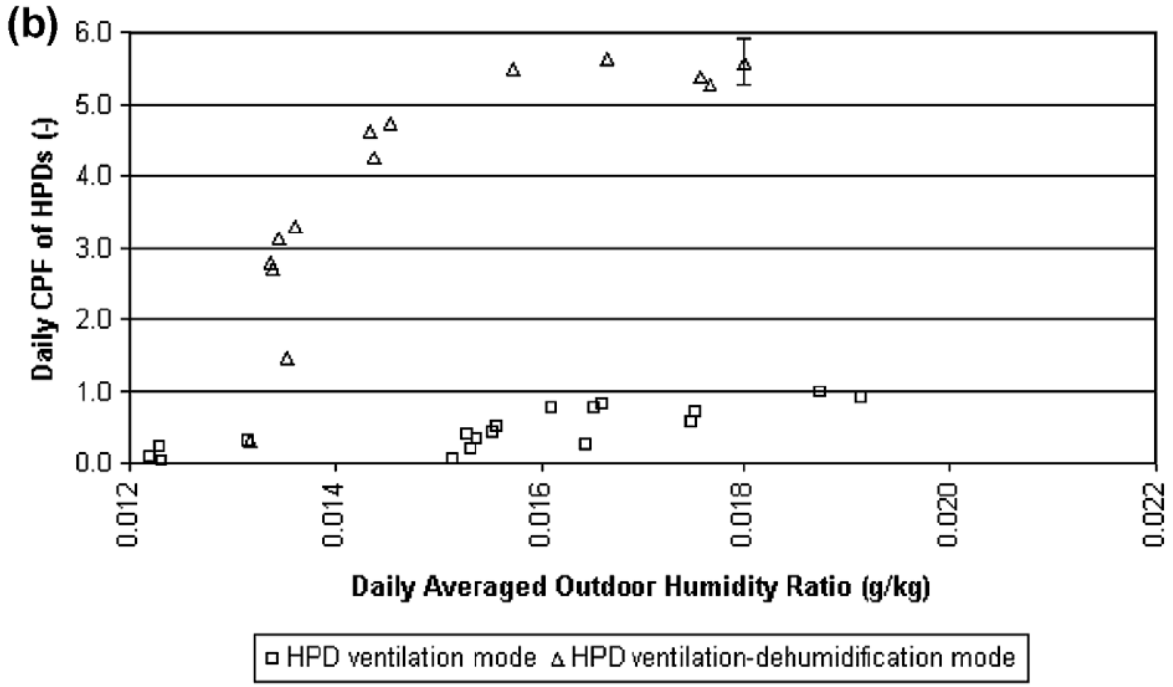

Heating & Humidification Mode

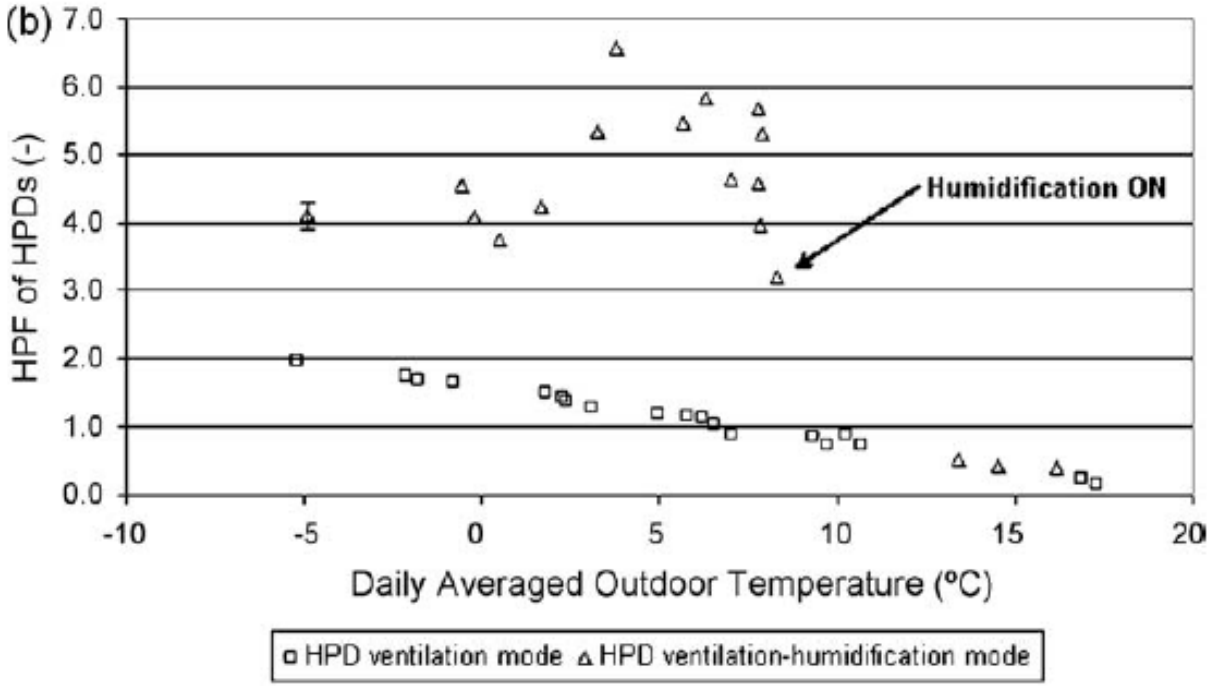

HPD Performance

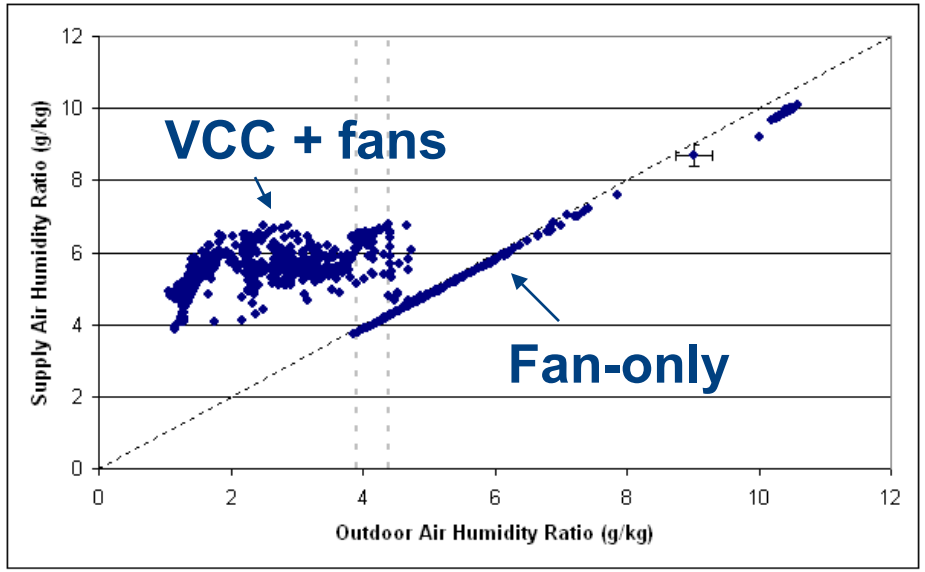

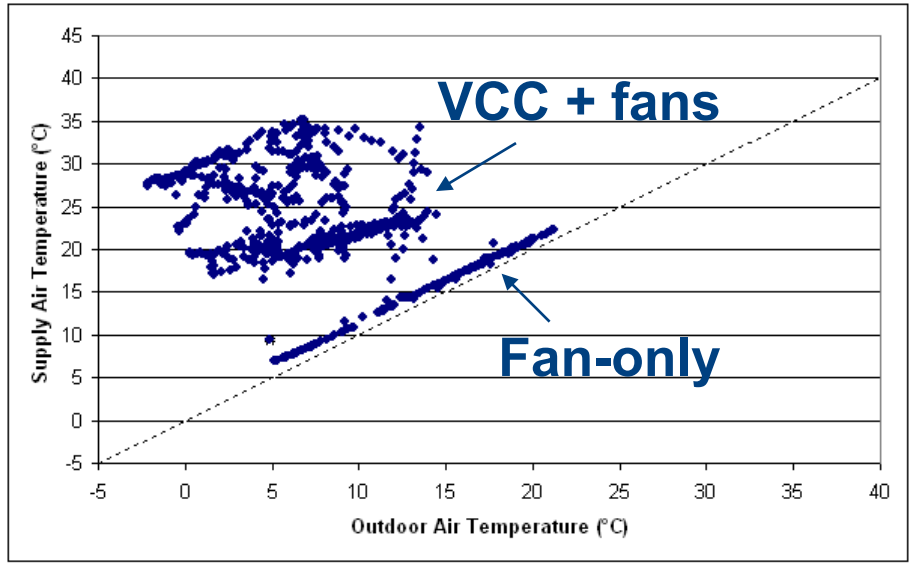

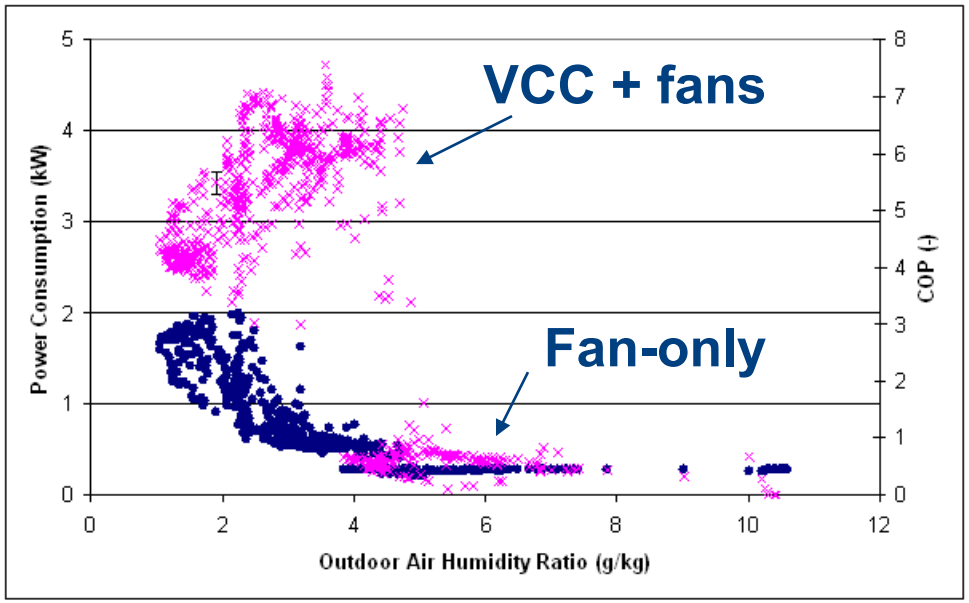

VCC: Vapor compression cycle

HPD Performance

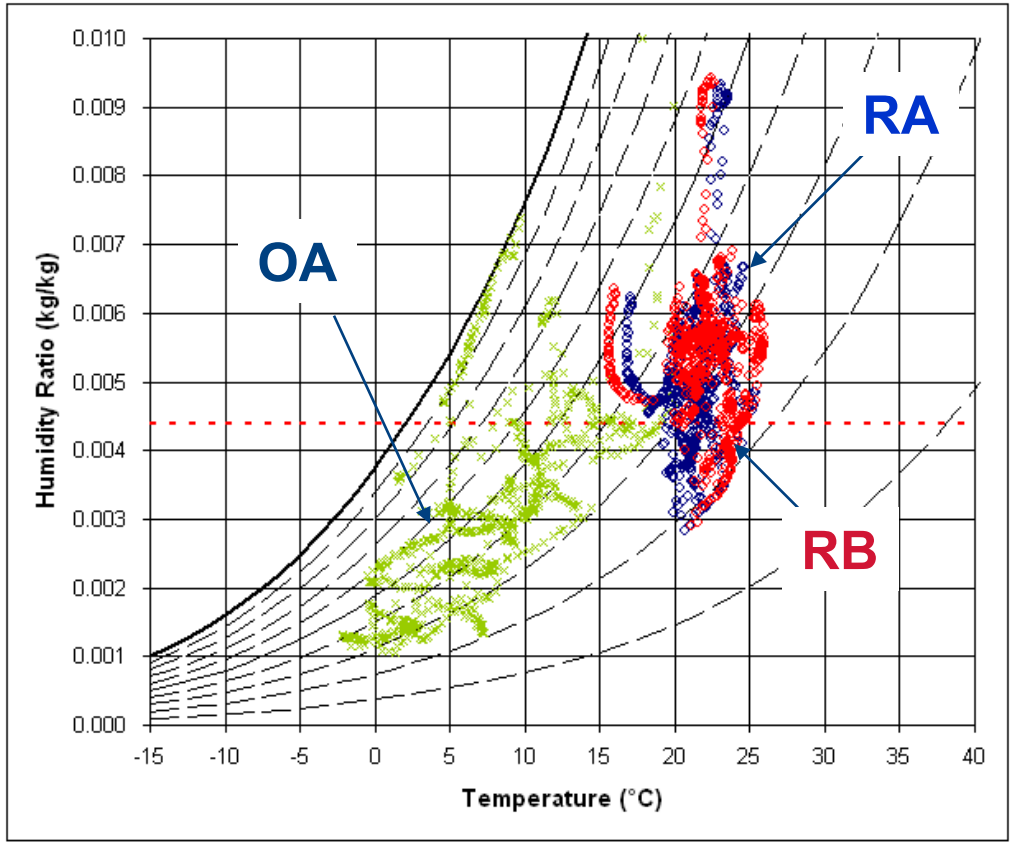

OA: Outdoor air
RA: Room A
RB: Room B

Seasonal Comparison

77.7% of all OA humidity ratio data ≤ 4.4 g/kg

78.2% of all RA humidity ratio data > 4.4 g/kg

85.8% of all RB humidity ratio data > 4.4 g/kg

SSLC AC Design Overview

Vapor Compression Cycle

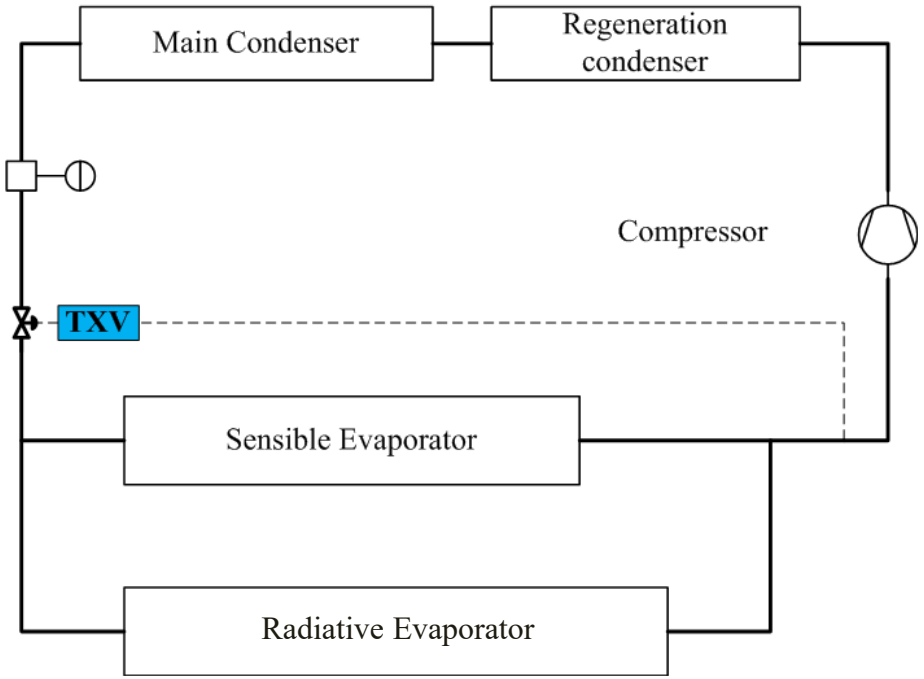

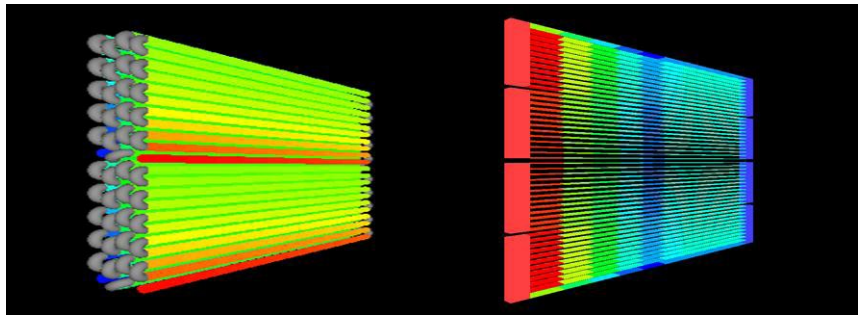

Desiccant Wheel

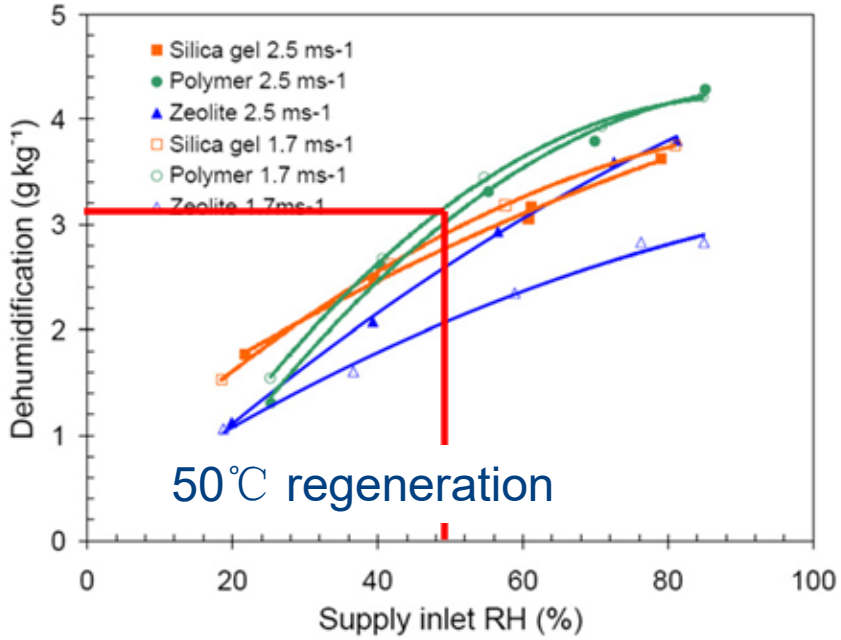

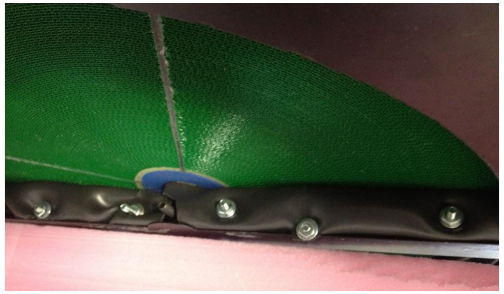

SSLC AC Components

High-efficient BLDC motor driven fan

Micro-channel condenser

Copper tubes at the back of RHX

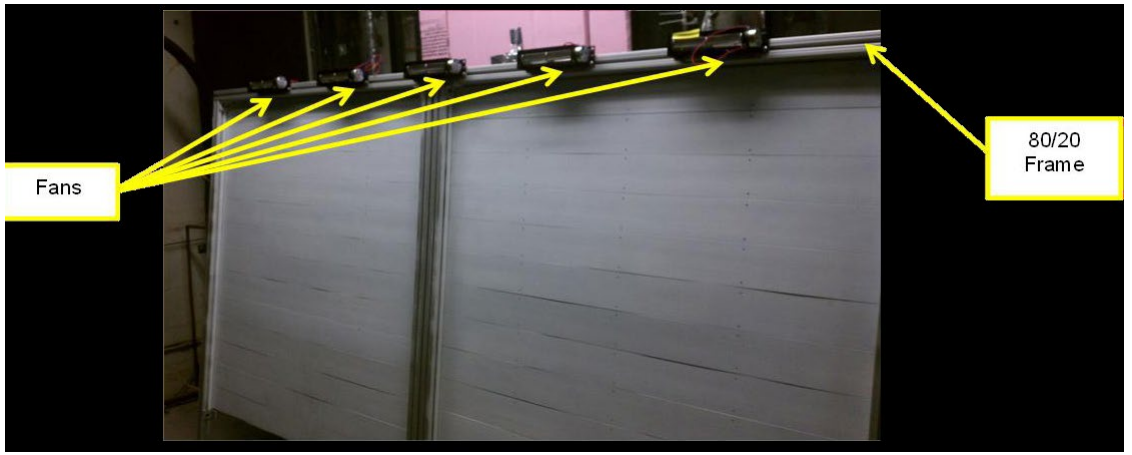

SSLC AC Design Overview

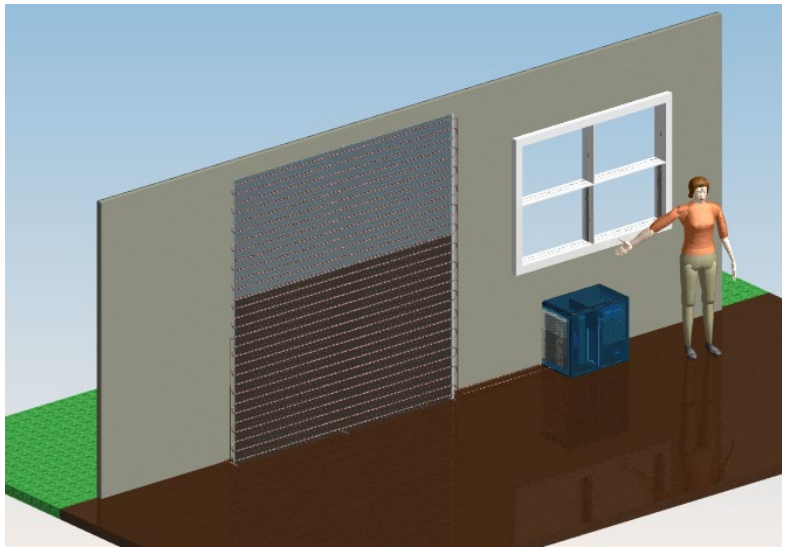

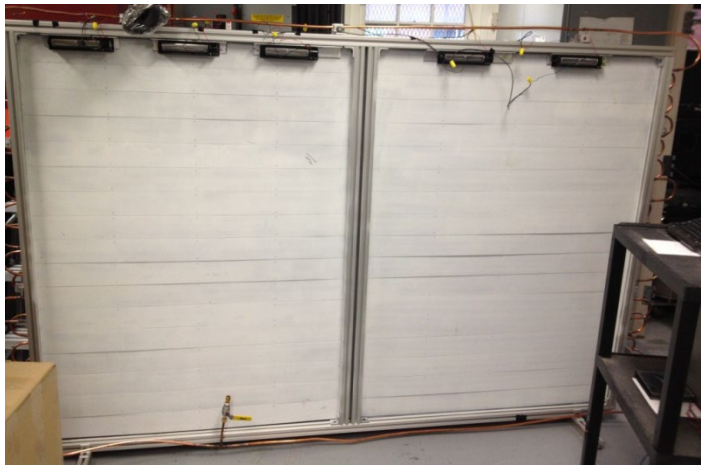

Radiative Heat Exchanger: Cooling Wall

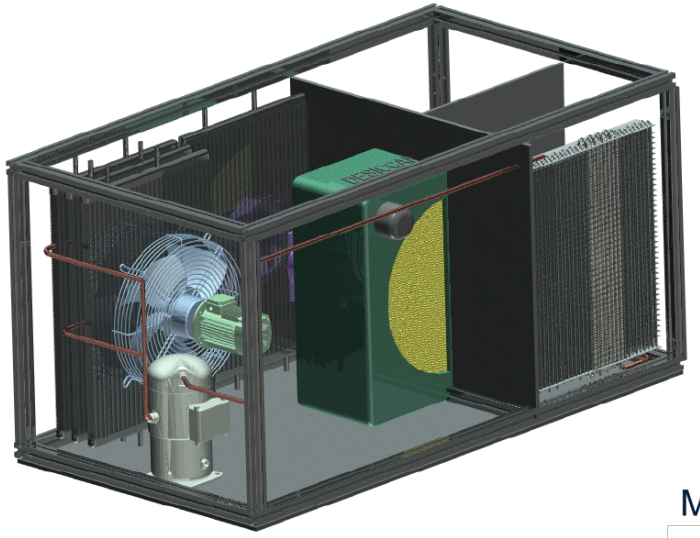

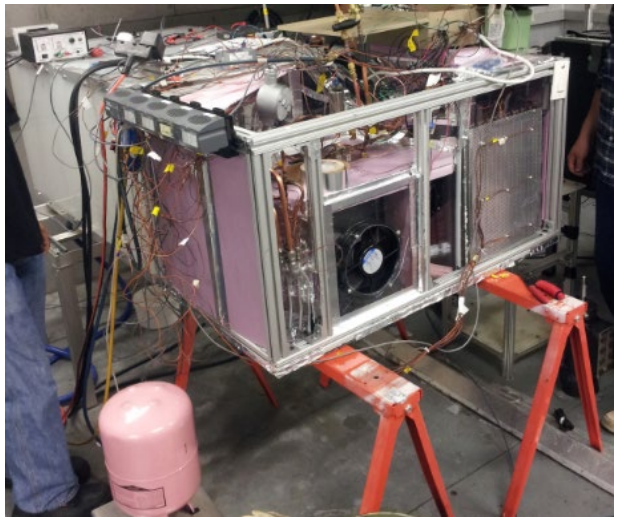

Prototype AC Unit

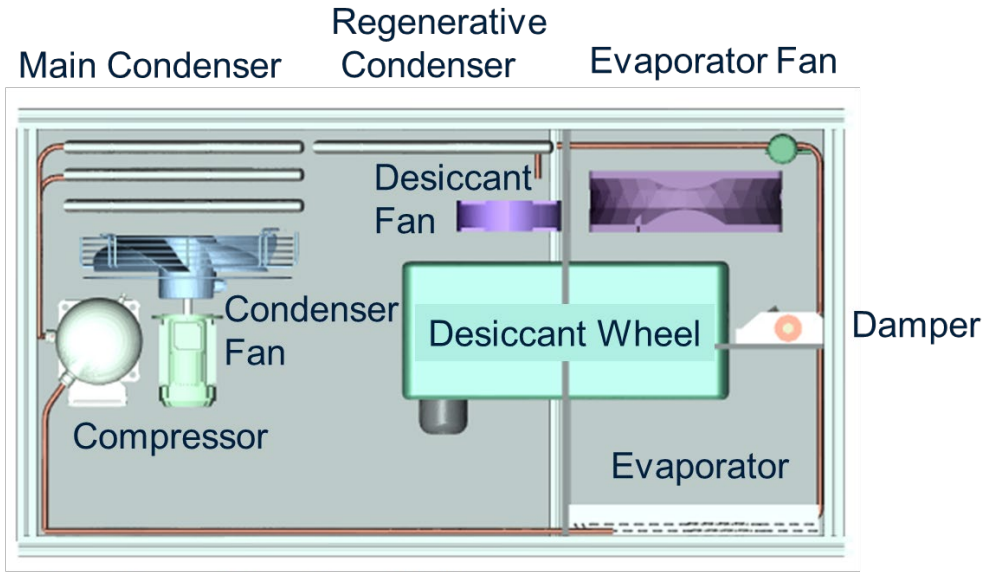

Top View of Contained Unit

SSLC AC Experimental Evaluation

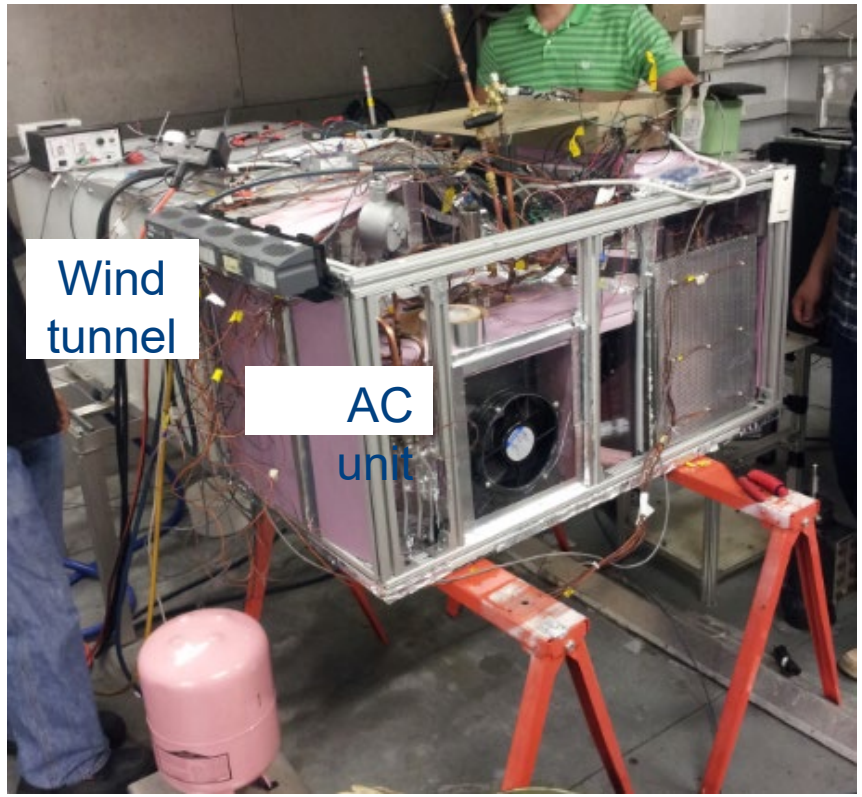

$$COP_e = \frac{Q_{evap}}{W_{compressor} + \sum_i W_{fan,i}}$$

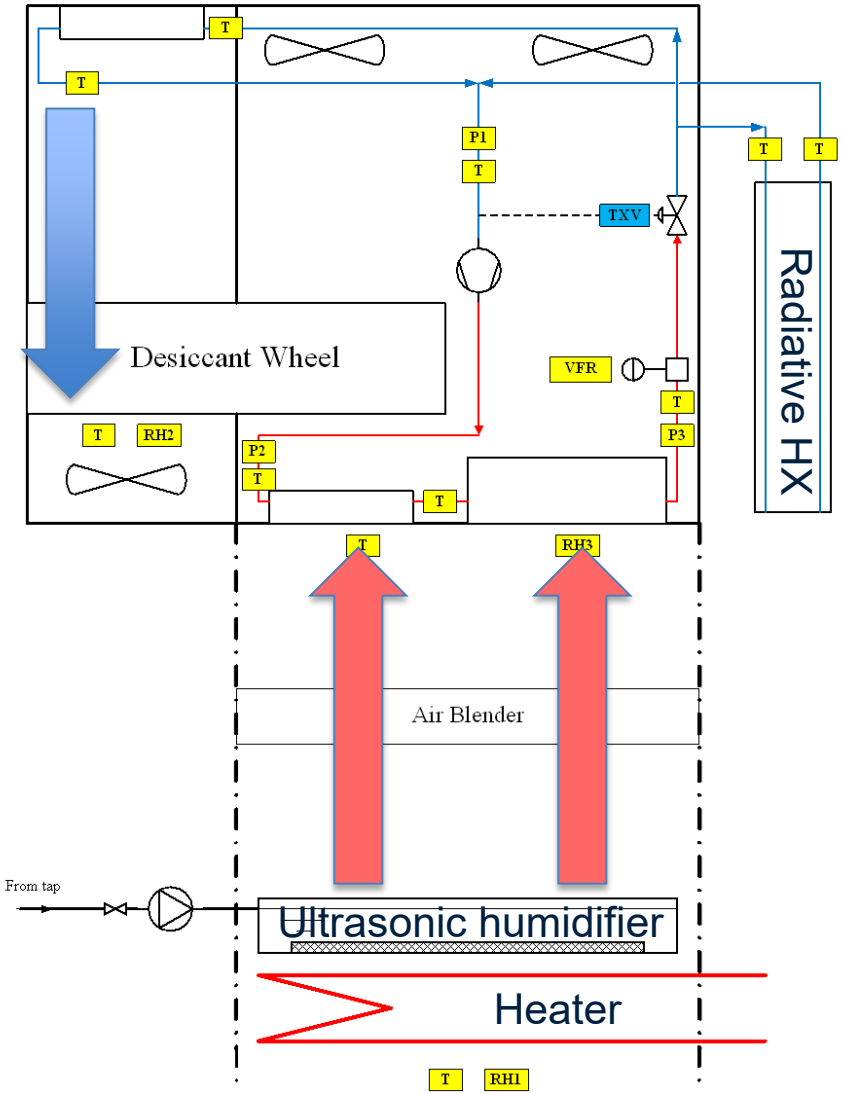

- T Thermocouples
- P Pressure transducer
- RH Relative humidity sensor
- VFR Turbine flow meter
- TXV Thermal expansion valve
- Fans
- Compressor
- Low pressure refrigerant line
- High pressure refrigerant line
- AC unit case
- Wind tunnel for test

IR Images of the RHX

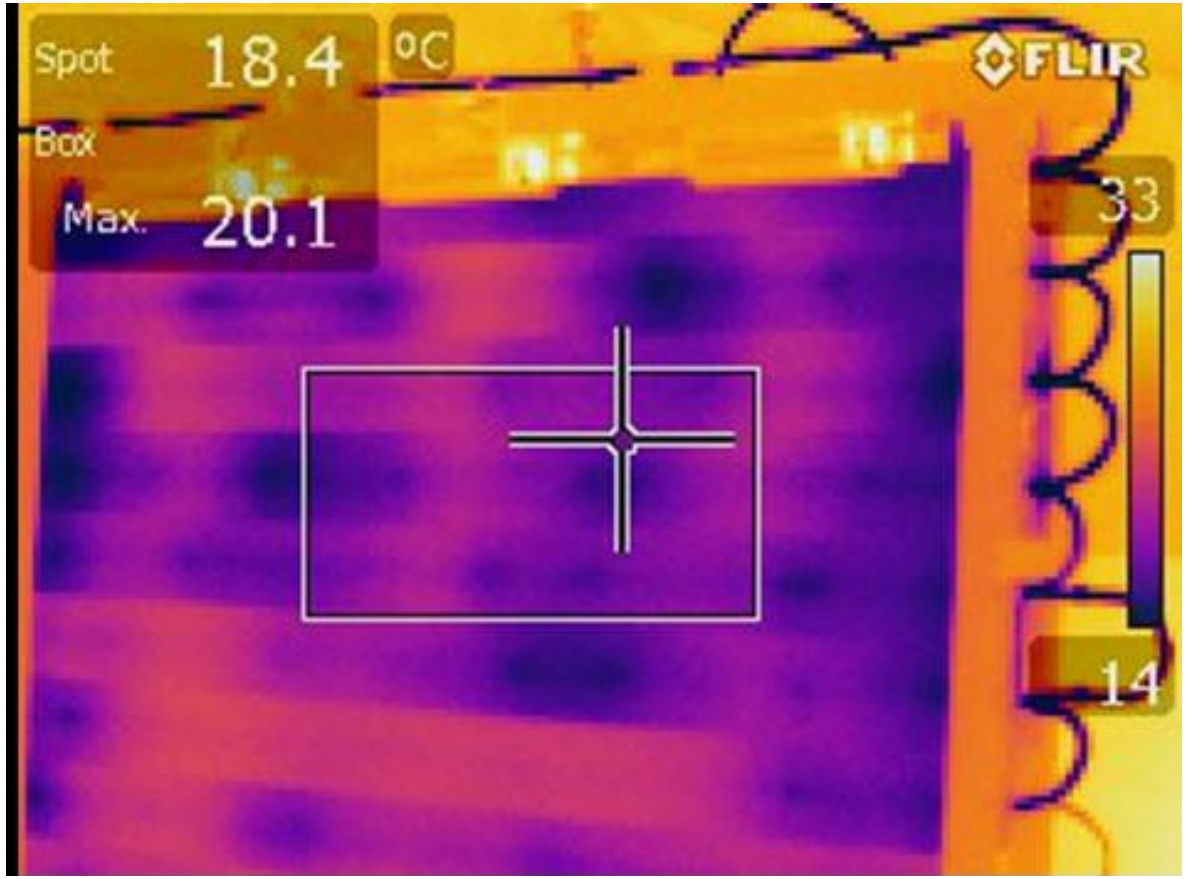

SSLC AC Test Results

Indoor air condition	**26.7 °C/ 50% RH**
Outdoor air condition	**35.0 °C/ 44% RH**

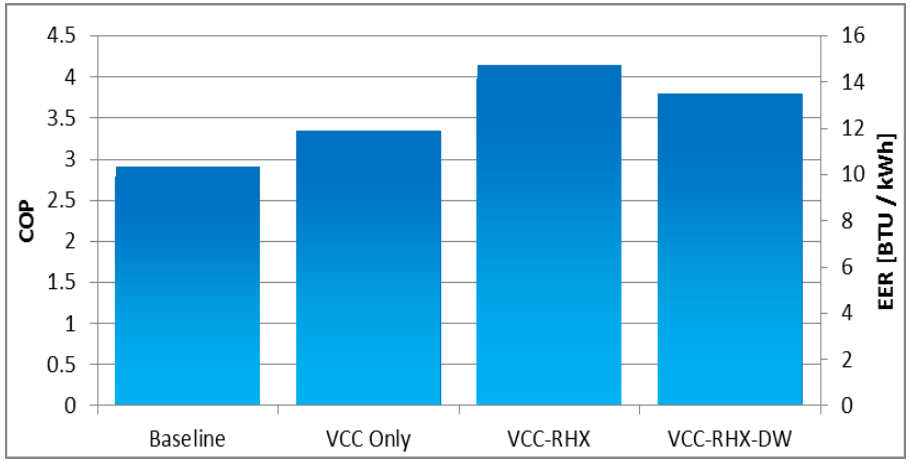

	Baseline Test	SSLC + RHX	SSLC + DW + RHX
Evaporating pressure (kPa)	951	1221	1091
Condensing Pressure* (kPa)	2481	2456	2310
Mass flow rate (g/s)	16.4	22.0	16.6
Cooling capacity (kW)	2.75	3.54	2.96
COP	2.91	4.15	3.8
COP improvement (%)	-	43	31

Part 3 Conclusions

- Separate Sensible and Latent Cooling was realized using a radiative cooling wall and a polymer desiccant wheel using waste heat from the superheated condenser.
- Achieved 31% COP enhancement
- There are many potential system integration opportunities (VCC + Enhanced Dehumidification).

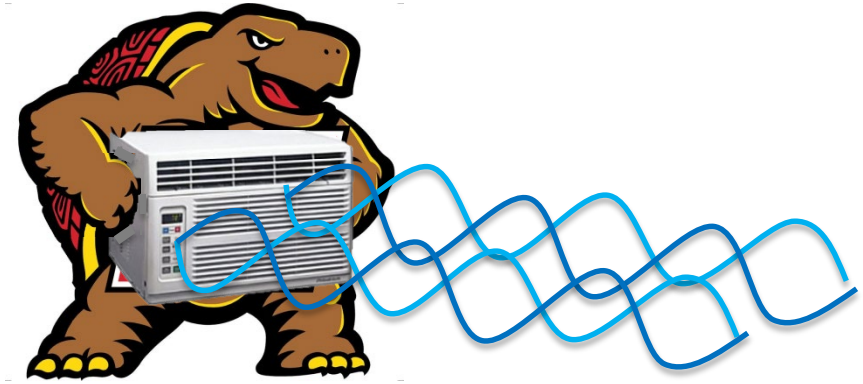

ECD Prototype Development

- **Design MEA for ECD-Mechanism**

Non-precious catalyst development: Dual active site design

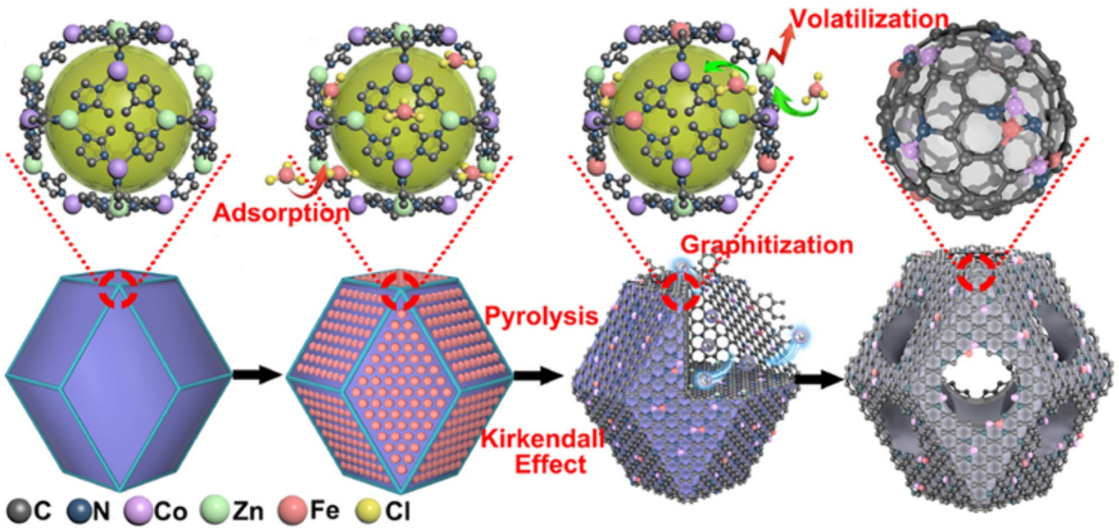

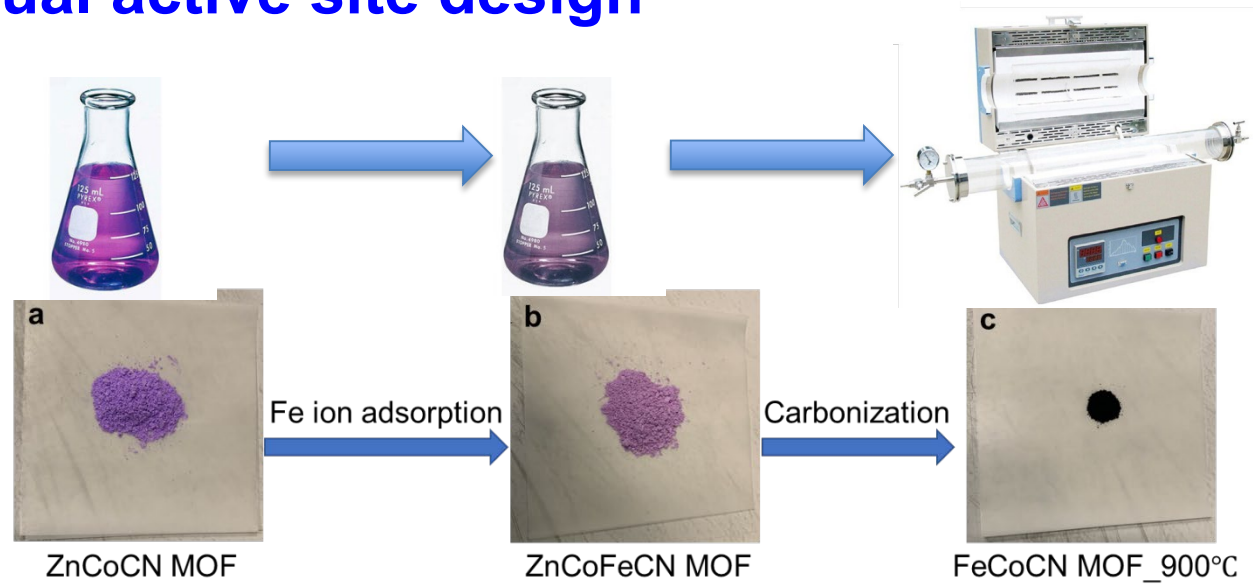

Preparation of FeCoCN MOF_900℃

2-methylimidazole+methanol→$Co(NO_3)_2 \cdot 6H_2O$+$Zn(NO_3)_2 \cdot 6H_2O$+methanol →ZnCoCN MOF

ZnCoCN MOF+hexane+$FeCl_3 \cdot 6H_2O$ → ZnCoFeCN MOF → heat → ZnCoFeCN MOF_900℃

10.1021/jacs.7b10385

Task 3: EHDECD Prototype Development

Direction of water transfer:

- No. 1 to 9: anode to cathode (proton exchange membrane)
- No. 10 to 12: cathode to anode (alkaline exchange membrane)

Carrier gas: No. 1 to 9 → air; No. 10 to 12 → O_2 (we will test with air in the future)

Performance Summary

No.	Electric Field (V)	Air inlet of Anode side				Air inlet of Cathode side				Water removal (g/day/m^2)	Dehumidification efficiency (g/(J·m^2))	Reference
		m_a (g/s)	V_a (mL/min)	T(°C)	HR (g/kg)	m_a (g/s)	V_a (mL/min)	T(°C)	HR (g/kg)			
1	3	0.0324	1502	21.5	14.7	0.0324	1502	21.5	10.7	4,020	0.0225	[2]
2	3	0.0111	516	21.5	14.7	0.0111	516	21.5	10.7	2,539	0.0195	[2]
3	3	0.0270	1251	22.6	13.2	0.0270	1251	22.9	12.6	2,610	0.0150	[2]
4	3	0.0111	516	22.6	13.2	0.0111	516	22.9	12.6	1,975	0.0155	[2]
5	3	0.0323	1497	21.9	11.3	0.0323	1497	22.3	11.6	2,116	0.0140	[2]
6	3	0.0111	516	21.9	11.3	0.0111	516	22.3	11.6	1,622	0.0150	[2]
7	3	0.0163	755	19.5	13.4	0.0163	755	19.3	8.6	2,821	0.0190	[3]
8	3	0.0113	524	17.7	12.1	0.0113	524	17.4	8.0	2,328	0.0190	[3]
9	3	0.0054	250	16.6	11.3	0.0054	250	16.5	8.0	1,693	0.0155	[3]
10	3	0.0143	600	20	7.2	0.0143	600	20	8.7	9,700	0.0417	Our work
11	2	0.0143	600	20	7.2	0.0143	600	20	8.7	6,900	0.0307	Our work
12	2	0.0190	800	20	7.2	0.0190	800	20	8.5	9,300	0.0619	Our work

Open-Air AEM ECD Results

- **Experimental results for EHD-ECD performance under different use cases**
- **Examined effect of EC potential and EHD enhancement**

For a 3-ton system, roughly 2 g/s dehumidification is required.

ECD-EHD Results

Moisture transfer rates under four electrode conditions and three different air-velocity conditions.

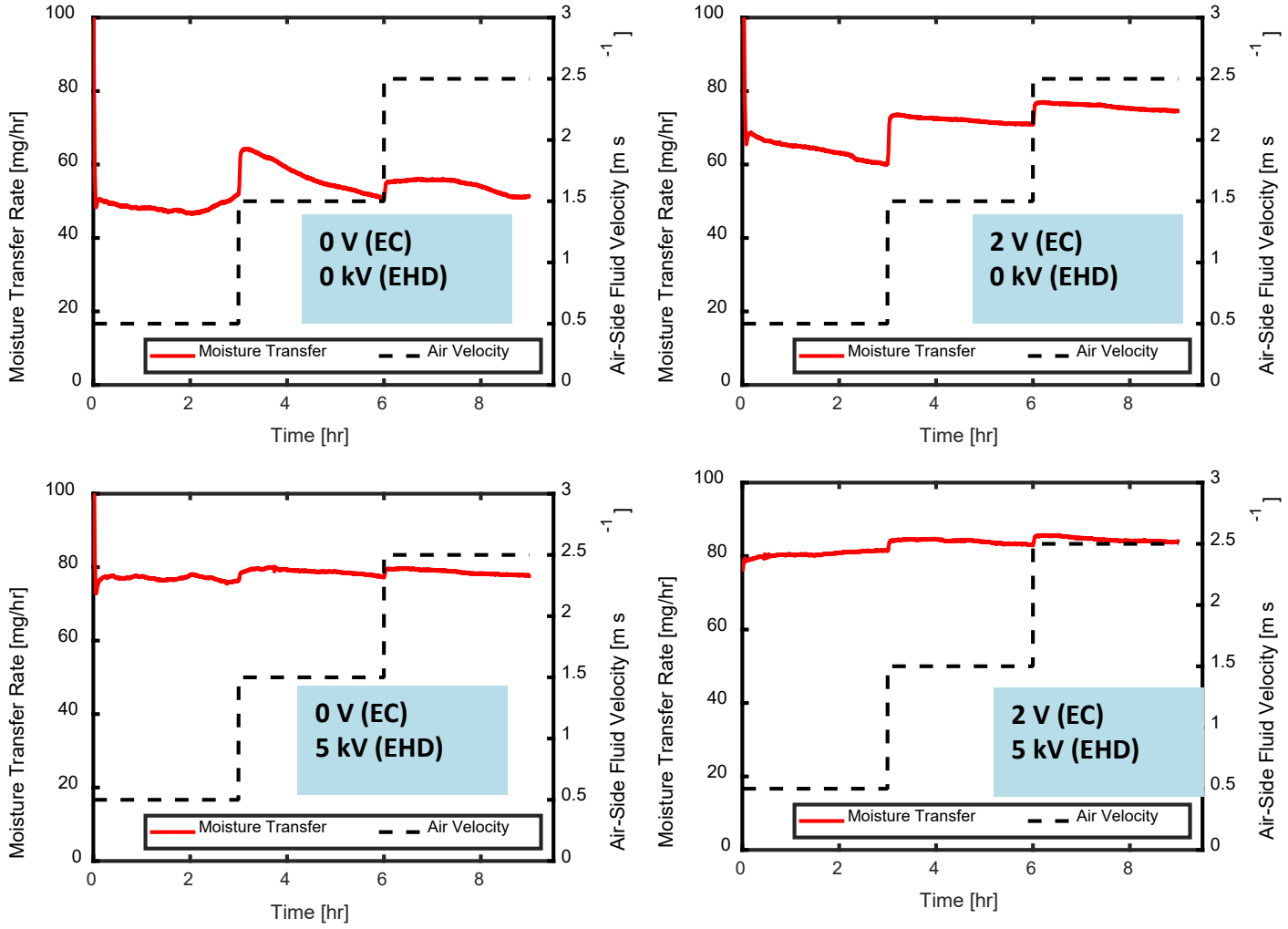

Open-Air PEM ECD Results

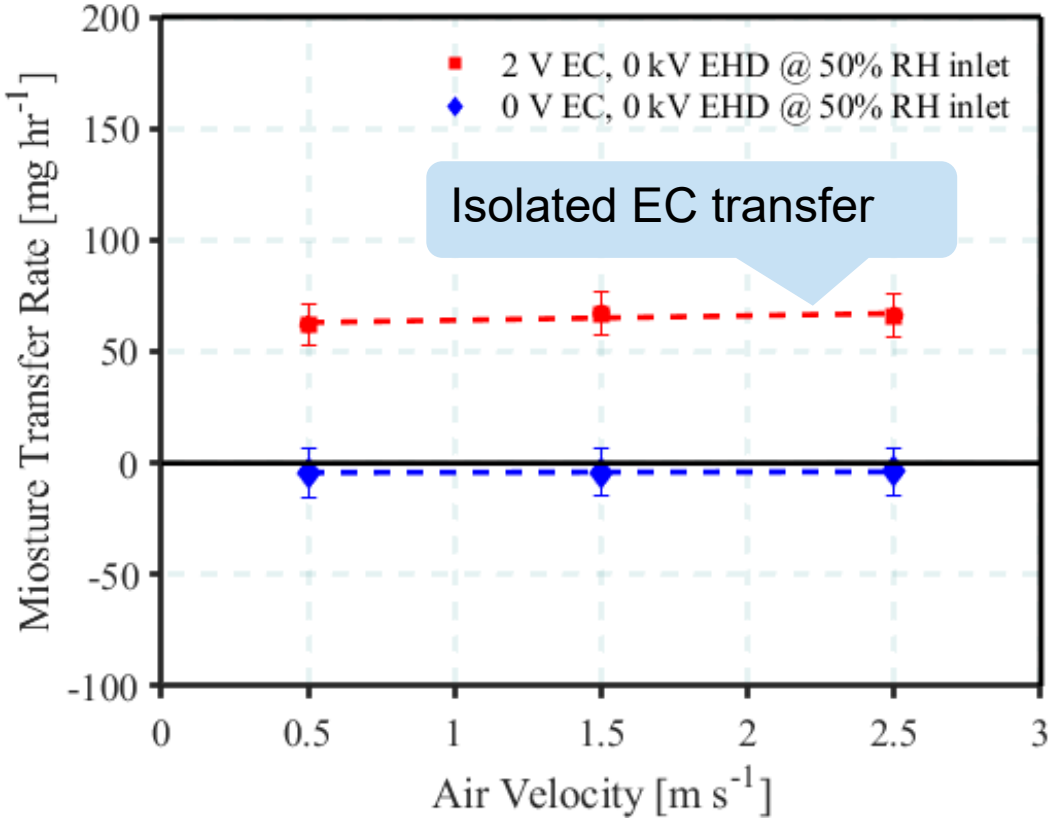

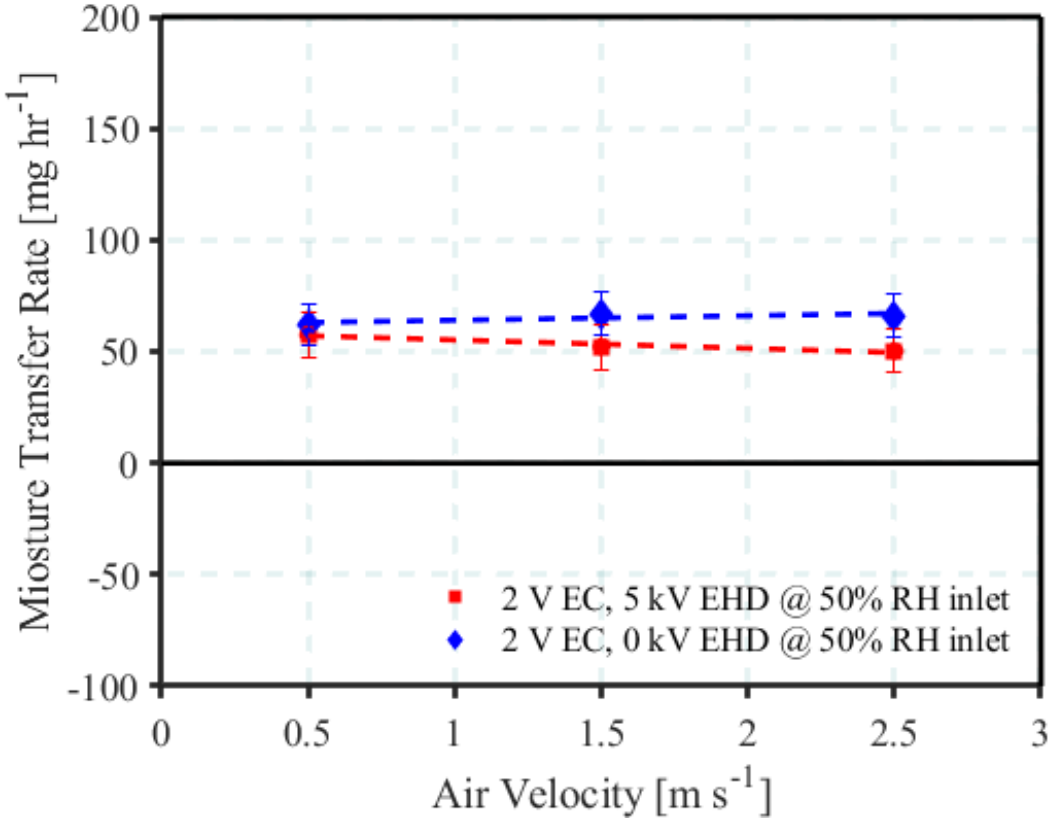

Effect of EC Potential

Comparison of pure diffusion in the MEA (blue) and total transfer rate with 2 V applied potential (red). Nafion 115. 26°C and 50% RH upstream (cathode) humidity; **50% RH anode inlet** at 200 sccm.

Effect of EHD Enhancement

Comparison 2 V EC 0 kV EHD the MEA (blue) and transfer rate with **2 V EC 5 kV EHD** voltage (red). Same conditions.

Task 8.1: Modeling EC Processes

- **We formulated the modeling methodology for predicting the performance of an integrated EHD-ECD system.**

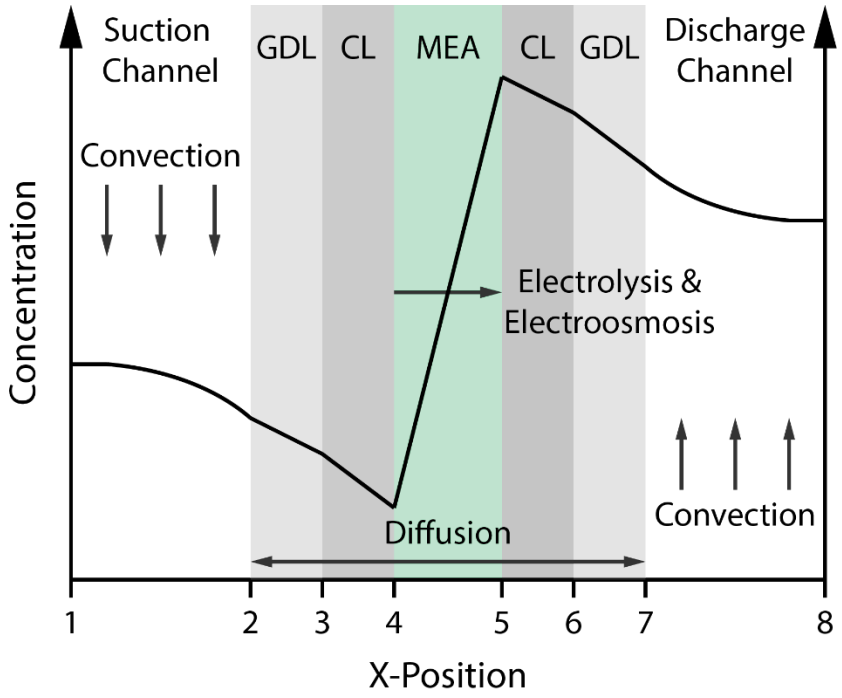

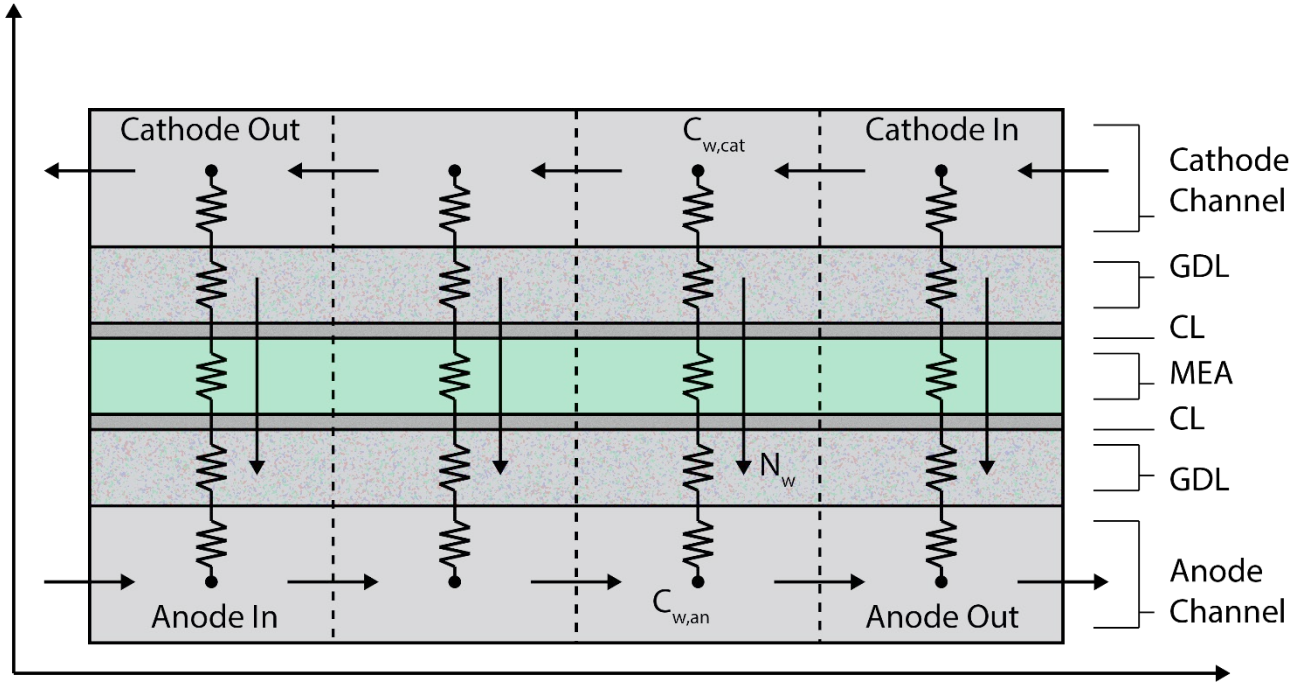

EC membrane model. Coupled mass transfer solved for a finite grid spanning the length of the flow channel.

Task 8.1: Solving ECD Element

- **Net water flux**

$$N_w = \alpha\left(\frac{I}{2F}\right)$$

- **Change in water concentration**

$$\frac{dx_i}{dz} = RT\sum_{j\neq i}\frac{x_i N_j - x_j N_i}{PD_{ij}}$$

- **Water Flux through the membrane**

$$N_{w,elec} + N_{w,diff} = \alpha\left(\frac{I}{2}F\right) = \frac{I}{2F} - \frac{\rho_{dry}}{M_m}D_\lambda\frac{d\lambda}{dz}$$

- **Cell voltage**

$$V_{cell} = \eta_{act,an} + \eta_{act,an} + Ir$$

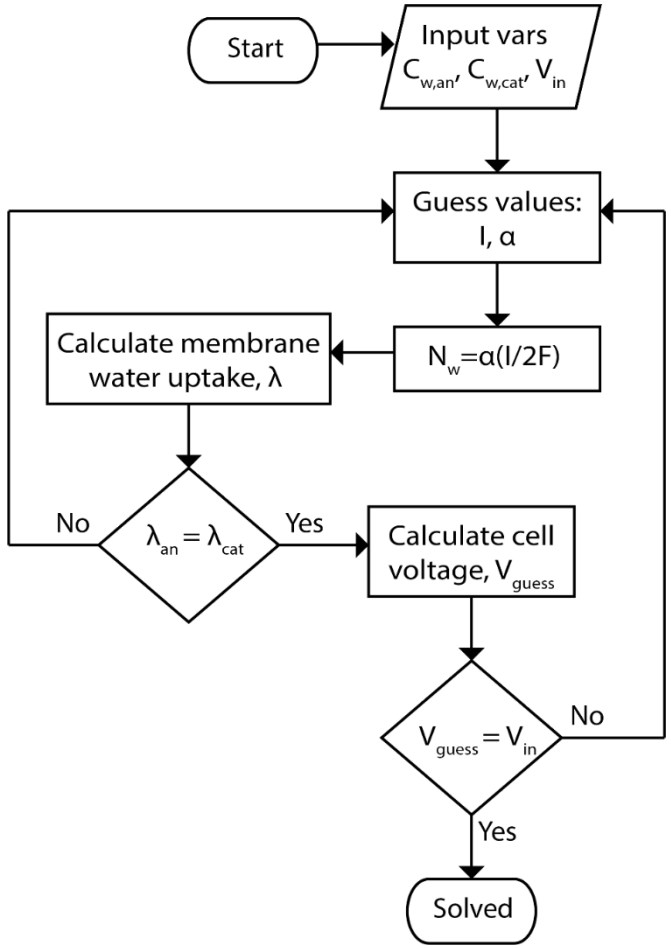

Flowchart of ECD Model

Task 8.2: Model Results

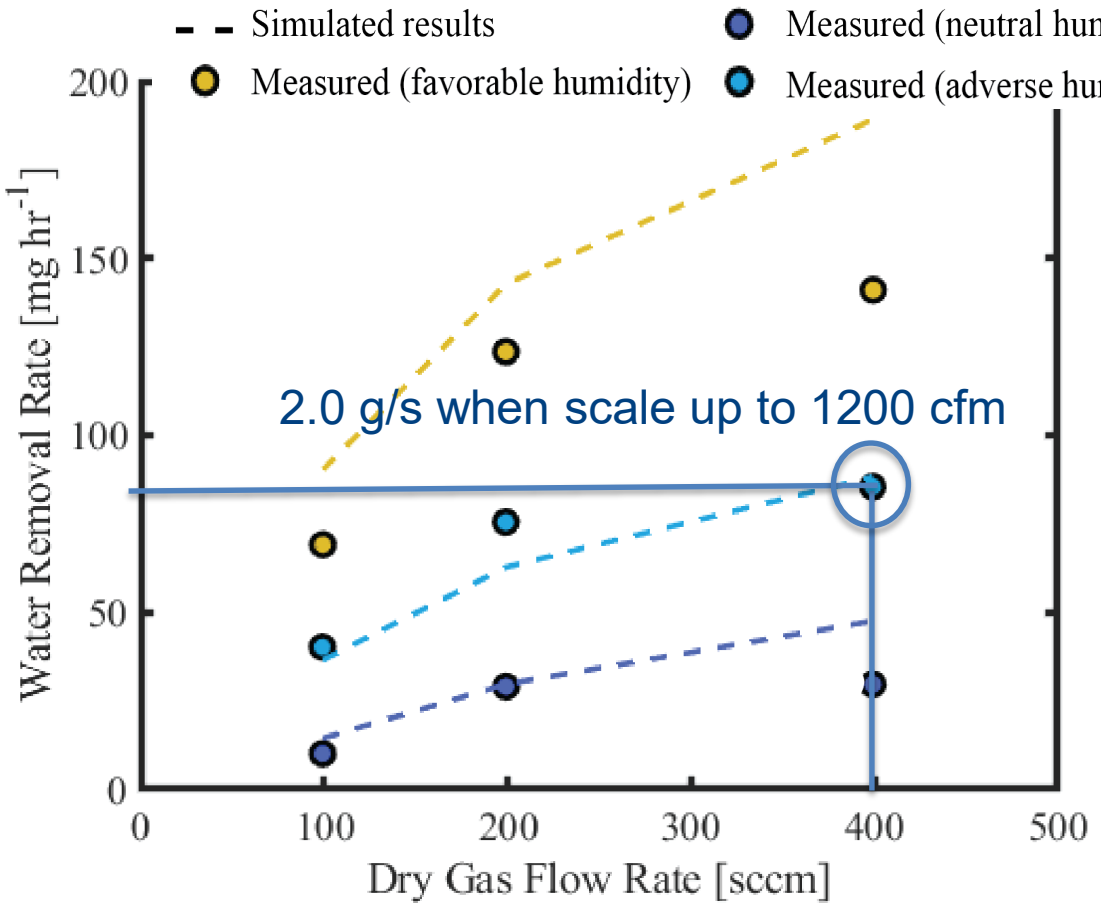

Model results. Simulated and measured values of moisture removal for various conditions.

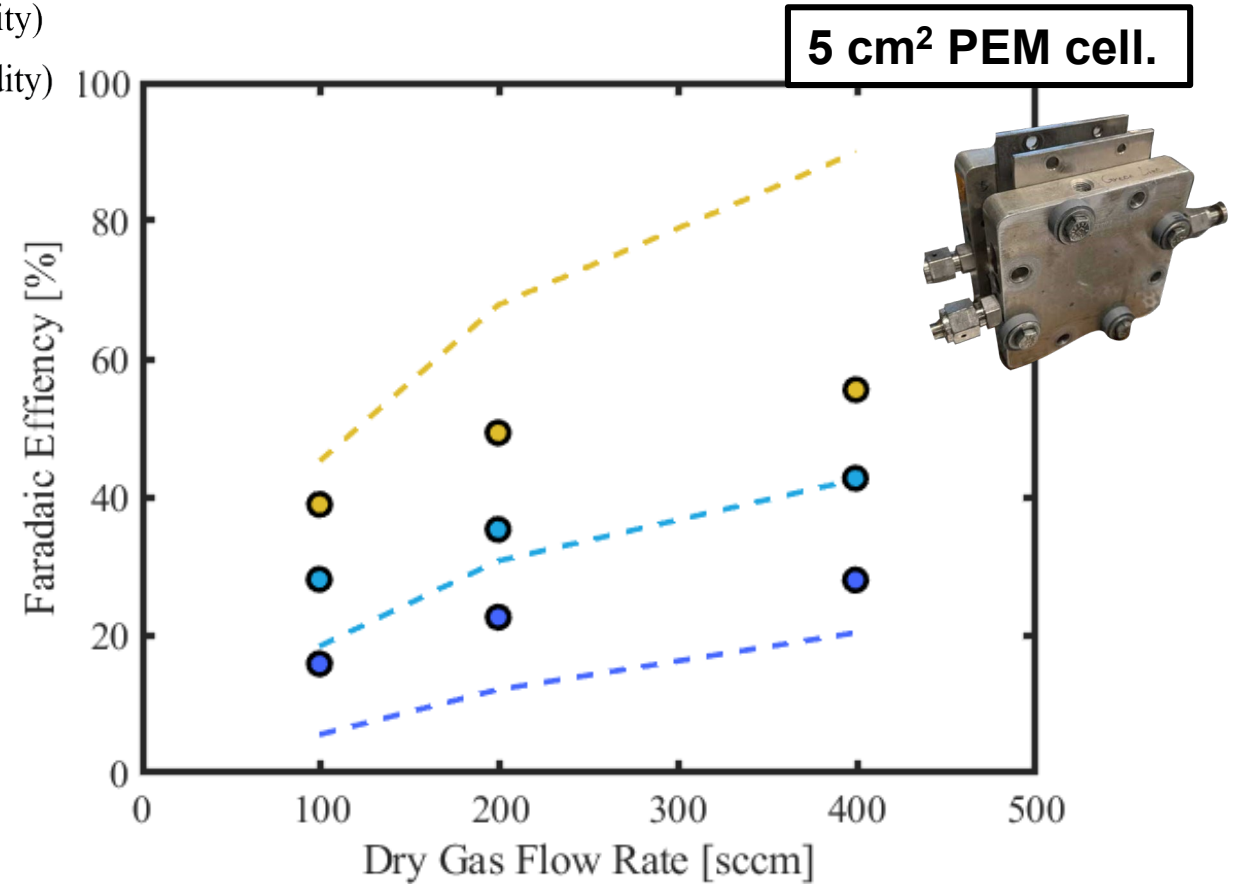

Model results. Simulated and measured values of faradaic efficiency for various conditions.

Task 8.2: Closed-Cell Model Accuracy

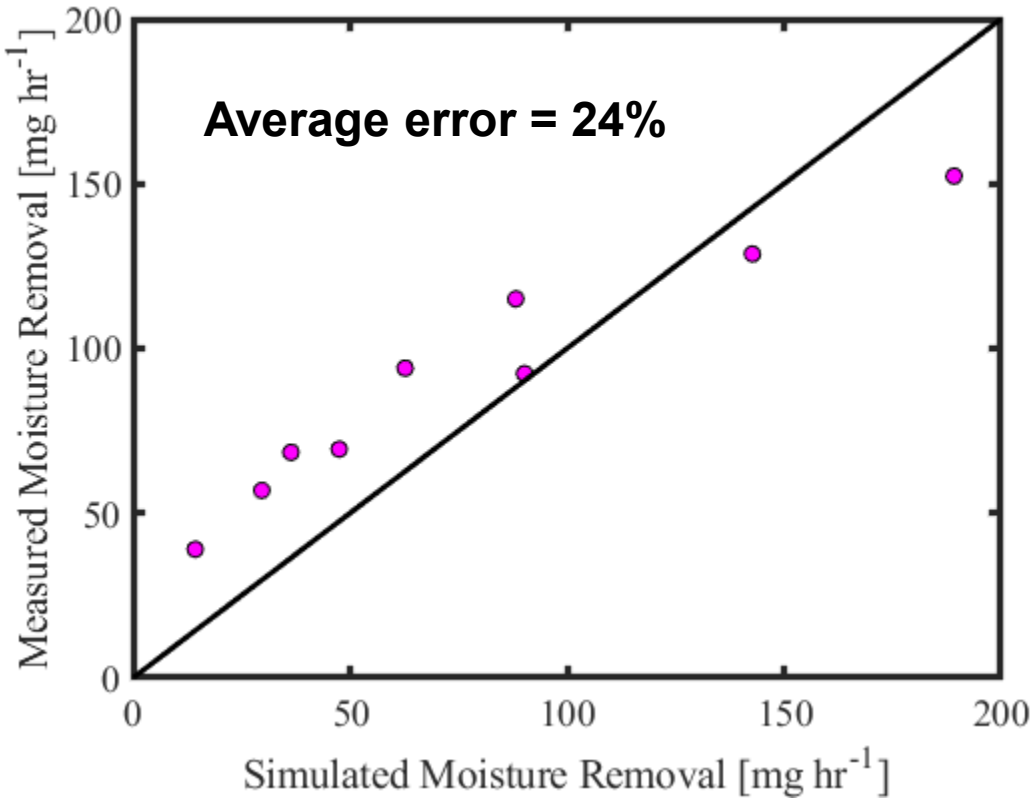

Model accuracy. Comparison on simulated moisture removal to measured values.

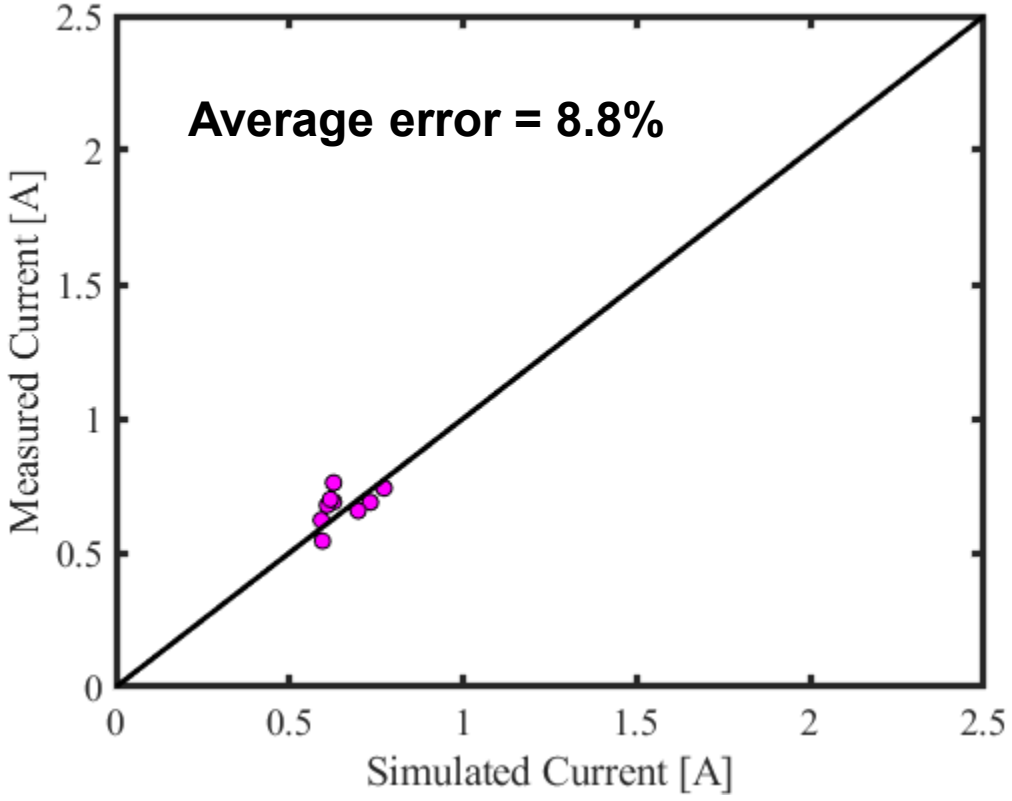

Model accuracy. Comparison on simulated current to measured values.

Configuration 1

- ECD used in a ventilator, outdoor air, w/ ventilation, 20% of total air flow through ECD
  - State 1: supply air stream before ECD (35°C, 44%, 15.6 gw/kgda)
  - State 2: supply air stream after ECD (same as return air)
  - Return air stream before ECD (27°C, 50%, 11.1 gw/kgda)
  - Supply air stream, the flow rate through ECD: 240 CFM
  - Latent load by ECD: 2.5 kW
  - Water removal rate: 0.56 g_wv/s (0.23 g_wv/s/kW, or 4.4 g_wv/kg_da)

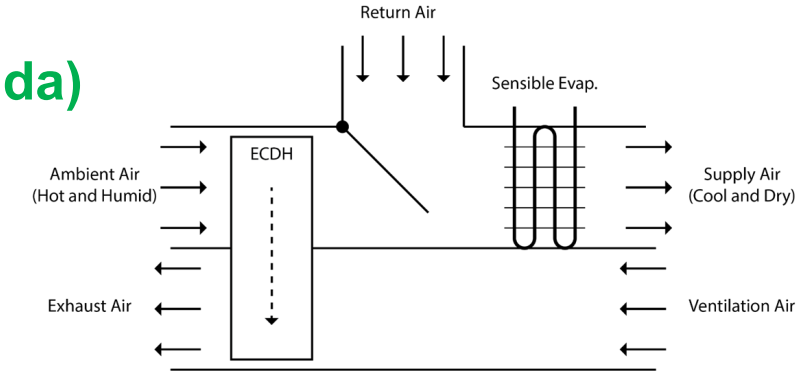

Main

Sort	1 T_i [C]	2 ρ_i [kg/m3]	3 RH_i	4 ω_i [kg/kg]	5 h_i [kJ/kg]	6 m_i [kg/s]	7 $m_{d,i}$ [kg/s]	8 $m_{w,i}$ [kg/s]	9 v_i [m3/s]
[1]	35	1.135	0.44	0.01558	75.13	0.1282	0.1263	0.001968	0.113
[2]	27		0.5	0.01115	55.54	0.1277	0.1263	0.001407	

Configuration 2

- EHD used in a DOAS, w/ 100% ventilation, 100% of total air flow through ECD
  - State 1: supply air stream before ECDEHD (35°C, 44%, 15.6 gw/kgda)
  - State 2: supply air stream after ECDEHD (same as return air)
  - Return air stream before ECDEHD (27°C, 50%, 11.1 gw/kgda)
  - Supply air stream, flow rate through ECDEHD: 1200 CFM
  - Latent load by ECD: 12.4 kW
  - Water removal rate: 2.8 g_wv/s (0.23 g_wv/s/kW, or 4.4 g_wv/kg_da)

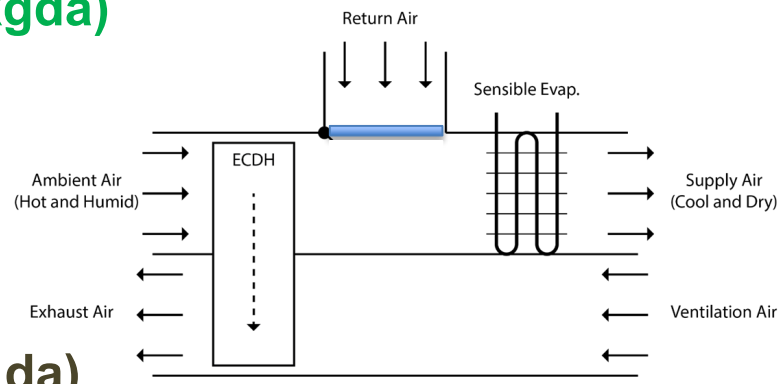

Main

Sort	1 T_i [C]	2 ρ_i [kg/m³]	3 RH_i	4 ω_i [kg/kg]	5 h_i [kJ/kg]	6 m_i [kg/s]	7 $m_{d,i}$ [kg/s]	8 $m_{w,i}$ [kg/s]	9 v_i [m3/s]
[1]	35	1.135	0.44	0.01558	75.13	0.6424	0.6325	0.009855	0.566
[2]	27		0.5	0.01115	55.54	0.6396	0.6325	0.00705	

Configuration 3

- ECD used after sensible evaporator, indoor air, w/o ventilation, 100% of total air flow through ECD
  - State 0: supply air stream before sensible evaporator (100% return air)
  - State 1: supply air stream before ECDEHD (100%, 11.1 gw/kgda)
  - State 2: supply air stream after ECDEHD (20°C, 8 gw/kgda)
  - Return air (27°C, 50%), Ambien air (35°C, 44%)
  - Supply air stream, flow rate through ECDEHD: 1200 CFM
  - Latent load by ECD: 2.3 kW; Sensible heat factor: 0.76
  - Water removal rate: 2.06 g_wv/s (0.88 g_wv/s/kW, or 3.1 g_wv/kgda)

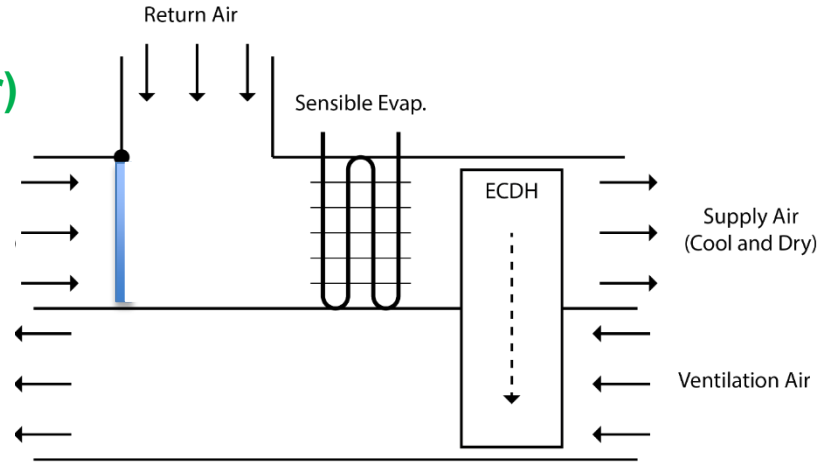

Arrays Table

Main

Sort	1 T_i [C]	2 ρ_i [kg/m3]	3 rh_i	4 ω_i [kg/kg]	5 h_i [kJ/kg]	6 m_i [kg/s]	7 $m_{d,i}$ [kg/s]	8 $m_{w,i}$ [kg/s]
[0]	27		0.5	0.01115	55.54	0.6612	0.6539	0.007288
[1]	15.7		1	0.01115	43.96	0.6612	0.6539	0.007288
[2]	20	1.198	0.5502	0.008	40.38	0.6592	0.6539	0.005231

Configuration 4

- ECD used before the sensible evaporator, indoor air, w/o ventilation, 100% of total air flow through ECD
  - State 0: supply air stream before ECDEHD (100% return air)
  - State 1: supply air stream after ECDEHD (31°C, 8 gw/kgda)
  - State 2: supply air stream after the sensible evaporator (20°C, 8 gw/kgda)
  - Return air (27°C, 50%), Ambien air (35°C, 44%)
  - Supply air stream, flow rate through ECDEHD: 1200 CFM
  - Latent load by ECD: 2.6 kW; Sensible heat factor: 0.74
  - Water removal rate: 2.06 g_wv/s (0.80 g_wv/s/kW, or 3.1 g_wv/kgda)

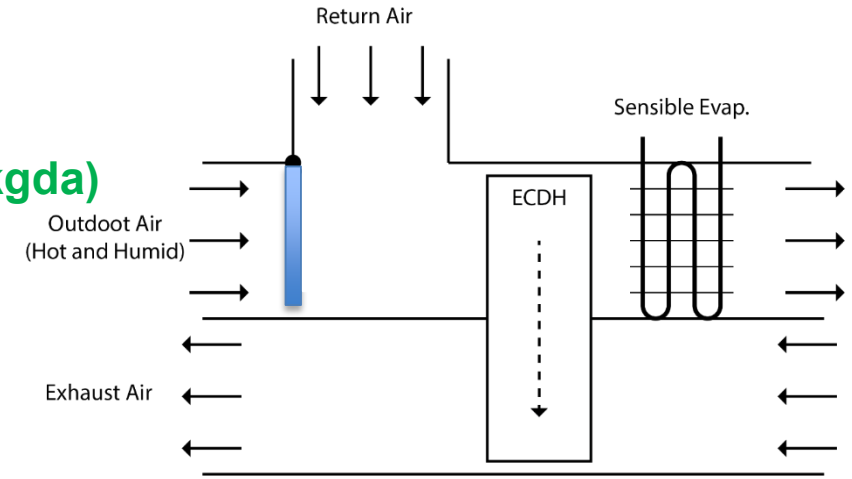

Main

Sort	1 T_i [C]	2 ρ_i [kg/m³]	3 rh_i	4 ω_i [kg/kg]	5 h_i [kJ/kg]	6 m_i [kg/s]	7 $m_{d,i}$ [kg/s]	8 $m_{w,i}$ [kg/s]
[0]	27		0.5	0.01115	55.54	0.6612	0.6539	0.007288
[1]	31		0.2862	0.008	51.6	0.6592	0.6539	0.005231
[2]	20	1.198	0.5502	0.008	40.38	0.6592	0.6539	0.005231

Configuration 5

- ECD used before sensible evaporator, indoor air, w ventilation, 100% of total air flow through ECD
  - State 0: supply air stream before sensible evaporator (80% return air + 20% ambient air)
  - State 1: supply air stream before ECD (100%, 12.0 gw/kgda)
  - State 2: supply air stream after ECD (20°C, 8 gw/kgda)
  - Return air (27°C, 50%), Ambien air (35°C, 44%)
  - Supply air stream, flow rate through ECDEHD: 1200 CFM
  - Latent load by ECD: 4.5 kW; Sensible heat factor: 0.63
  - Water removal rate: 2.60 g_wv/s (0.58 g_wv/s/kW, or 4.0 g_wv/kgda)

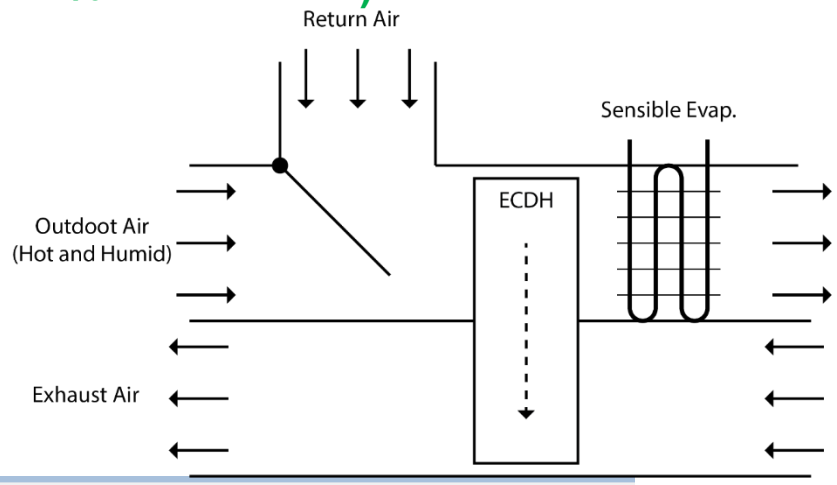

Main

Sort	1 T_i [C]	2 ρ_i [kg/m3]	3 rh_i	4 ω_i [kg/kg]	5 h_i [kJ/kg]	6 m_i [kg/s]	7 $m_{d,i}$ [kg/s]	8 $m_{w,i}$ [kg/s]
[0]	28.57		0.491	0.01201	59.35	0.6575	0.6497	0.007801
[1]	16.85		1	0.01201	47.32	0.6575	0.6497	0.007801
[2]	20	1.198	0.5502	0.008	40.38	0.6549	0.6497	0.005197

Configuration 6

- **ECD used before sensible evaporator, indoor air, w 20% ventilation, 100% of total air flow through ECD**
  - **State 0: supply air stream before ECDEHD (80% return air + 20% ambient air)**
  - **State 1: supply air stream after ECDEHD (32.57°C, 8 gw/kgda)**
  - **State 2: supply air stream after the sensible evaporator (20°C, 8 gw/kgda)**
  - **Return air (27°C, 50%), Ambien air (35°C, 44%)**
  - **Supply air stream, flow rate through ECDEHD: 1200 CFM**
  - **Latent load by ECD: 4.0 kW; Sensible heat factor: 0.68**
  - **Water removal rate: 2.60 g_wv/s (0.65 g_wv/s/kW, or 4.0 g_wv/kgda)**

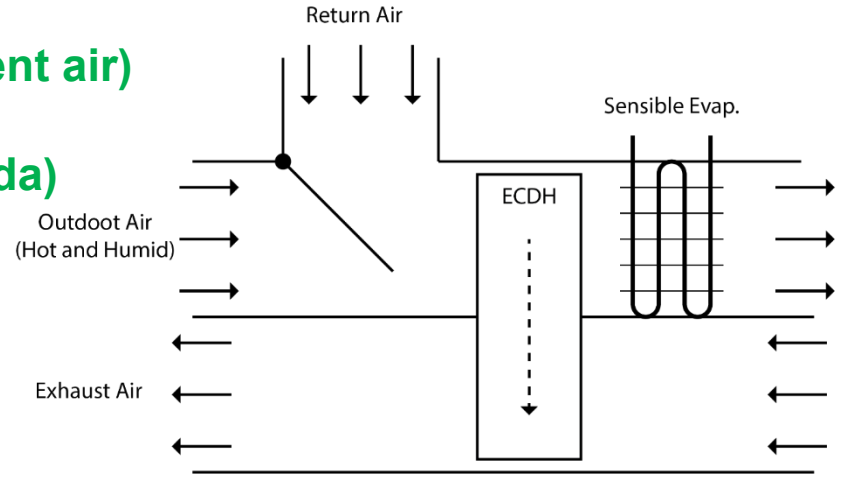

Main

Sort	1 T_i [C]	2 ρ_i [kg/m³]	3 rh_i	4 ω_i [kg/kg]	5 h_i [kJ/kg]	6 m_i [kg/s]	7 $m_{d,i}$ [kg/s]	8 $m_{w,i}$ [kg/s]
[0]	28.57		0.491	0.01201	59.35	0.6575	0.6497	0.007801
[1]	32.57		0.2618	0.008	53.2	0.6549	0.6497	0.005197
[2]	20	1.198	0.5502	0.008	40.38	0.6549	0.6497	0.005197

Reference

1. Alem-Rajabi, A. and F. Lai, "EHD-Enhanced Drying of Partially Wetted Glass Beads," Drying Technology, vol. 23, pp. 597-609, 2005.
2. Lai, F.C. and R. Sharma, "EHD-enhanced drying with multiple needle electrode," Journal of Electrostatics, vol. 63, pp. 223-237, 2005.
3. Poós, T. and Varju E. Mass transfer coefficient for water evaporation by theoretical and empirical correlations. International Journal of Heat and Mass Transfer vol. 158, 2020.
4. Qi, R., D. Li, H. Li, H. Wang and L.-Z. Zhang, "Heat and mass transfer in a polymeric electrolyte membrane-based electrochemical air dehumidification system: Model development and performance analysis," International Journal of Heat and Mass Transfer, vol. 126, pp. 888–898, 2018.
5. Qi, R., Tian, C., Shao, S., Tang, M. and Lu, L. Experimental investigation on performance improvement of electro-osmotic regeneration for solid desiccant. Applied Energy vol. 88, pp. 2816-2823, 2011.

MEA Materials

MEA	Material	Cathode CL	Anode CL	Cathode GDL	Anode GDL
Open-Cathode (5 cm^2)	Nafion 115	Pt B (3 mg/cm^2)	IrRuOx (3 mg/cm^2)	Ti Frit	Ti Frit
PEM A (5 cm^2)	Nafion 115	Pt C (60%) (0.5 mg/cm^2)	IrOx (4 mg/cm^2)	Carbon Cloth	Ti Frit
PEM B (5 cm^2)	Nafion 115	Pt B (3 mg/cm^2)	IrRuOx (3 mg/cm^2)	Carbon Cloth	Ti Frit
AEM (5 cm^2)	Fumasep	Pt C	RuO2	Carbon Cloth	Carbon Cloth
AEM (50 cm^2)	Fumasep	Pt C	RuO2	Carbon Cloth	Carbon Cloth

ECD Modeling Methodology

	Anode GDL	Anode CL	Membrane	Cathode CL	Cathode GDL
H2 (C_H)	$-D_{Hv}\nabla C_H$	$-D_{Hv}\nabla C_H - \frac{1}{2F}i$	-	-	-
O2 (C_O)	-	-	-	$\sum_{j\neq i}^{N} -D_{ij}\nabla C_j - \frac{1}{4F}i$	$\sum_{j\neq i}^{N} -D_{ij}\nabla C_j$
N2 (C_N)	-	-	-	$\sum_{j\neq i}^{N} -D_{ij}\nabla C_j$	$\sum_{j\neq i}^{N} -D_{ij}\nabla C_j$
vH2O (C_v)	$-D_{Hv}\nabla C_v$	$-D_{Hv}\nabla C_v$ $- h_m(C_m - C_v)$	-	$\sum_{j\neq i}^{N} -D_{ij}\nabla C_j$ $- h_m(C_m - C_v)$	$\sum_{j\neq i}^{N} -D_{ij}\nabla C_j$
mH2O (C_m)	-	$-D_m(\varepsilon_m)^{1.5}\nabla C_m$ $+ h_m(C_m - C_v)$	$\xi\frac{i_x}{F} - D_m\nabla C_m$	$-D_m(\varepsilon_m)^{1.5}\nabla C_m$ $+ h_m(C_m - C_v) + \frac{1}{2F}i$	-
e^- (Φ_s)	$-\sigma_0\varepsilon^{1.5}\nabla\Phi_s$	$-\sigma_0\varepsilon^{1.5}\nabla\Phi_s + i$	-	$-\sigma_0\varepsilon^{1.5}\nabla\Phi_s - i$	$-\sigma_0\varepsilon^{1.5}\nabla\Phi_s$
H^+ (Φ_m)	-	$-\kappa(\varepsilon_m)^{1.5}\nabla\Phi_m + i$	$-\kappa\nabla\Phi_m$	$-\kappa(\varepsilon_m)^{1.5}\nabla\Phi_m - i$	-

Introduction

- **Comparison of H_2O electrochemical dehumidifier and AEMFC**

H_2O electrochemical dehumidifier (HEC)

High H_2O partial pressure outlet

$4OH^- \rightarrow 2H_2O+O_2+4e^-$

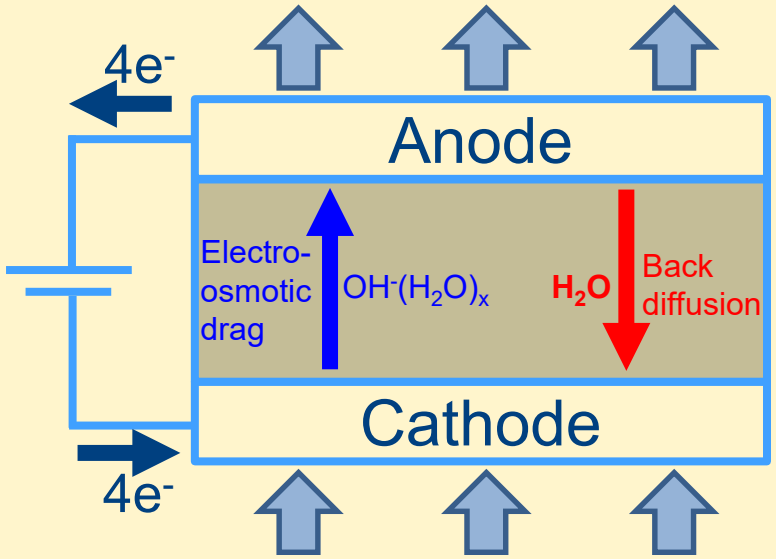

$2H_2O+O_2+4e^- \rightarrow 4OH^-$

Low H_2O partial pressure inlet

Alkaline fuel cell (AEMFC)

High H_2O partial pressure outlet

$2H_2+4OH^- \rightarrow 2H_2O+4e^-$

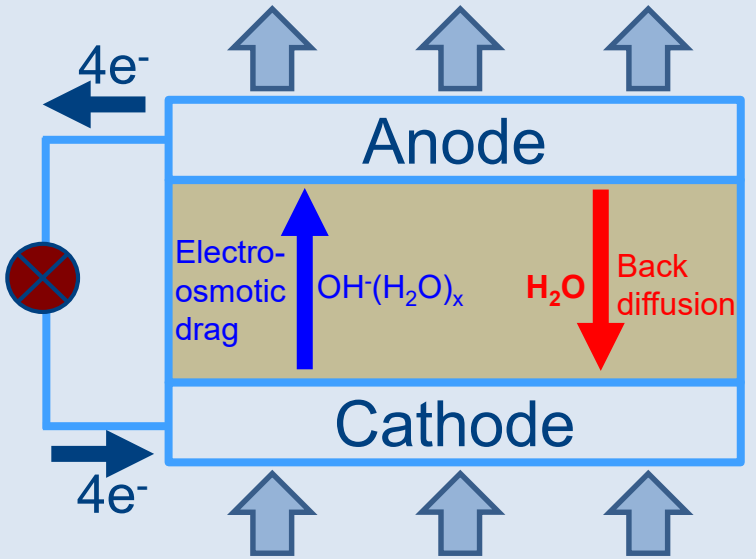

$2H_2O+O_2+4e^- \rightarrow 4OH^-$

Low H_2O partial pressure inlet

Introduction

- Dehumidification using an electrochemical (EC) membrane
- Electrohydrodynamic (EHD) promotes mass transfer

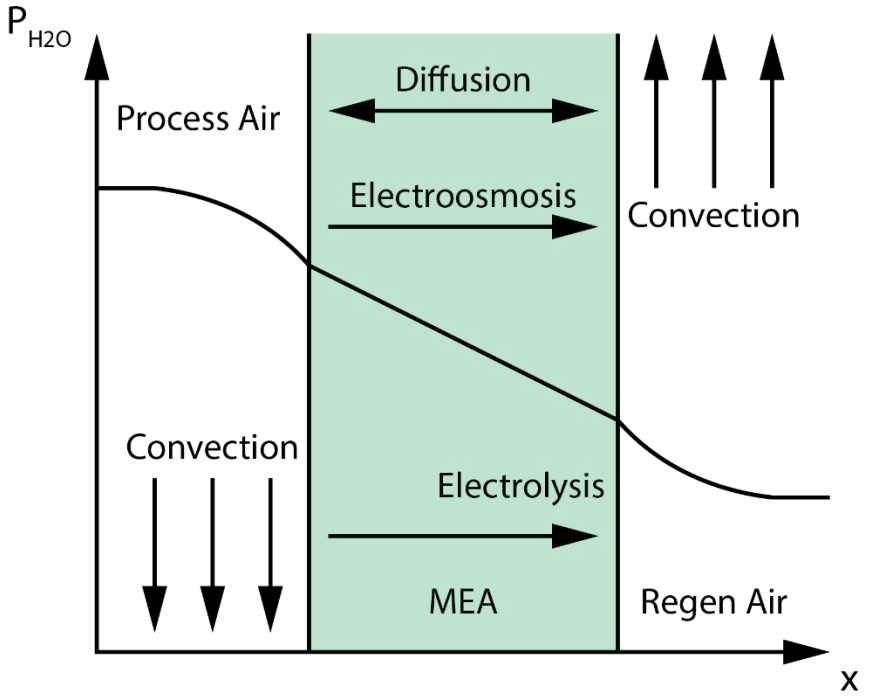

Membrane Transport Phenomena

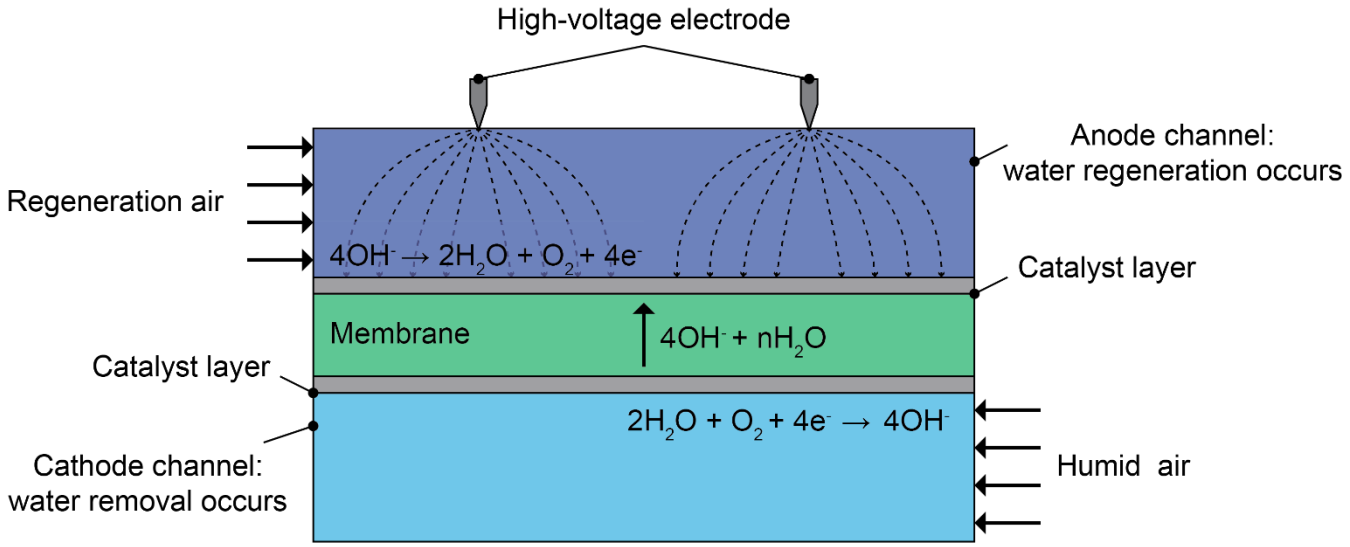

EHD Enhanced Water Transport
(Anode/cathode can be switched for EHD water extraction)

Task 3: EHDECD Prototype Development

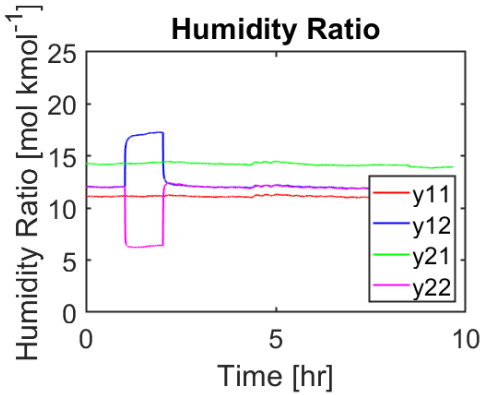

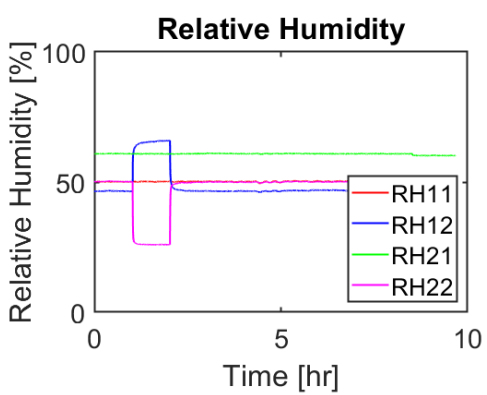

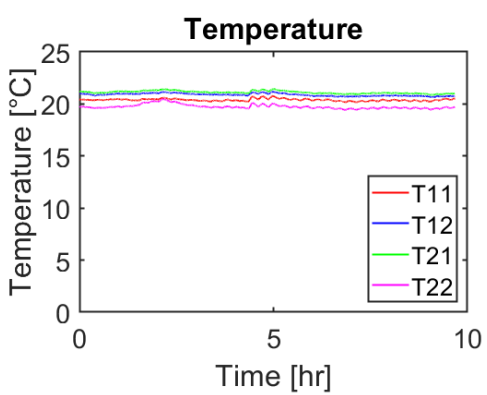

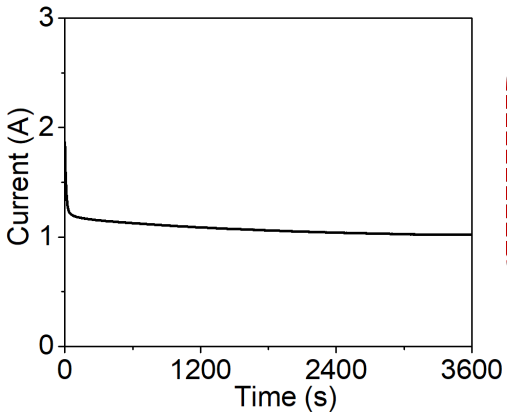

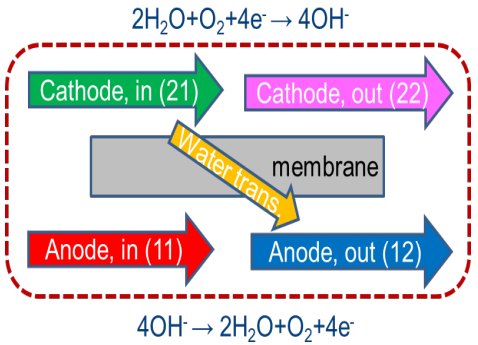

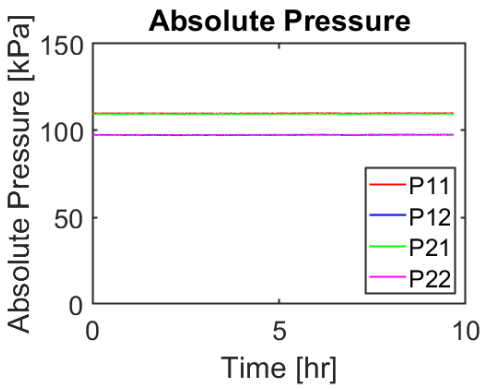

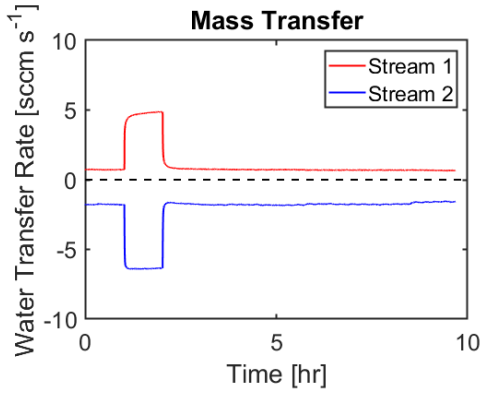

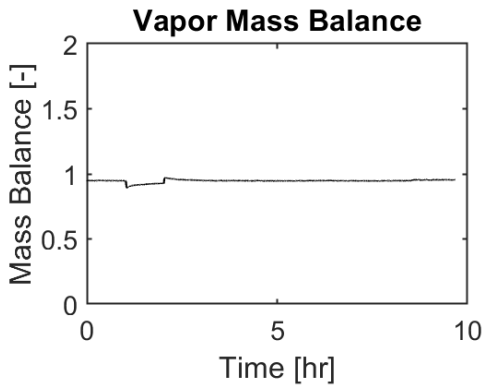

Actual water removal rate 1.48 g/day/cm^2 is 20% smaller than Faradic water removal rate 1.85 g/day/cm^2 when water is moved from high RH 61% to low RH 50% at 3 V (forward diffusion).

5 cm^2 RPI membrane, cathode catalyst 1 mg$_{Pt}$/cm^2 (60wt.%Pt/40wt.%C), anode catalyst 1 mg$_{IrO2}$/cm^2, Ti endplate. Operation voltage 3 V. Anode in (11) dry oxygen flow rate 800 mL/min, cathode in (21) dry oxygen flow rate 800 mL/min. 20 °C.

EHDECD Prototype Development

- **Developed a new prototype for ECD with integrated EHD enhancement**

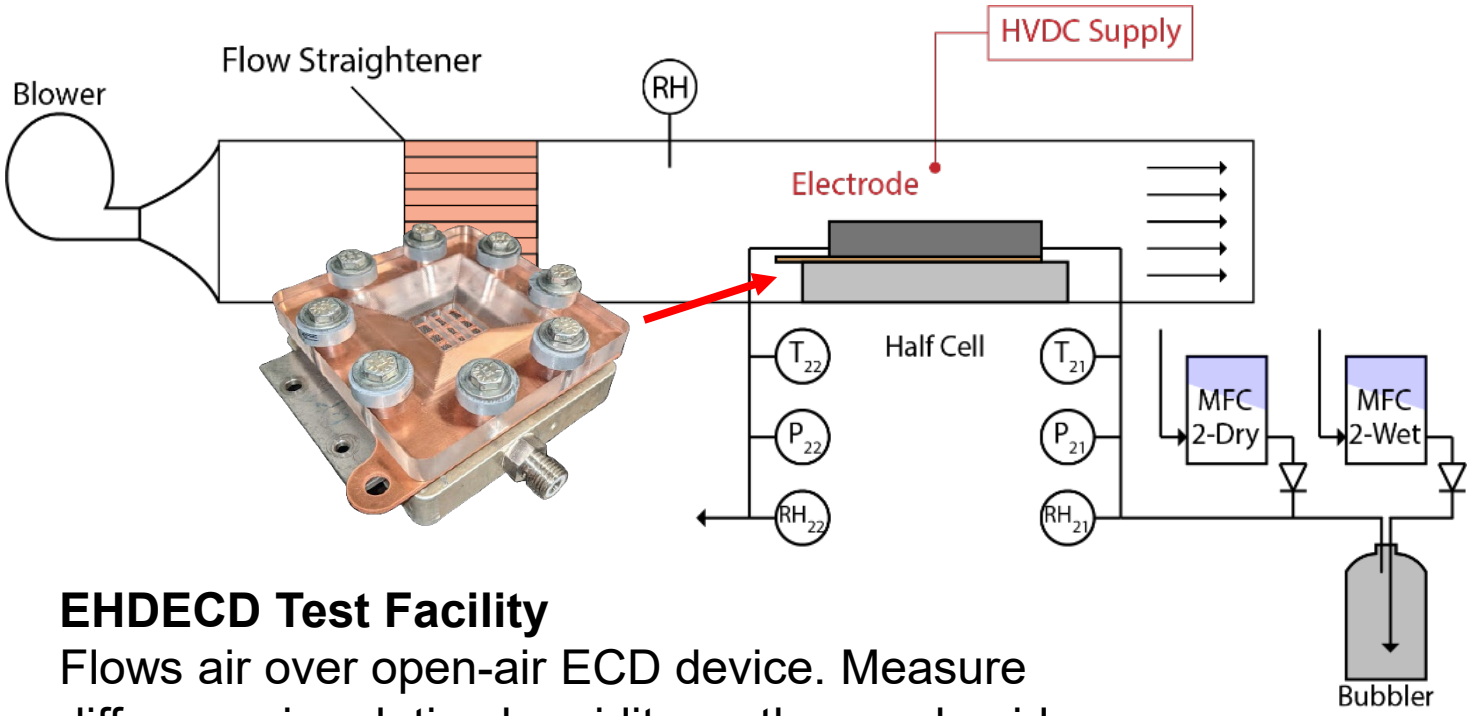

EHDECD Test Facility
Flows air over open-air ECD device. Measure difference in relative humidity on the anode-side.

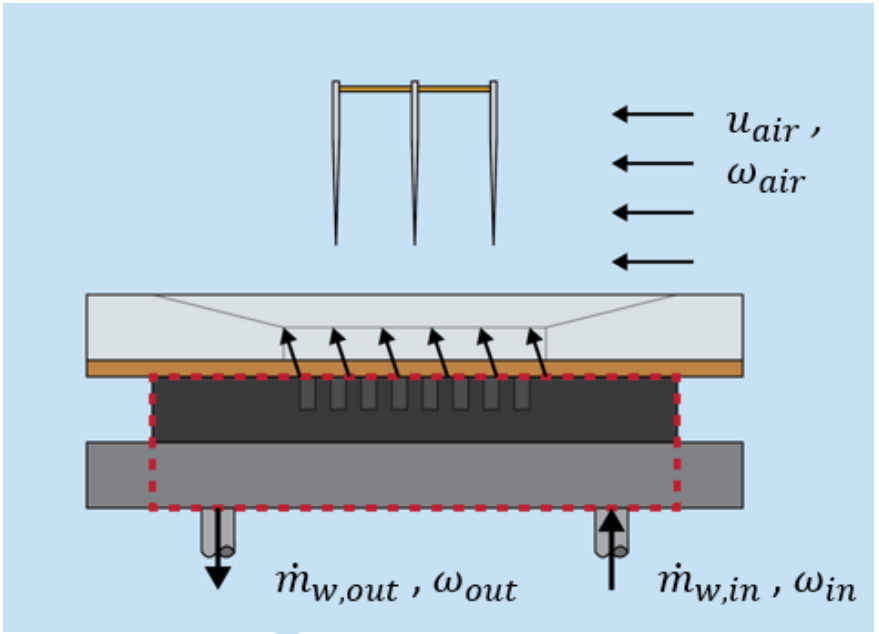

Open-air ECD Prototype

Polycarbonate top plate with copper grounding plate (common ground for ECD and EHD).

EHDECD Prototype Development

- **Summary of steady-state experimental performance**

H_2O Ratio → 2.5: Adverse humidity gradient
H_2O Ratio → 0: Favorable humidity gradient

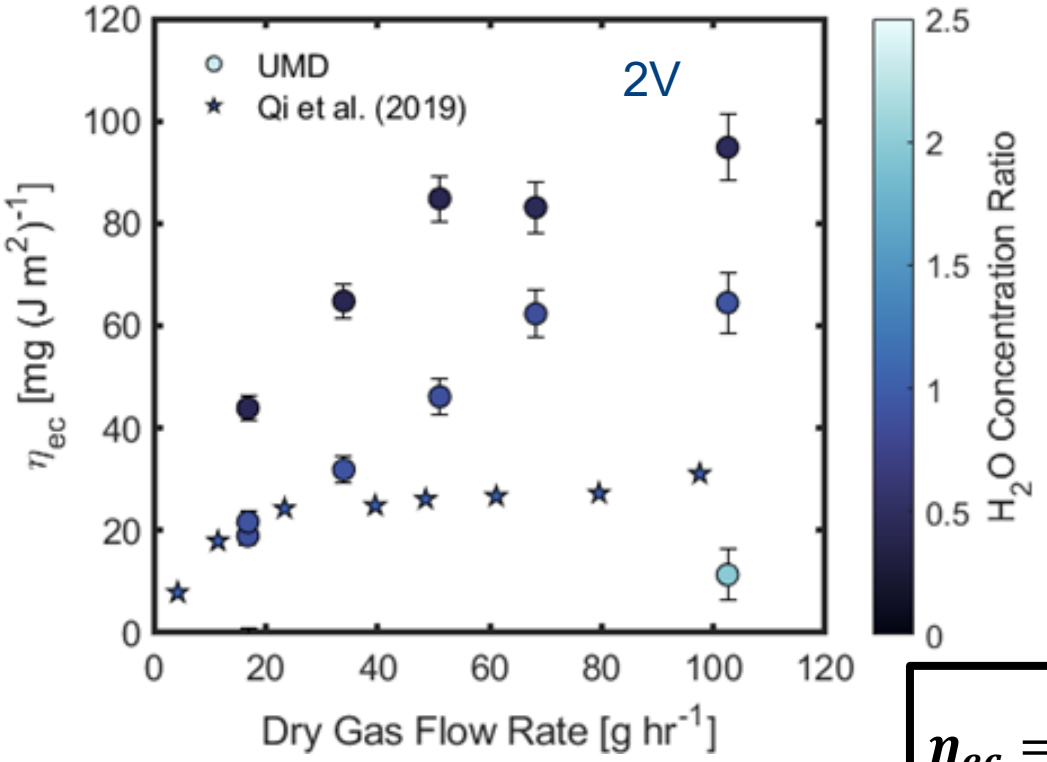

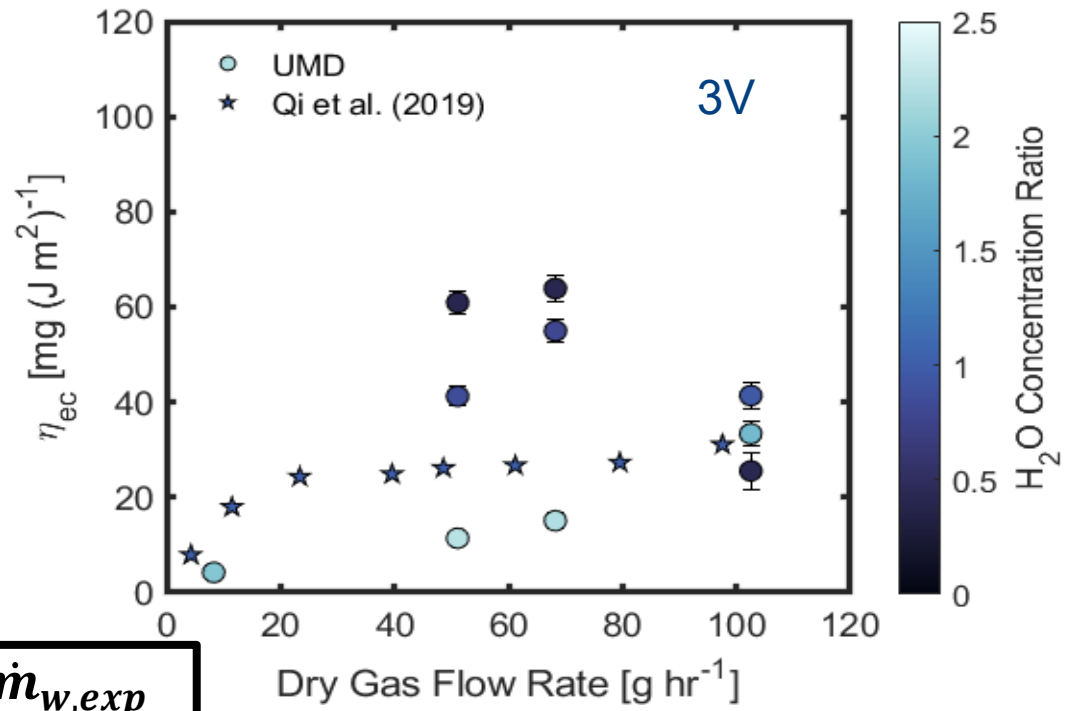

$$\eta_{ec} = \frac{\dot{m}_{w,exp}}{A\,V\,I}$$

Steady-state water removal efficiency 2V applied potential (left) 3V applied potential (right) comparted with best available performance from similar experiment by Qi et al. (2019)

Modeling of EC Processes

- Used numerical simulation to predict measured experimental data
- Model inputs:
  - Voltage
  - Inlet flow rates
  - Inlet pressures
  - Inlet relative humidities
- Compare simulated moisture removal rate and current to measured values

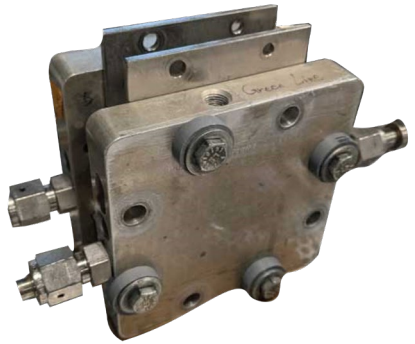

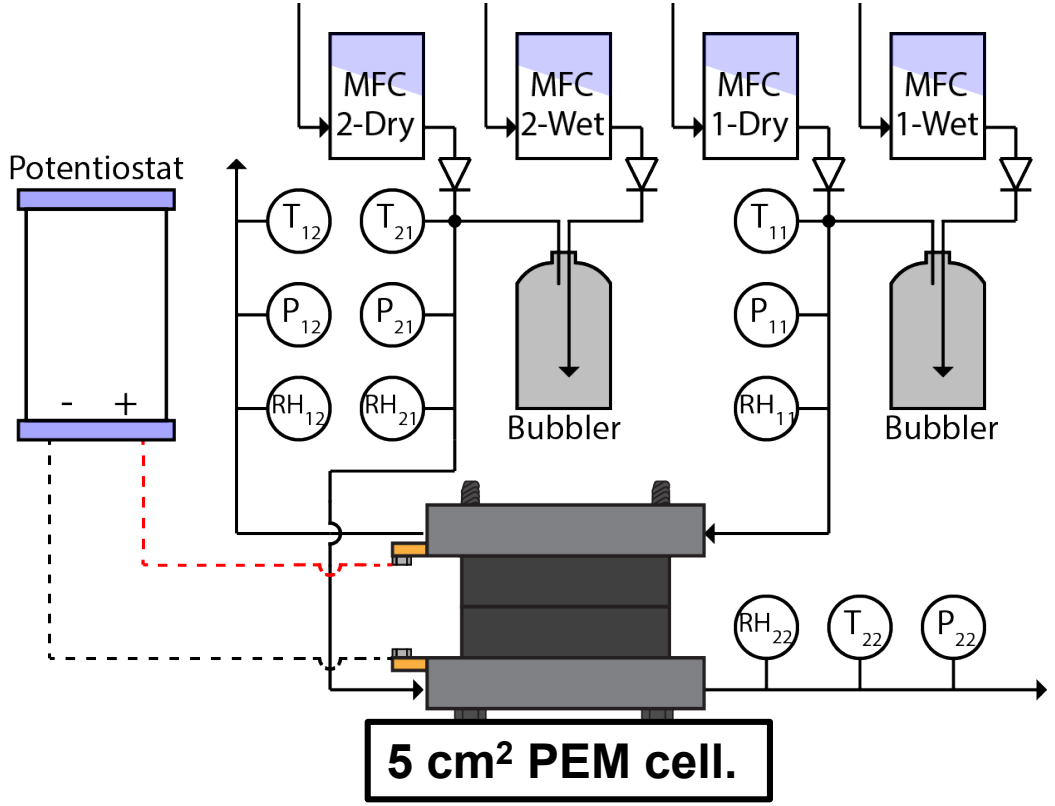

MEA Test Facility
Measure difference in RH before and after MEA. Placed heaters in cell hardware to test effect of temperature.

Proposed System Modeling Approach

- **Use experimental data and other modeling approaches to simulate:**
  - **EC dehumidifier**
  - **EHD enhancement**
  - **Sensible evaporator**
- **Combine system components using numerical model**

Conveniently solve different system configurations

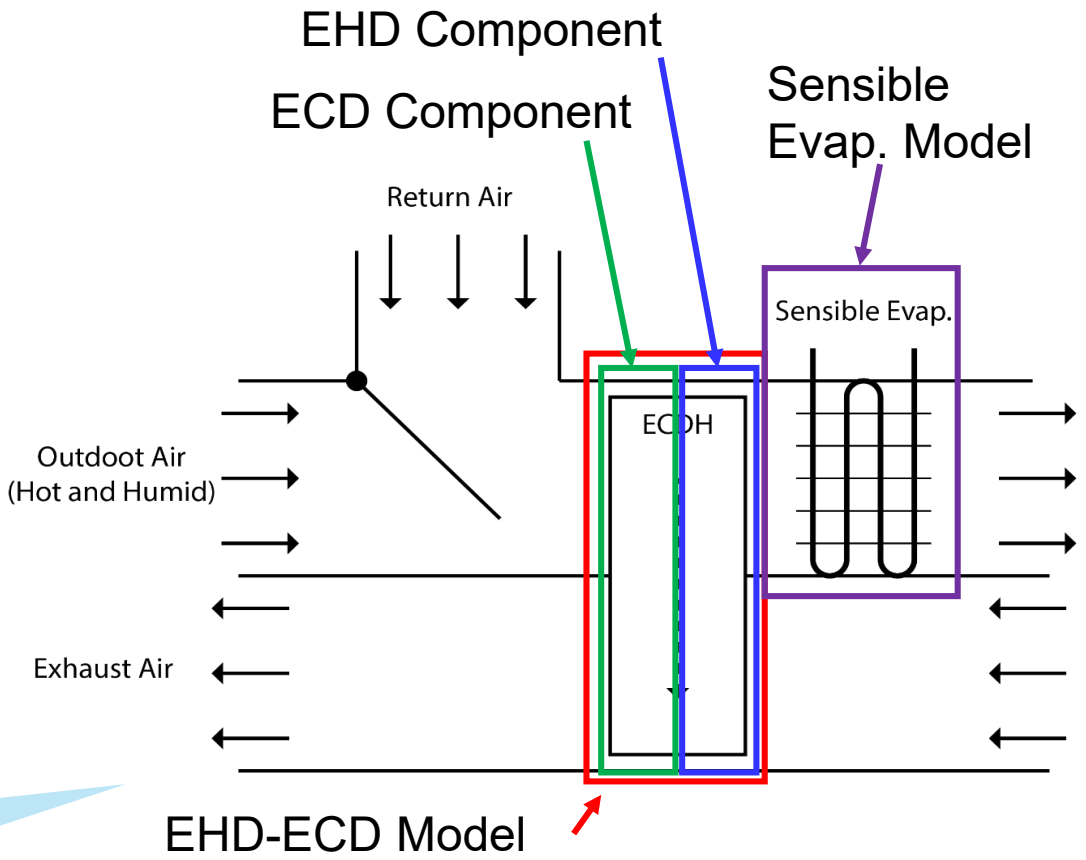

Proposed modeling approach: combine system components using independent sub-models validated by experimental data.

SSLC System Configurations

Conf. 1: 20%V, ECDin OA

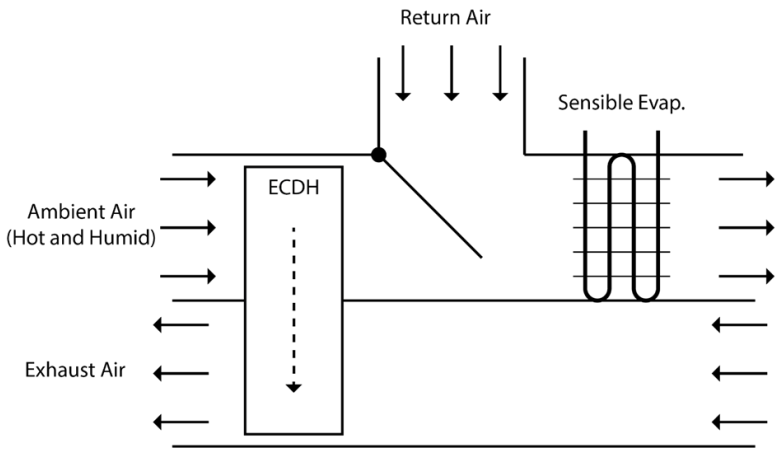

Conf. 2: 100%V, ECDin OA

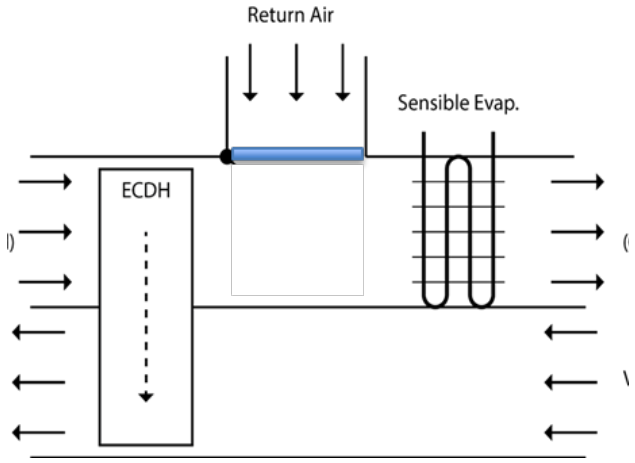

Conf. 3: 0%V, ECDin RA

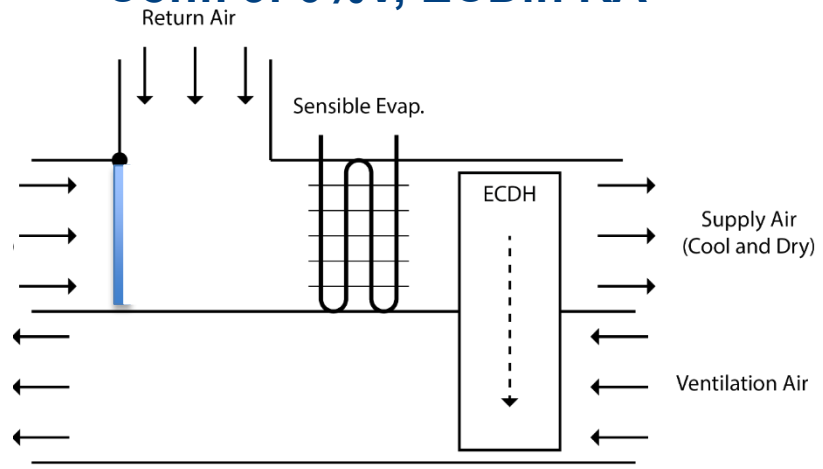

Conf. 4: 0%V, ECDin RA

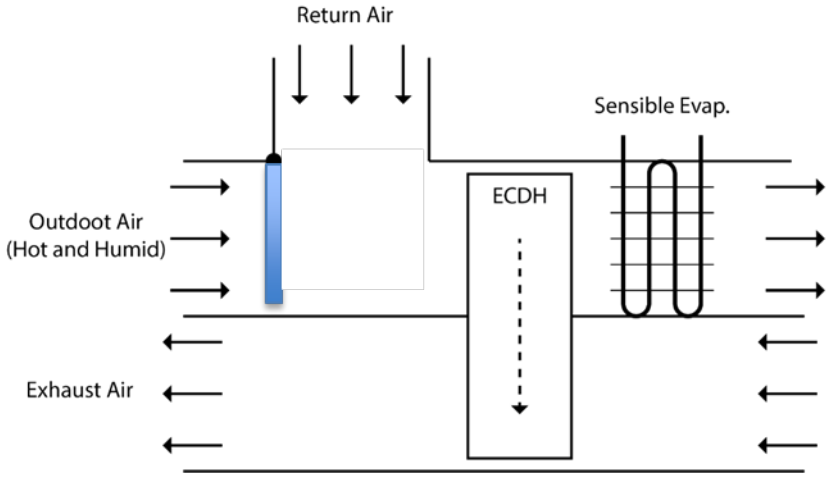

Conf. 5: 20%V, ECDin MixA

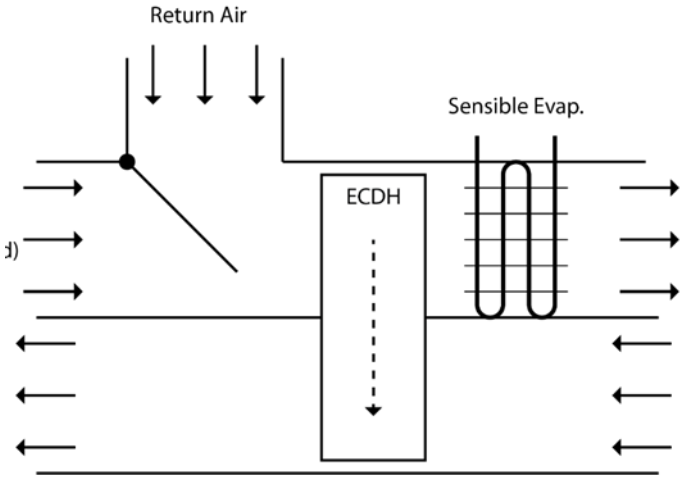

Conf. 6: 20%V, ECDin MixA

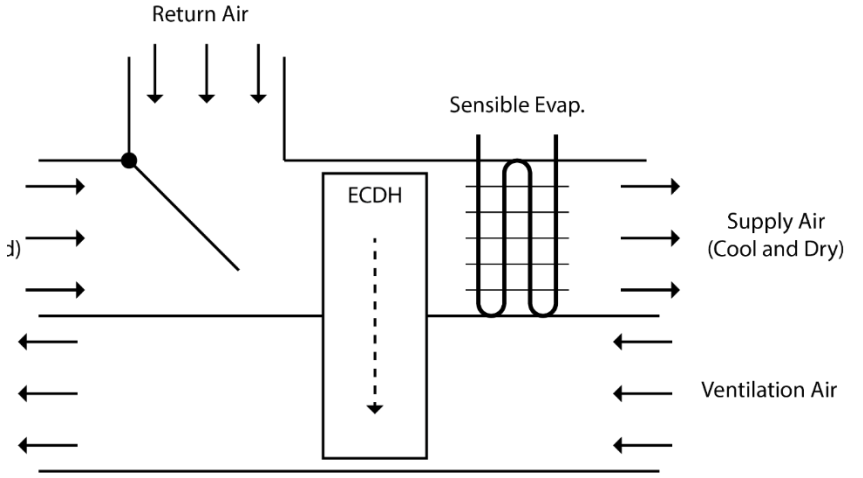

ECD Requirements

Configuration	Ventilation	Airflow Rate (CFM)	Cathode-side Inlet Temperature (°C)	Cathode-side Inlet Relative Humidity (%)	Cathode-side Inlet Humidity Ratio (g/kgda)	ECD Latent Load (kW)	Moisture Removal (g_w/s)
1	20%	240	35	44	0.01558	2.5	0.6
2	100%	1,200	35	44	0.01558	12.4	2.8
3	0%	1,200	15.7	100	0.01115	2.3	2.1
4	0%	1,200	27	50	0.01115	2.6	2.1
5	20%	1,200	16.9	100	0.01201	4.5	2.6
6	20%	1,200	28.6	49	0.01201	4.0	2.6

Anode-side inlet conditions: 27°C, 50% RH, 0.01115 g/kgda

Sensible Evaporator Requirements

- System: ~ 1 ton
- Airflow: 400 CFM[1]
- Ref. Mass Flow Range: 8~16 g/s[2]

Configuration[3]	Evaporator Mode[4]	Airflow Rate [CFM]	Air Inlet Temperature & Humidity[5]	Target Capacity[6] [kW]	Ref. Inlet Temperature & Quality[7]
1	Wet	400	27°C / 50%	3.2	10°C / 0.2
2					
2.5	Dry	400	27°C / < 20%	1.5	10°C, 14°C / 0.2
3	Wet	400	27°C / 50%	2.5	10°C / 0.2
4	Dry	400	32°C / < 20%	2.7	10°C, 14°C / 0.2
5	Wet	400	29°C / 49%	2.6	10°C / 0.2
6	Dry	400	34°C / < 20%	3.0	10°C, 14°C / 0.2

1. Using standard 400 CFM/ton; can be adjusted for your coil capacity and test facility
2. A suggested range for capacity ranging from 1.5 to 3.2 kW; please finalize design flow rate based on simulations
3. All are corresponding to configurations in previous slides, 2.5 is a variation assuming dry inlet conditions can be achieved in configuration 1 and 2
4. Under some configurations, the inlet are still wet conditions (which means the sensible evaporator needs to take care of some latent load as well)
5. Inlet air conditions for dry tests is flexible on humidity as long as it is below 20%, per AHRI 210/240
6. This is the design capacity (variations are expected depending on real test and operating conditions)
7. A higher evaporation temperature (14°C) is used for dry tests to validate the benefits from SSLC (a higher evaporation temperature for sensible evaporator), according to Ling et al. (2011)

Part 1 Conclusions

- Experimentally evaluated the ECD systems
- Scaled-up ECD Development with Commercial MEA Manufacturer
- Developed Component Models for the novel SSLC System
  - Formulated modeling methodology for closed-cell and open-cathode EC dehumidifiers
  - Implemented EC dehumidifier models in MATLAB
  - Achieved reasonably good agreement between modeled and measured moisture removal rates and cell currents